UNIVERSITEIT VAN PRETORIA
UNIVERSITY OF PRETORIA
YUNIBESITHI YA PRETORIA

Layered Double Hydroxides as PVC thermal stabilisers: The effect of particle size and concentration

HC Wright

February 2016

UNIVERSITEIT VAN PRETORIA
UNIVERSITY OF PRETORIA
YUNIBESITHI YA PRETORIA

Layered Double Hydroxides as PVC thermal stabilisers: The effect of particle size and concentration

Harry Charles Wright

A thesis submitted as partial fulfilment of the degree

Master of Engineering

in the

Institute of Applied Materials
Department of Chemical Engineering
Faculty of Engineering, the Build Environment and Information Technology
University of Pretoria
Pretoria

February 2016

Supervisor: Dr FJWJ Labuschagne

Layered Double Hydroxides as PVC thermal stabilisers: The effect of particle size and concentration

Abstract

Layered double hydroxides have shown promise as PVC thermal stabilisers, however how the properties of these clays effect their stabilising abilities is not fully understood. The purpose of this research was to help understand the relationship between the LDH clays properties and their ability to thermally stabilise PVC. The main property that was analysed was the particle size of the LDH clays. The particle size was varied by milling the clays. The effect of concentration of the clays was also tested.

Two separate LDH clays were synthesised, a magnesium aluminium clay (MgAl) and a calcium aluminium clay (CaAl). These clays were then milled to four different particle sizes and characterised. XRD analyses was done to understand the crystal structure of the LDH's. PSA ensured that four different particle sizes had been reached, BET was done to analyse the surface area of the clays. Samples were also observed using SEM to understand their morphology and acid reactivity tests were done to observe the reactivity of the clays. The clays were added to a PVC dry blend, which was processed and then thermally degraded via three testing methods. The three instruments used was: Torque Rheometer, Testing oven and a PVC Thermomat.

Characterisation showed that the two LDH's were successfully synthesised and milling had successfully reduced the particle size. We also noted the expected platelet shape from SEM. Reduction in particle size had little effect on the surface area of the particles.

Results from the thermal degradation tests indicated that particle size had very little effect on the thermal stability of the PVC. This could have been due to bad dispersibility or agglomeration and it is suggest that further tests be done to determine whether dispersibility was a problem. An increase in concentration of the LDH's increased the stability time of the PVC in the majority of the thermal degradation tests.

The CaAl LDH severally discoloured during processing and the MgAl caused only slight degradation. The MgAl LDH outperformed the CaAl LDH in the majority of the tests, the exception was the PVC Thermomat. This tests for HCl evolution, and the CaAl LDH may have performed better as it was shown to be much more reactive with acids. It was noted that different degradation tests led to different results, this important as a degradation method that is suitable for the application of the PVC should be used.

KEYWORDS: poly(vinyl chloride), thermal degradation, layered double hydroxides.

Acknowledgments

- My supervisor Dr FJWJ Labuschagne for his useful comments and engagement through the duration of my thesis.
- The National Research Foundation (NRF) for their funding.
- Wiebke Grote for her XRD analysis.
- Ansie Wiid and Hendrik Venter for their help with the synthesis of the LDH clays.
- Monique Schmidt for her help with D-spacing analysis.
- Isbe van der Westhuizen for her help with Rancimat testing.
- Washington Mhike for his help with training on polymer processing equipment.

Contents

List of Figures

List of Tables

1. Introduction

Poly (vinyl chloride) (PVC) is the third most used polymer, after the polyolefins (polyethylene and polypropylene). PVC however is thermally unstable and needs thermal additives to make it processable. In the past heavy metal based stabiliser have been used, however due to health and environmental concerns these are being phased out. This has led to the need for greener and safer thermal stabilisers. Layered double hydroxides (LDH's) have shown to be successful as well as green thermal stabilisers.

LDH's are a class of anionic clays which are made up of mixed metals. These clays have mixed metal cationic layers and an anionic interlayer. The mixed metals can be varied during synthesis and the anionic interlayer can also be substituted.

Layered double hydroxides have already been used as PVC thermal stabilisers, however the effect of different material properties have not been extensively studied. Properties such as particle size, concentration and the metals used in the metal layers are expected to influence the effect of the LDH's as PVC thermal stabilisers. Research into these properties would help optimise the LDH's as PVC stabilisers.

There are several thermal degradation testing methods used for the thermal degradation of PVC. The most common methods include: Hydrogen Chloride (HCl) measurement, colour change measurement, torque rheometry and thermogravimetric analysis. It is often required to use several of these methods to examine the stability behaviour of PVC. The use of several of these tests can be time consuming and require a lot of PVC material, which may be problematic as stabilisers are often synthesised on a small scale.

The purpose of this research is to examine some of the properties of the LDH's which are expected to effect the thermal stability of PVC. The properties which were examined were the particle size, metals used in mixed metal layers as well as concentration. A secondary objective of this study was to examine the results from several thermal stability tests and identify any possible interactions between the

testing methods that could help optimise the amount of experimental time needed to fully understand the stabilising effect of a stabiliser.

This was done by synthesising LDH's with two separate mixed metal layers. These LDH's were then milled in a hydraulic mill to different particle sizes. LDH's were analysed using X-ray diffraction (XRD), scanning electron microscopy (SEM), particle size analysis (PSA), surface area analysis (BET) as well as acid reactivity tests.

This LDH's were then mixed into a PVC dry blend at three different concentrations and processed, using extrusion and pressing.

The PVC plastic was then thermally degraded using three different pieces of equipment. The equipment used was a Metrohm 895 Professional PVC Thermomat, Metrastat testing oven and a Haake Polylab OS Rheomix torque rheometer. Results were then analysed to determine the effect of varying the LDH properties as well as to examine any interactions between the results from the different testing methods.

2. Theory

2.1. Introduction to PVC

2.1.1. History of PVC

Poly(vinyl Chloride) (PVC), is the third most produced and used polymer, after Polyethylene and Polypropylene (Braun, 2001). This means that PVC is an important polymer in the modern age. However the discovery of PVC is not a new one, with the first synthesis being done by Baumann in 1872 (Mulder & Knot, 2001). This was a purely academic discovery at this point and no industrial uses were proposed for PVC at this time.

The invention of PVC was credited to F Klatte, who in 1913 polymerised the vinyl chloride monomer (VCM) with organic peroxides and developed a production process of PVC. He also suggested that PVC could be used as a substitute for films, fibres as well as lacquers (Braun, 2003). Although a method had now been invented for the production of PVC there were still several shortcomings. The major shortcoming was the fact that the PVC was difficult to process as it started to degrade at temperatures as low as 100 °C. Due to these shortcomings Klatte's patent lapsed in 1926 allowing other companies to start producing PVC.

2.1.2. Commercialisation of PVC

PVC was finally commercialised in 1930 with the development of plasticisation, these early plasticisers had a tendency to migrate to the surface of the PVC and cause the PVC to become brittle prematurely (Utracki, 1995). The use of plasticisers made it easier to process the PVC and as a result PVC started to find commercial applications. The first commercial PVC products were shock absorber seals and tank linings. These initial products were shortly followed by flame retardant cable insulation and PVC-coated textiles (Semon & Stahl, 1982).

This early compounded PVC still had problems as the plasticisers would volatilise as they migrated to the surface of the PVC giving off bad odours. The migration of the plasticisers also leads to bad mechanical properties. For this reasons PVC was initially negatively received by the general public (Meikle, 1997, 83).

These problems were overcome with the invention of newer and better plasticisers as well as other additives which helped the processability of PVC. This occurred from the 1930's till the 1960's and new additives for PVC are currently still being invented. With all new processing aids and additives PVC started to internationalise in the 1950's (Mulder & Knot, 2001).

2.1.3. Modern PVC and Applications

Since the 1950's PVC utilisation has been growing at a rate above 4 % per year and is currently the second most used plastic after the polyolefins (Braun, 2001). Figure 2.1 shows the growth of PVC since it was first synthesised in the 1930's (Braun, 2003). One of the major advantages of PVC over the polyolefins is the fact that PVC consists of 50 % chlorine, which comes from salt as opposed to crude oil. PVC prices are therefore more stable and less susceptible to oil price fluctuations (Wilkes *et al*, 2005: 1). PVC did however have a dip in sales in recent times, between 2004 and 2009, growth was a mere 1.3 %. This was due to the worldwide economic crisis. (Ertl *et al*, 2010).

PVC is a plastic which is used in several different industries in the current day. Some of the typical uses of PVC are : Piping, cable insulation, panels, bottles. Figure 2.2 shows the worldwide applications of PVC in 2010 (Attenberger *et al*, 2011).

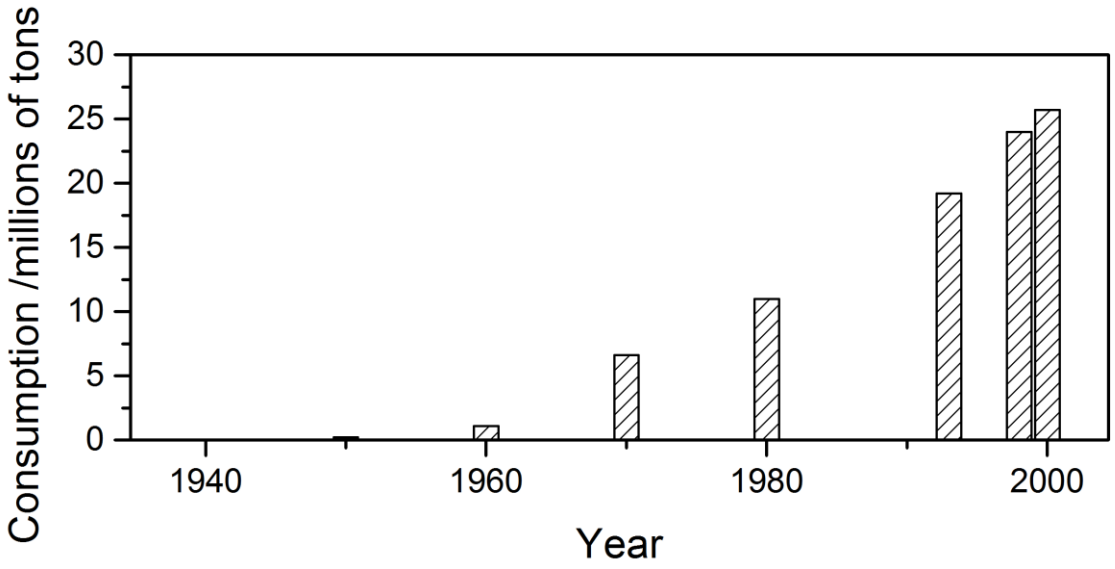

Figure 2.1: Worldwide consumption of PVC from 1930 till 2010.

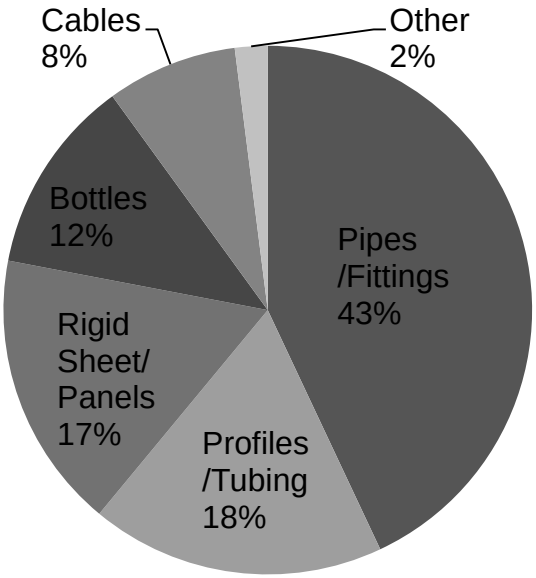

Figure 2.2: Worldwide application of PVC in 2010.

2.1.4. Setbacks and the Future of PVC

PVC has however had several setbacks along the way. These setbacks are due to the fact that some of the additives used have had negative effects on people as well as the environment. The use of phthalates as plasticisers has had a negative effect as some of the phthalates can interfere with the human hormones (Duty *et al*, 2005). This

has been a major issue as the majority of plasticisers used are based on the phthalates.

A further problem with PVC is that when scrap PVC is combusted it produces dioxins which can cause reproductive problems, cause cancer, damage the immune system and interfere with hormones (Schecter *et al*, 2005).

The heavy metals used as additives have also had negative effects on the environment; this is also a major problem as the most efficient PVC stabilisers are based on heavy metals (Anon, 2007).

To counter these setbacks the Vinyl industry committed itself to Vinyl 2010, a 10 year program to make the PVC industry a cleaner industry. The program reached several of these goals and the most important include: discontinuing the use of cadmium stabilisers, reducing the amount of lead stabilisers, the shifting of plasticisers away from the dangerous phthalates and increasing the amount of PVC recycling (Attenberger *et al*, 2011).

With initiatives like the one mentioned above and the continued improvement of environmentally and human friendly stabilisers and additives and more efficient recycling, PVC should flourish as a polymer into the future.

2.2. Chemistry of PVC

2.2.1. Basic Structure

Figure 2.3 shows the basic structure of the PVC molecule. PVC is white solid which is brittle in its pure form. The fact that PVC is polar, a property which isn't found in the other major polymers (polyethylene and polypropylene), gives PVC unique properties amongst polymers. The most important of these properties is the fact PVC has better compatibility with a lot of additives (especially plasticisers).This means that additives will be slightly more effective in PVC than in the other polymers (Titow, 1984: 94).

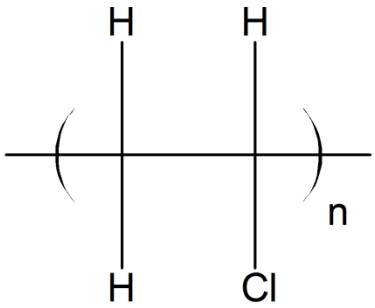

Figure 2.3: The chemical structure of the PVC molecule.

2.2.2. Polymerisation of the Vinyl Chloride Monomer (VCM)

2.2.2.1. Polymerisation Mechanism

The polymerisation of the VCM occurs in three steps, initiation, propagation and termination. This process occurs via the radical reaction of the monomer.

Initiation occurs in a two-step process, as shown in Equation 2.1 and 2.2. Equation 2.1 shows the process whereby an initiator (I) produces free radicals, Equation 2.2 shows the imitator radical, radicalising the monomer.

$$I \rightarrow 2I^{\bullet} \quad (2.1)$$

$$I^{\bullet} + VCM \rightarrow PVC^{\bullet} \quad (2.2)$$

Where VCM is the monomer and PVC is the growing polymer chain. The radical reaction can then be explained by Equation 2.3, whereby the polymer grows in length and molecular weight.

$$PVC^{\bullet} + VCM \rightarrow PVC^{\bullet} \quad (2.3)$$

The termination of the polymerisation reaction occurs when two $PVC^{\bullet}$ react with each other and therefore cancel each other out (Wypych, 2008:26).

In the modern manufacture of PVC there are three main methods for the polymerisation of the VCM. These methods are suspensions polymerisation, emulsion and bulk polymerisation. These three methods will now be further explained.

2.2.2.2. Suspension Polymerisation

Suspension polymerisation accounts for approximately 80% of all PVC manufactured. The method of suspension polymerisation involves using 1-2 parts of water per part VCM and adding them to a reactor with an initiator. This mass is then reacted until approximately 90% of all the VCM is reacted. The PVC/water mixture is then heated until all the monomer has been removed; the PVC resin is then removed and dried. The dried resin is then transferred to be stored in storage vessels (Wheeler, 1981; Endo, 2002).

2.2.2.3. Emulsion Polymerisation

Emulsion polymerisation accounts for approximately 12% of the industrially produced PVC. A water soluble initiator system will be used to explain the emulsion polymerisation method further. The method involves using 1-2 parts water per part of VCM as well as 0.01-0.03 parts of a surfactant and adding them to a reactor with an initiator. This mass is then reacted until approximately 90% of the VCM has been reacted. The PVC forms a latex solution and this can be stripped of remaining VCM or further reacted with further addition of an initiator. This PVC product can be shipped as a latex solution or the polymer can be recovered as a dry resin (Wheeler, 1981; Endo, 2002).

2.2.2.4. Bulk Polymerisation

Bulk polymerisation accounts for the remaining PVC production. The process whereby bulk polymerisation occurs is as follows: VCM and initiator is charged to a reactor and about 10% of the VCM is reacted. This is then transferred to a secondary reactor where additional VCM and initiator are added and reacted to about 85%. The unreacted VCM is then removed; the PVC is then moved to storage vessels. The

absence of water means that the PVC does not need to be dried (Wheeler, 1981; Endo, 2002).

2.3. Thermal Degradation of PVC

2.3.1. Basic Understanding of Thermal Degradation

PVC has relatively bad thermal stability and degrades during processing, at temperatures just above its glass transition temperature (Palma & Corenza, 1970). Considering that processing happens at temperature much higher than PVC's glass transition temperature, it is important to understand the chemistry behind the degradation of PVC.

The process which occurs during the degradation is known as a dehydrochlorination process whereby the PVC loses a hydrogen chloride (HCl), this loss causes a zipper like process whereby double bonds (polyenes) form within the PVC polymer. This process is further explained in Figure 2.4 (Nagy *et al*, 1980).

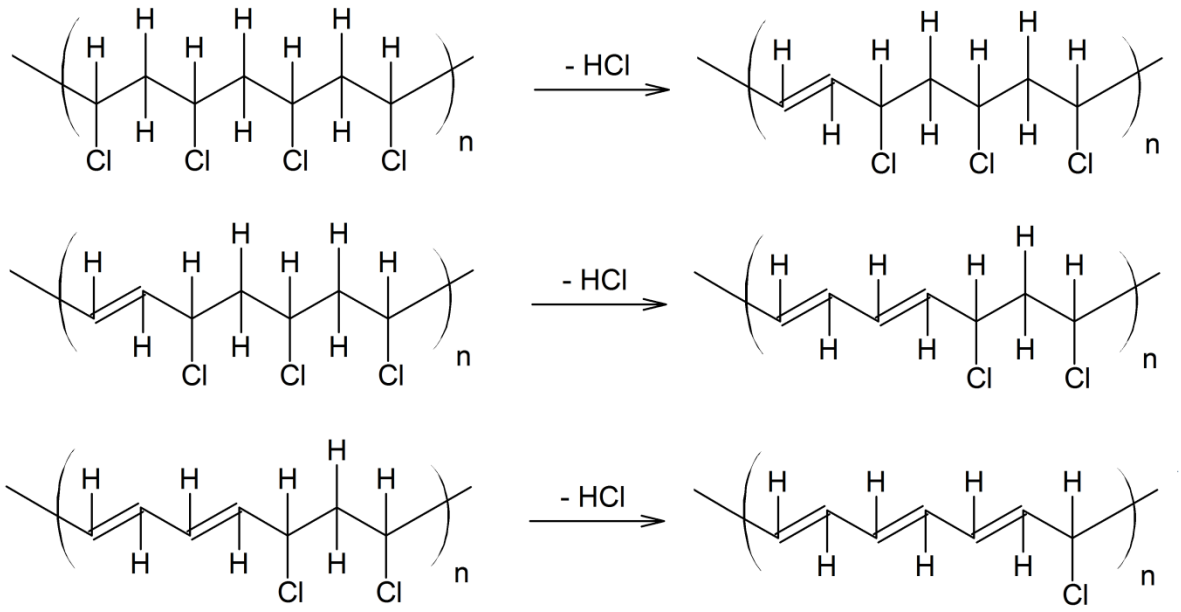

Figure 2.4: The dehydrochlorination of PVC and formation of polyenes.

It is generally accepted that this zipper like process is the primary process of degradation and can generally be broken into 3 different steps (Ivan, Kelen and Tudos, 1989).

1 – Initiation: this could be due to defects in the PVC or several other reasons.
2 – Zip Elimination: The elimination of HCl and the formation of the polyene structures.
3 – Termination: The process which stops the Zip elimination from continuing.

These three steps will be further explained in Section 2.3.2 as this helps in the understanding of the main mechanisms that occur during degradation.

The dehydrochlorination of PVC is an autocatalytic reaction, as any free HCl will further cleave off more HCl molecules from the PVC chain.

2.3.2. Degradation Mechanisms of HCl evolution

There have been lots of papers published on the mechanisms which control PVC thermal degradation, and lots of different hypotheses on which mechanism is indeed the correct one (Wypych, 2008: 98,). For this reason only some of the mechanisms will be included in this literature review. Although all of the mechanisms are correct under a certain set of conditions, a mechanism to fully explain the degradation behaviour of PVC has yet to be suggested. The most popular mechanisms have been selected and investigated further.

2.3.2.1. Molecular Mechanisms

a) Basic Molecular Mechanism

The molecular mechanism predicts that the initiation of the PVC dehydrochlorination reaction occurs when an HCl molecule reacts with a regular unit within the PVC chain. This is the simplest mechanism and does not include any radical formation or formation of ionised groups (Wypych, 2008: 98, Amer and Shapiro, 1980). The basic outline of the molecular mechanism is shown in Figure 2.5: The molecular mechanism for the Dehydrochlorination of PVC.Figure 2.5.

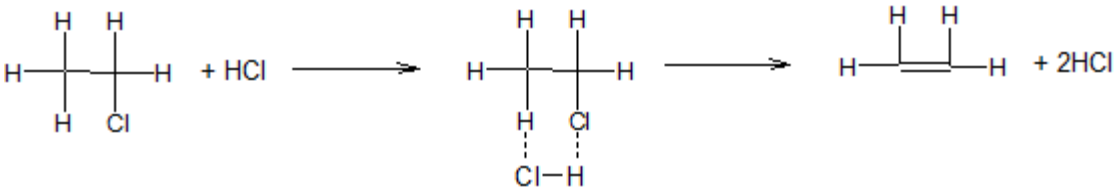

Figure 2.5: The molecular mechanism for the Dehydrochlorination of PVC.

b) Amer-Shapiro and Six Centre HCl elimination

The Amer-Shapiro mechanism (Amer and Shapiro, 1980) was suggested as a three step mechanism to explain the thermal degradation of PVC. The first step, or the initiation of degradation involved the formation of a cis double bond within the PVC chain. This could be done by one of two mechanisms, which are both shown in Figure 2.6.

Figure 2.6 (a) describes the process as a molecular process whereby HCl is eliminated by a 1,2-unimolecular elimination. Figure 2.6 (b) describes this first step as a radical process.

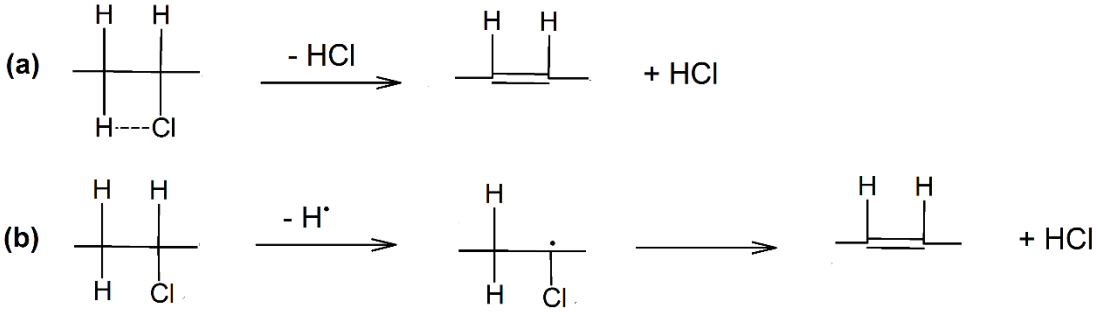

Figure 2.6: The two mechanisms for forming a cis double bond within PVC.

The second step in this process consists of a six centre elimination of HCl and this causes an HCl catalysed double bond shift. Step three shows how this can continue as long the correct conformation is retained. Step two and step three can be seen in Figure 2.7.

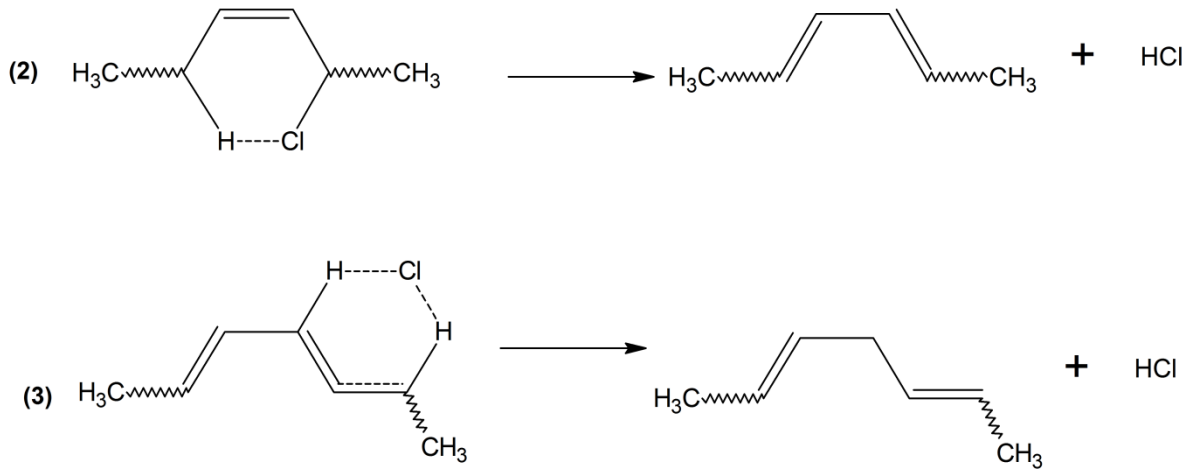

Figure 2.7: Shows step two and step three of the six centre elimination of HCl during PVC degradation.

Step three of the above mentioned mechanism has been altered by Bacaloglu and Fisch (1995) to explain why polyenes stop growing when they reach a certain length, normally between 1-30 in length, with an average of about 10 (Hjertberg, Martinsson, & Sorvik, 1987). This is explained by the fact that if the double bond forms in the cis conformation then the reaction can continue further however if the double bond forms in the trans conformation then it forms a stable unreactive product. This is shown in Figure 2.8.

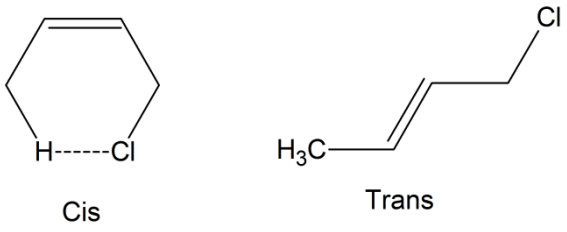

Figure 2.8: The cis and trans form of the polyene double bond.

2.3.2.2. Radical Mechanism

The radical mechanism has been used to explain PVC thermal degradation in the presence of impurities such as catalysts or unreacted monomer. It has also been used to explain degradation in PVC copolymers. There have been several different combinations or radicals which can start the process of dehydrochlorination and lots

of these have been examined in literature (Bamford & Fenton, 1969; McNeil and Neil, 1969).

The basic mechanism for the radical dehydrochlorination of PVC is shown in Figure 2.9 (Braun, 1981), where $R^{\bullet}$ is a radical that is able to initiate the PVC degradation and the C-Cl bond which is weak can then be cleaved due to the radical formation in the PVC chain (Yousufzai, Zafar and ul-Hasan, 1972).

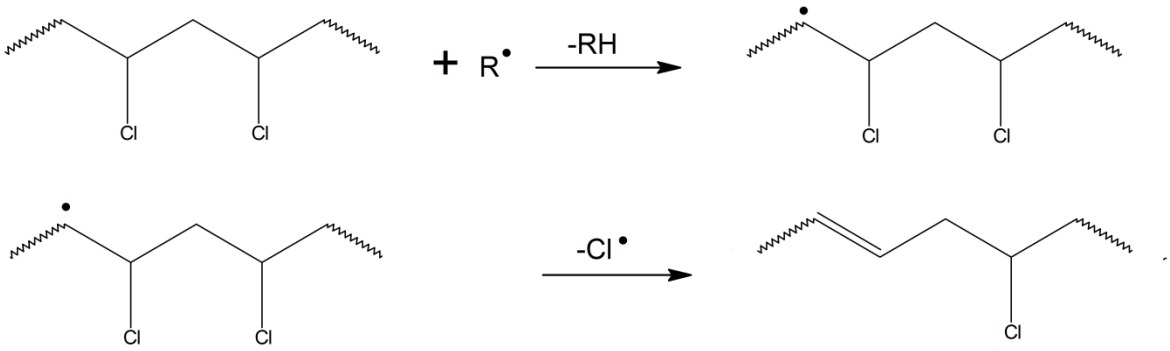

Figure 2.9: Radical Mechanism for the Dehydrochlorination of PVC.

2.3.2.3. Ionic Mechanism

Although there isn't a lot of experimental work to back up the ionic mechanism for the dehydrochlorination of PVC however it is still worth mentioning. The quasi-ionic mechanism is given in the Figure 2.10 (Starnes, 2005).

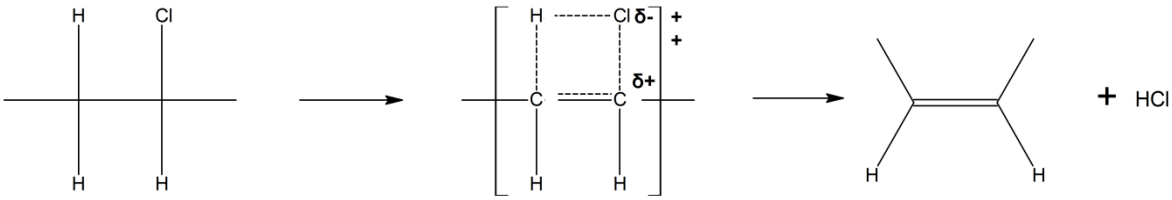

Figure 2.10: The quasi-ionic mechanism for the dehydrochlorination of PVC.

2.3.2.4. Polaron Mechanism

A final mechanism is mentioned however not explained in detail. The propagation reaction is explained in terms of polarons instead of allylic chlorines or radical. This

mechanism also describes the chain degradation reaction. For further reading on the polaron mechanism see (Van Hoang & Guyot, 1990; Tran *et al*, 1991).

2.3.3. Degradation Mechanisms of Cross Linking and Benzene Formation

The dehydrochlorination of PVC is the major method of thermal degradation, however a few other mechanisms are of importance. The two which will be mentioned here are the cross linking of PVC as well as the formation of benzene rings.

The crosslinking of PVC is a process which is catalysed by the availability of HCl (Bacalogulu & Fisch, 2004) and crosslinking causes a loss of mechanical properties of PVC. The most important reaction of crosslinking is known as the Diels Alder mechanism and is shown in Figure 2.11 (Kelen *et al*, 1978).

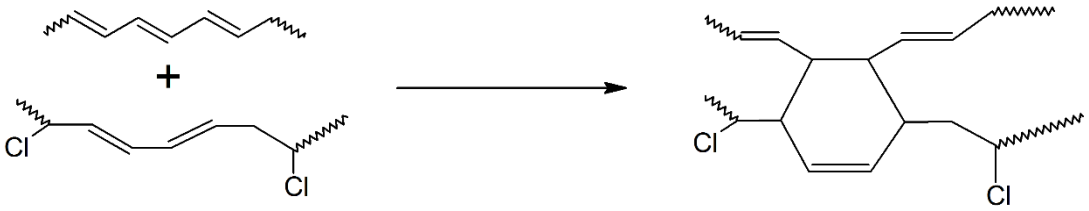

Figure 2.11: Diels Alder mechanism for the crosslinking of PVC.

During the process of crosslinking some benzene can also be formed. This is a side reaction of the Diels Alder Mechanism. The mechanism for this formation is shown in Figure 2.12 (Marongiu *et al*, 2003).

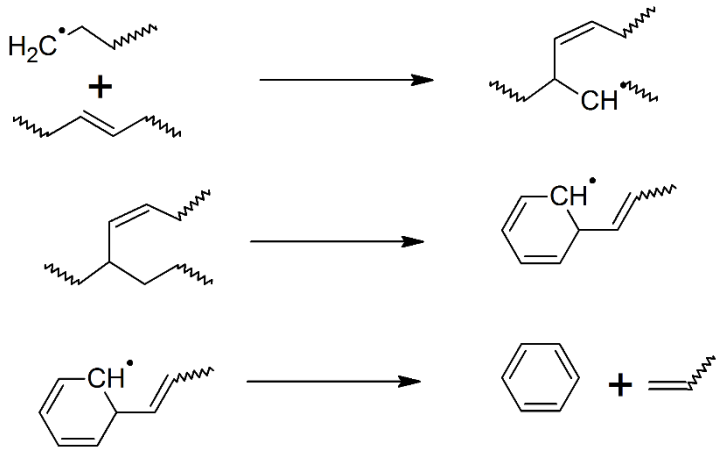

Figure 2.12: Mechanism for the formation of benzene during PVC degradation.

2.3.4. Results of Thermal Degradation

2.3.4.1. Volatile Formation

The degradation of PVC leads to the formation of several products. The first and most obvious of these volatiles is HCl. This is due to the dehydrochlorination of the PVC chain. The release of HCl is slow and at the stage whereby HCl evolution is noticible, degradation has progressed to such an extent that the mechanical properties are destroyed and the product is no longer suitable to its application.

The other major volatiles which form during the degradation are the polyenes (McNeill, Memetea and Cole, 1995). The majority of these structures are benzene based and aromatic in nature.

There are some volatiles that are found in low concentrations which are toxic. These dioxin compounds can be found in very low concentrations however this can still be very dangerous as PVC has several household applications (Carroll, 1996). There are very few oxygen containing volatiles.

2.3.4.2. Mechanical Properties

The mechanical properties of all polymers decrease until the polymer is no longer useful when they are degraded thermally. This is no different for PVC, however additives are normally added to try and counter this loss of mechanical properties (Wypych, 2008: 125).

2.3.4.3. Colour Change

PVC is very sensitive to discolouration during the thermal degradation process; this is in fact the most sensitive method for measuring PVC thermal degradation (Geddes, 1967).

The discolouration of PVC is said to be due to the formation of the double bonds within the PVC polymer chain (Ocskay *et al*, 1971). The number of initial conjugated double

bonds (after processing) therefore determines the colour of the product. There is therefore the thought that HCl evolution can be related to the colour change of PVC. There has however been very little progress in relating colour change to the evolution of HCl within the sample. Ocskay *et al* (1974) claims a correlation between colour change and HCl, however the method for measuring colour change were not extremely sensitive and subjective.

PVC changes from its initial colour to yellow then yellow-orange, red-orange, red, brown and then finally black during the degradation process (Van der Laan, 2004).

2.3.4.4. Other Changes

There are other changes which occur during the degradation of PVC. These include changes in electrical properties, changes in molecular weight, weight loss, char formation and the formation of ash. The change in these properties are expected as they would be for the majority of thermally degraded polymers.

An important change in the PVC is the change of the conductivity of the polymer. This is an important change as it is due to the release of hydrogen chloride. For this reason the conductivity of the polymer during degradation can be measured, and the amount of HCl evolved can be calculated.

For further reading on these and other property changes see Wypych (2008: 119 - 126).

2.4. Thermal Stabilisation of PVC

Due to the fragile nature of neat PVC as a thermoplastic, stabilisation is required to ensure that the PVC is processable at elevated temperatures. This has been a problem since PVC was first synthesised in the lab, and the reason why it took so long for PVC to become a viable plastic.

PVC was first commercialised as a flexible product with the discovery of plasticisers, these early PVC formulations borrowed thermal stabilisers such as white lead and sodium silicate from the rubber industry to help stabilise flexible PVC (Dworkin, 1989).

The first stabilisers created directly for the PVC market were the metal soaps. These were patented in 1934 (Dworkin, 1989). The next patented stabilisers for the dehydrochlorination of PVC were the cadmium-zinc and barium-cadmium soaps which were patented in 1940 (Yngve, 1940). In the 1950's the organotin stabilisers started being produced. This is an important discovery as the organotins are still used today, whereas the majority of the stabilisers discovered during this age have been phased out due to health and environmental reasons. The 1950's also lead to the discovery of several other stabilisers including: antimony mercaptoesters, polyols and mixed alkyl/aryl phosphites.

The first of processing aid for the processing of rigid PVC was patented in 1953 and the first processing aid which was made commercially available was introduced in 1957. The first processing aid for rigid PVC was an acrylic based processing aid. This marks the beginning of the commercialisation of rigid PVC (Dunkelberger, 1987).

Due to the current environmental and health standards, there has been a need to develop new and safer stabilisers. These stabilisers include zinc and calcium stearates, hydrotalcite type stabilisers as well as new organic stabilisers (Conroy, 1999). These new stabilisers have shown promising stability improvement however these are not a major part in the market yet due to high prices.

PVC stabilisers can be broken up into two separate groups, primary and secondary stabilisers.

2.4.1. Primary Stabilisation

Primary stabilisers work by stabilising the unstable allylic groups on the PVC backbone, this process needs to happen rapidly as it needs to occur before a double bond is formed within the PVC (Wypych, 2008: 15). This stabilisation stops the formation of polyenes with lengths longer than 4 or 5. Primary stabilisation is also

known to give PVC good early colour retention (Zweifel, Maier & Schiller, 2008: 438). A list of some primary stabilisers can be seen in Table 2.1, which is adapted from (Fisch & Bacaloglu, 1999).

An example of the mechanism for a primary stabiliser is shown in Figure 2.13 (adapted from Abbas and Sorvik, 1980). This example of a primary stabilising mechanism is for zinc stearate. The reaction that occurs is an exchange reaction, whereby the ester group replaces the allylic chlorine atom and slows the propagation of polyene sequence formation (Abbas and Sorvik, 1980). Step 1 in Figure 2.13 shows the zinc stearate reacting with the allylic chloride, stabilising the allylic intermediate. Step 2 shows this process repeating with the second ester group, finally forming zinc chloride.

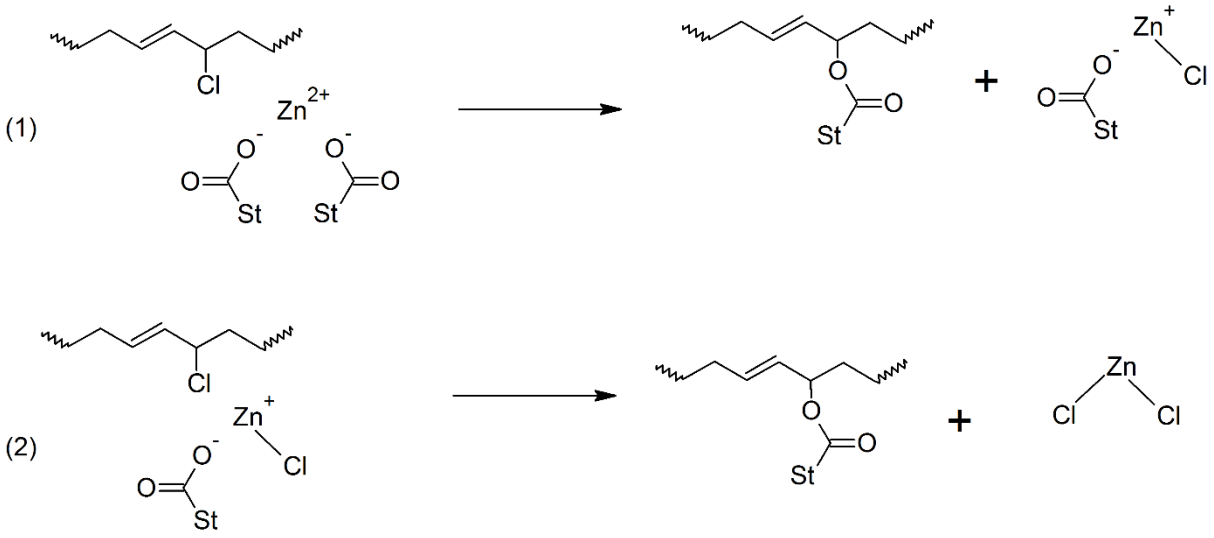

Figure 2.13: Mechanism for zinc stearate, a primary thermal stabiliser.

Table 2.1: Examples of some Primary and Secondary Stabilisers

Stabiliser	Primary Stabiliser	Secondary Stabiliser
Alkyltin Thioglycolates	Yes	Minor
Alkyltin Mercaptopropionates	Yes	Minor
K, Ba, Ca carboxylates	No	Yes
Zn, Cd carboxylates	Yes	Minor
Alkyl phosphites	Minor	Yes
Zn/alkyl phosphites	Yes	Minor
Zn/b-diketones	Yes	Minor
Epoxides	No	Yes
Zn/epoxides	Yes	Minor
Hydrotalcites	No	Yes

2.4.2. Secondary Stabilisation

Secondary stabilisers are hydrochloric acid (HCl) scavengers; scavenging HCl can stop the unzipping of PVC chains and therefore slow the autocatalytic degradation of PVC (Van der Laan, 2007). These scavengers cannot stop the degradation altogether though, as allylic intermediates are still able to form with the PVC backbone (Zweifel, Maier & Schiller, 2008: 437). A list of some secondary stabilisers can be seen in Table 2.1, which is adapted from (Fisch & Bacaloglu, 1999).

An example of the mechanism for a secondary stabiliser is shown in Figure 2.14. This example of a mechanism is for calcium stearate (Fisch & Bacaloglu, 1999). This is a simple ion exchange reaction

Figure 2.14: Mechanism for Calcium Stearate, a secondary PVC stabiliser.

2.4.3. Thermal Co-Stabilisation

If primary and secondary stabilisers are used together PVC thermal stability can be drastically increased and synergistic effects have been seen between some stabilisers (such as Calcium/Zinc stearate systems) (Balkose, Gokcel & Goktepe, 2001). There is another reason why primary and secondary stabilisers need to be used together. Some of the primary stabilisers have the ability to react with the free HCl and form strong lewis acids. These lewis acids are detrimental to the stabilisation process. It is therefore important that free HCl is scavenged by the secondary stabilisers (Zweifel, Maier & Schiller, 2008: 437). Table 2.1 shows that some stabilisers act as both primary and secondary stabilisers, and are known as co-stabilisers. A list of some co-stabilisers can be seen in Table 2.1Table 2.2, which is adapted from (Fink, 2010: 158).

Table 2.2: Examples of some Co-stabilisers.

Co-Stabiliser
Phosphite esters
Epoxy compounds
Poly(ols)
Phenolic antioxidants
1,3-Diketones
Dihhydropyridines
β-Ketocarboxylic acid esters

The mechanism of the synergistic effect of Calcium stearate and zinc stearate is shown in Figure 2.15 (Briggs & Wood, 1971). The calcium stearate acts as a secondary stabiliser as shown in Figure 2.14 is able to react with the zinc chloride, which is formed as zinc stearate acts as a primary stabiliser. This reaction regenerates the zinc stearate which allows further primary stabilisation to occur (Briggs and Wood, 1971).

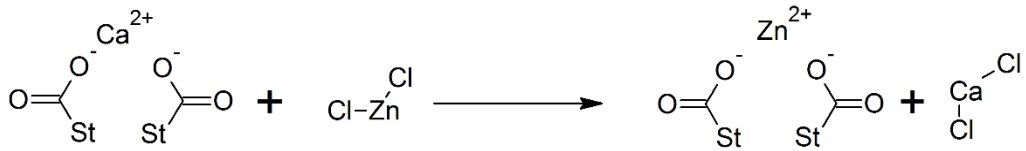

Figure 2.15: Mechanism of the synergism of zinc stearate and calcium stearate.

2.5. Layered Double Hydroxides (LDH) as PVC Thermal Stabilisers

2.5.1. Introduction to LDH's

2.5.1.1. Structure of LDH's

Layered double hydroxides are a class of anionic clays made up of layers of mixed metals. The general structure of a LDH is shown in Figure 2.16.

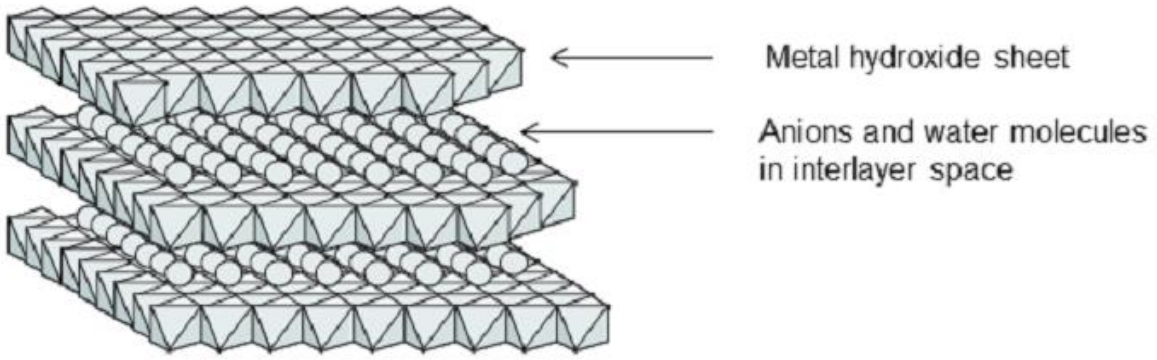

Figure 2.16: General structure of a LDH clay (from Forano *et al*, 2006).

From Figure 2.16 we see the mixed metal hydroxide layers, as well as the anions and water which are intercalated between the layers of the LDH. These clays have the general formula shown in Equation 2.4 (Forano *et al*, 2006). The most prevalent of these LDH's is hydrotalcite, which consists on aluminium and magnesium as the metal cations and carbonate in the interlayer.

$$M^{2+}_{1-x}M^{3+}_{x}(OH)_2X^{q-}_{x/q}nH_2O \qquad (2.4)$$

In Equation 2.4 M^{2+} represents a metal cation with two free valence electrons, M^{3+}represents a metal cation with three free valence electrons and X^{q-} represents the negatively charged interlayer anion.

There are several possibilities with regard to which metals cations be used in LDH's and these are shown in Figure 2.17.

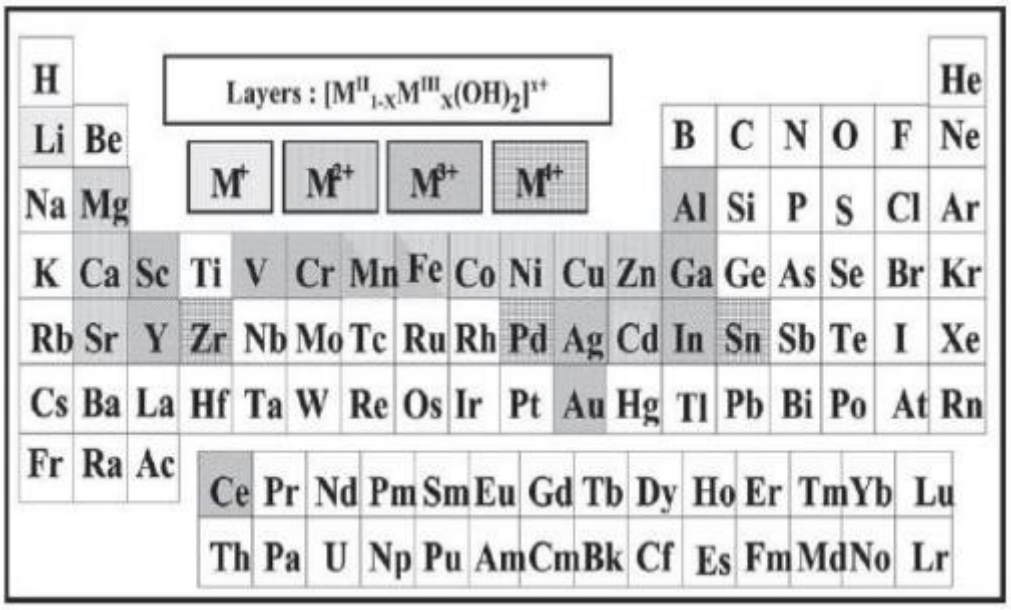

Figure 2.17: Metal cations which can be used to from LDH's (from Forano *et al*, 2006).

The interlayer anion can consist of any negatively charged compound, and is theoretically unlimited (Forano *et al*, 2006). It has been found that LDH's do however have preferences for interstitial ions. The following shows the preferences for some monovalent and divalent interlayer anions in hydrotalcite (Miyata, 1983). $OH^- > F^- > Cl^- > Br^- > I^-$ for monovalent anions and $CO_3^{2-} > NYS^{2-} > SO_4^{2-}$ for divalent anions.

2.5.1.2. Synthesis of LDH's

a) Co-precipitation Method

Co-precipitation is the most common method of LDH synthesis (De Roy, Forano & Besse,2006: 8). It is based on the addition of mixed metal salts (M(II) and M(III)) to a reactor in the correct amounts. This method can be done at constant or variable pH (Crepaldi, Pavan & Valim, 2000). This reactor is filled with water, and a second, alkaline solution is added to the water to maintain the solution's pH. This process leads to the precipitation of the two metallic salts. This method leads to high crystallinity of the particles (Bergaya *et al*, 2006: 1028). A further advantage is that the equipment required is simple.

A sub method of the co-precipitation method is known as the urea hydrolysis method. This method differentiates itself from the co-precipitation method as it uses urea as the alkaline medium solution. At a temperature of 363 K, the urea decomposes into ammonium and carbonate, this then acts as the basic medium as well as the interlayer anion (Zeng, 2009). This method is advantageous as the product is easier to wash, it also leads to having a narrower particle size distribution (Adachi-Pagano, Forano & Besse, 2003).

b) Sol-Gel Technique

The Sol-Gel method, involves forming a mobile colloidal suspension (sol) which then gels (gel) due to the formation of crosslinks within the LDH (Brinker and Scherer, 1990:2). LDH's formed by this method result from hydrolysis and pyrolysis of metal alkoxide solutions (Braterman *et al*, 2004: 383). The metal alkoxides are dissolved in an organic solvent and then water is slowly added to this solution to cause the crosslinking. LDH's formed by this method are known to have higher specific area than those synthesised by the co-precipitation method (Aramendia *et al*, 2002).

c) Mixed Oxide (Reconstruction)

The mixed oxide or reconstruction method involves calcining of mixed metal oxides with a liable interlayer anion (Grey & Ragozzini, 1991). These amorphous oxides are then rehydrated in the presence of the liable anion and LDH forms (Mascolo, 1995). This formation is due to a memory characteristic of the LDH's.

d) Dissolution Precipitation

A dissolution precipitation method of mixed metal oxides/hydroxides has been proposed by Labuschagne *et al* (2006). This method involves dissolving the mixed metal oxides/ hydroxides as well as an anion source into water and subjecting the slurry to elevated temperature and pressure. During this process, the mixed metal oxides may precipitate as a precursor to the LDH and then again dissolve, with the anion intercalating into the interlayer and forming the LDH.

This process has been used to synthesise several different LDH's and has the added advantage of having little to no effluent.

e) Hydrothermal Post-Treatment

LDH's formed by any of the above methods can be hydrothermally treated. This hydrothermal treatment can improve the crystallinity of the resulting LDH's (Forano *et al* 2006). This treatment is done in water and at an elevated temperature. This treatment may also increase the particle size.

2.5.2. Mechanism of PVC Thermal Stabilisation

The LDH's act as secondary stabilisers to PVC, scavenging HCl that evolves during the thermal degradation. Secondary stabilisers have been discussed in section 2.4.2. The specific mechanism for the thermal stabilisation of PVC by LDH's is shown in Figure 2.18: Mechanism by which LDH's scavenge HCl.Figure 2.18 (adapted from Gupta, Agarwal & Banerjee, 2008).

The method by which this scavenging occurs is relatively simple. CO_3^{2-} is easily replaced in the interlayer by the chloride ion, the CO_3^{2-} ion is released as H_2O and CO_2 (Constantino *et al* 1998). This ion exchange is the sole method of stabilisation if standard LDH's are used, if certain anions (these need to be PVC stabilisers, either primary or secondary) are intercalated into the LDH further stabilisation may occur.

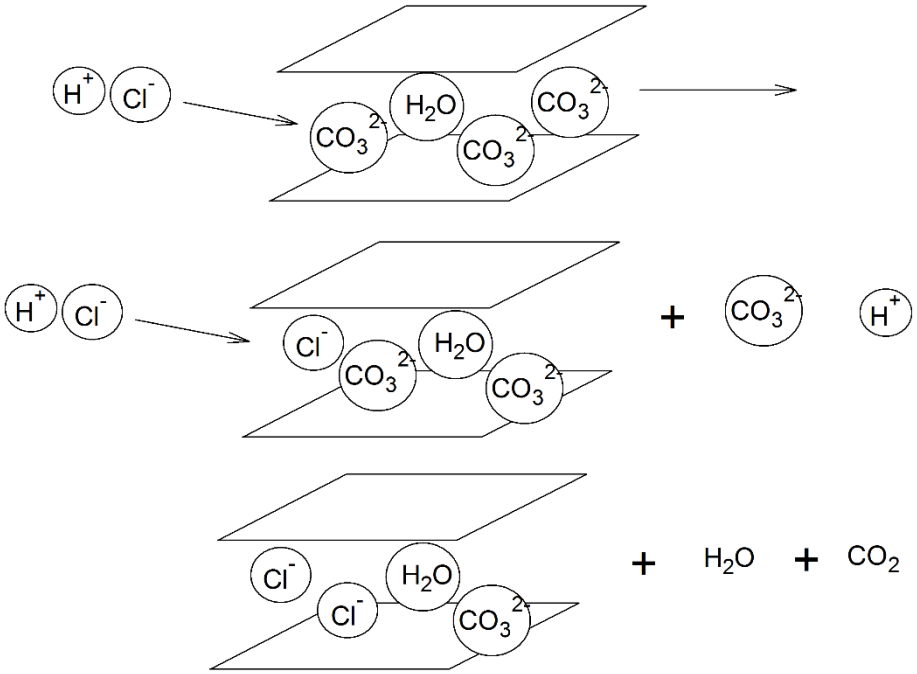

Figure 2.18: Mechanism by which LDH's scavenge HCl.

2.5.3. Factors Affecting Stabilisation

There are several different factors affecting the amount of thermal stability achieved by a LDH. These factors will be further discussed.

2.5.3.1. Mixed Metal Layers

The metals used for the metal layers in the LDH have shown to have an influence on the thermal stability of PVC. Labuschagne *et al* (2015) showed that a Magnesium Zinc Aluminium LDH had better colour stability than the conventional Magnesium Aluminium LDH. They showed further that Magnesium Copper Aluminium scavenged more HCl than the conventional LDH. This study also showed that different metals performed differently in different heat stability tests for flexible PVC.

Calcium Aluminium LDH has also been shown to outperform conventional hydrotalcite with regards to colour change and HCl scavenging (Sauerwien, 2008). Wen *et al* (2012) proved that Zinc Aluminium Lanthanum LDH had a better stabilising effect than other mixed metal LDH's. These above mentioned examples make it clear that the

metals used in the LDH's can have a major effect on their ability to thermally stabilise PVC.

2.5.3.2. Interspacial Anion

The anion intercalated between the mixed metal layers has also been proven to affect the way LDH's thermally stabilise PVC. Gupta *et al* (2008) synthesised a Calcium Aluminium LDH and varied the anion. Several ions were intercalated (NO_3^-, CO_3^{2-}, Cl^-, SO_4^{2-}, PO_4^{3-}) into the LDH, added to PVC and thermally tested. These tests showed that the nature of the anion had a predominant effect on the thermal stability of PVC.

Lin *et al* (2006) formed an Mg-Al-Zn LDH and changed the intercalated anion from carbonate to maleate, and tested the colour change of thermally degraded PVC. They found that the maleate anion drastically improved early colour in the sample, however degraded to black sooner than the LDH with the carbonate anion.

Some other anions that have been intercalated and shown to vary PVC thermal stability include antinomy sulphide (Lui *et al*, 2015), various amines (Xue, Zhang & Zhang, 2014) and a sulphonic acid (Zhang *et al*, 2014).

2.5.3.3. Surface Modification

LDHs are hydrophilic by nature, and PVC is largely hydrophobic, therefore to increase their synergy a surface coating may be added to the LDH. Coatings that have been used to increase the hydrophobicity of the LDH include oleate (Xu *et al*, 2006), alkyl phosphate (Bao *et al*, 2008) as well as stearic acid (Focke *et al*, 2009). This increase in hydrophobicity generally leads to a more uniform distribution of the additive within the polymer matrix.

2.5.3.4. Particle Size

There has been little work into the effect of particle size of LDH's as PVC stabilisers. In his thesis Papino (2010) found that ultra-fine hydrotalcite improved the thermal

stability of PVC over larger platelets. This was however with a PVC formulation that only consisted of PVC resin and a thermal stabiliser. Plasticised formulations may behave differently. Other than this research, there is very little stating how particle size affects PVC thermal stability. Wang & Zhang (2004) mention that the particle size of hydrotalcite plays a critical role in its applications and Miyata & Nosu (1988) state in their patent that a smaller LDH particle size is preferred however no evidence is presented.

This lack of research leads to an opportunity, as most other thermal stabilisers have shown a trend to perform better with decreasing particle size. Lui, Zhao & Guo (2006) showed that a decrease in calcium carbonate particle size increased the thermal stability of PVC. Wypych (2008: 140) also shows that decreasing the particle size of fillers changes the fusion time of PVC.

2.6. Analytical Testing Methods for Thermal Degradation

2.6.1. Hydrogen Chloride Measurement

HCl evolution measurement is normally done by the isothermal heating of a PVC sample and the HCl gas is absorbed in water. The HCl evolution determination is then done by one of the following methods (Wypych, 2008: 230).

2.6.1.1. Potentiometric Titration

For potentiometric titration a change in potential is measured between suitable electrodes, this change in potential can then be used to calculate the amount of HCl in the solution (Grzybkowski, 2002).

2.6.1.2. Argentopotentiometric titration

Argentopotentiometric titration measures a loss of weight of the sample and the potential between two cells are measured; this means that two indications of HCl

evolution are given (Guyot & Benevise, 1962). This method was governed by ASTM D 793-44T however this standard has since been withdrawn (1981).

2.6.1.3. Pehametric titration

The Pehametric or pH-metric method consists of measuring the time taken to neutralise a certain basic compound, this is then used to calculate the concentration of HCl in the solution (Lerke & Szymanski, 1977).

2.6.1.4. Conductometric Measurement

Conductometric measurement involves the dissolving of the HCl gas in distilled water, the increase in conductivity of the water is then measured and this can be translated into a voltage. This can then be used to calculate the amount of HCl dissolved in solution (Arlman, 1954).

Conductometric measurement is the most used of the four methods mentioned above as it is the most sensitive at recording data about HCl evolution in distilled water.

When using the method of isothermal heating and then the measurement of HCl in distilled water, it is important that experimental care is taken to ensure that the results are accurate and that the measurement is correct.

The first important step to take is in insuring that your sample is of the same size, weight and thickness for each experiment. The weight and thickness of the sample important as this will affect how long it takes to reach isothermal heating of the sample.

The next important step in this experimental method is trying to ensure isothermal conditions, this is the hardest to do and there has been some work done to find correction factors for the non-isothermal conditions seen during these experiments (Vymazal *et al*, 1974).

In the past these methods were quite unreliable and it was difficult to get reproducibility of data due to the reasons mentioned above as well as several other experimental

issues. This however is all starting to change as companies like Metrohm have released products like the 895 Professional PVC Thermomat. This product contains 8 sample holders which can then be used to degrade PVC and the HCl evolution calculated. The sample vessels are disposable and all these improvements means that more reliable data can be collected. The Thermomat also tests according to the required standards. Figure 6.1 shows the Metrohm 895 Professional PVC Thermomat.

Figure 2.19: The Metrohm 895 Professional PVC Thermomat.

2.6.2. Colour Change Measurement

The colour change of PVC is usually testing by aging a sample in the oven and then taking out part of the sample and given time intervals to see how the colour has changed. This is normally measured by eye and can be a rather subjective method of viewing colour change. A slightly improved method of doing this type of testing is to use an automatic testing oven, such as the Metrastat 780 Testing oven, where the PVC sample is slowly ejected from the oven, so that the time scale spent in the oven can be viewed on the sample. An example of a sample tested in a conventional oven as well as one tested in a Metrastat automated oven is shown in Figure 2.20. Figure 2.21 shows the Metrastat 780 Testing Oven.

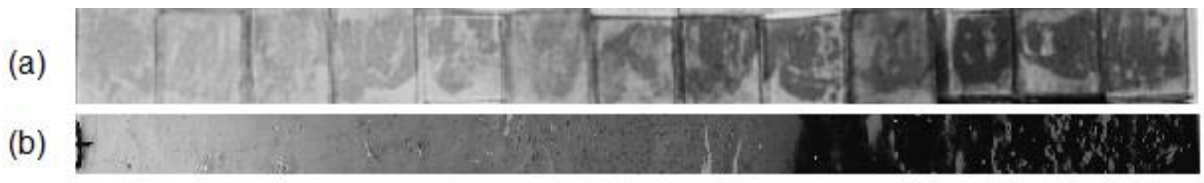

Figure 2.20: (a) Thermally degraded PVC, tested in a conventional oven (Fiaz & Gilbert, 1998), (b) Thermally degraded PVC, tested in an automatic Metrastat testing oven.

Figure 2.21: The Metrastat 780 Testing oven.

A more modernised technique has been developed and used by (Bacaloglu & Stewen, 2001) whereby PVC was degraded in an oven and then scanned in and measured using the Fluoscan program , the RGB colours as well as CIE lab colours were then found and could be used for further analysis. This method is much more accurate however it has a few drawbacks. The first of these drawbacks is the price; it is a very expensive method to get better colour readings. The other drawback is that no kinetic measurements can be made, as samples are first prepared and then only measured after externally (Wypych, 2008: 239).

A device that measured the rate of dehydrochlorination as well as reflectance (a form of colour change) has been used in the past and a patent was applied for such a device (Wypych *et al*, 1985). However no device that directly measures HCl evolution as well as colour change, with regards to CIE Lab or RGB colours has been used.

2.6.3. Torque Rheometer

A torque rheometer, is a batch mixer that measures the torque required to rotate its rotors at a fixed speed, whilst at an elevated temperature. It can be used to evaluate the flow properties of polymers as well as the rate of degradation of polymers (Ari, 2010). The two most popular torque rheometers are the Brabender mixer and the Haake Polylab OS Rheomix. The Haake Rheomix will be further explained. Figure

2.22 shows the basic shape of a torque rheometer chamber, the numbered parts are shown in Table 2.3.

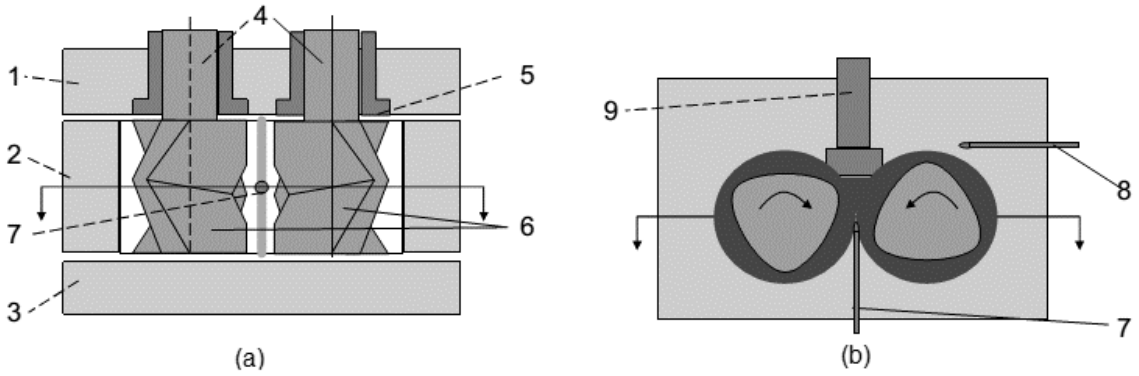

Figure 2.22: Torque rheometer chamber (a) Top view (b) Front View (adapted from Thermo Fischer Scientific).

Table 2.3: Parts list for the torque rheometer.

Part Number	Part
1	Back Section
2	Centre Bowl
3	Front Plate
4	Rotor Shafts
5	Bushings
6	Rotors
7	Melt Thermocouple
8	Control Thermocouple
9	Ram

The back section, front section as well as the centre bowl are all heated, this gives a very even temperature throughout the centre bowl. The rotors then turn at a constant speed and the temperature as well as torque are recorded. The torque curve can then be further analysed to determine the stability of the PVC.

2.6.4. Thermogravimetric Analysis (TGA)

TGA as well as TGA-Mass spectrometry can also be used to test the degradation of PVC. A TGA weight loss curve can be generated and this allows us to see at what temperature volatiles form (Perkin Elmer, 2010). The TGA can be coupled to a mass spectrometer and the volatiles can then be identified. The connection of the mass

spectrometer gives a more complete analysis of the polymer degradation processes (TA Instruments).

2.6.5. Governing International Standards

The following Table 2.4 is a list of governing standards which relate to the dehydrochlorination of PVC as well as the change in colour which is observed during the thermal degradation of PVC.

Table 2.4: A List of the governing standards which regulate the testing of dehydrochlorination as well as colour change of PVC.

Standard	Standard Number	Title
ASTM	D2115-04	Standard Practice for Oven Heat Stability of Poly(Vinyl Chloride) Compositions.
ASTM	D3045-92	Standard Practice for Heat Aging of Plastics Without Load.
DIN EN ISO	305	Plastics - Determination of thermal stability of poly(vinyl chloride), related chlorine-containing homopolymers and copolymers and their compounds - Discoloration method.
DIN	53381-1	Testing of plastics; determination of thermostability of polyvinyl chloride (PVC); dehydrochlorination methods.
IEC	60811-3-2	Methods specific to PVC compounds. Loss of mass test. Thermal stability test.
ISO	182-1	Determination of the tendency of compounds and products based on vinyl chloride homopolymers and copolymers to evolve hydrogen chloride and any other acidic products at elevated temperatures - Part 1: Congo red method.
ISO	182-2	Determination of the tendency of compounds and products based on vinyl chloride homopolymers and copolymers to evolve hydrogen chloride and any other acidic products at elevated temperatures - Part 2: pH method.
ISO	182-3	Determination of the tendency of compounds and products based on vinyl chloride homopolymers and

		copolymers to evolve hydrogen chloride and any other acidic products at elevated temperatures - Part 3: Conductometric method.
ISO	182-4	Determination of the tendency of compounds and products based on vinyl chloride homopolymers and copolymers to evolve hydrogen chloride and any other acidic products at elevated temperatures - Part 4: Potentiometric method.
JIS	K 7103	Testing methods for yellowness index and change of yellowness index of plastics.
JIS	K 7212	Plastics -- Determination of thermal stability of thermoplastics -- Oven method.
JIS	K 7373	Determination of yellowness index and change of yellowness index.

3. Experimental

3.1. Experimental Planning

Some of the factors which alter the effectiveness of LDH's as PVC thermal stabilisers (thoroughly discussed in Section 2.5.3) were investigated. Two important factors that influence this are the particle size of the LDH as well as the mixed metals used in the LDH layers. It was therefore decided to alter these two factors and test how this changed the effectiveness of the LDH's.

The mixed metal layers were altered by changing the reagents used to synthesise the LDH's. Two different mixed metal LDH's were synthesised. The particle size was altered by hydraulically milling the LDH samples. The LDH's were milled to four different particle sizes.

It was decided to leave the LDH samples uncoated. This was done as coating the LDH samples can change several properties of the LDH's. These properties include the surface area, as well as the way the stabiliser interacts with the PVC matrix. The downside of leaving the stabilisers uncoated is that this may reduce the compatibility as well as dispersibility of the stabiliser within the PVC matrix.

The stabilisers were then characterised by several different analytical techniques (including PSA, SEM, BET and XRD). Once characterised the LDH's were incorporated into the PVC matrix by mixing and processing. The LDH's were incorporated into the PVC in three different concentrations, 1, 2 and 5 PHR.

This lead to a total of 25 PVC samples, a total of 24 with the LDH stabilisers present and one sample with no LDH stabiliser.

The PVC samples were thermally degraded by 3 methods (Metrastat testing oven PVC Thermomat and Rheomix torque rheometer) and the stability as well as degradation times of the PVC recorded. Each test was run three times and the standard average

from the runs was calculated. All thermal stability and degradation graphs have this standard average shown, unless otherwise specified (although hard to see in some graphs, this is due to very low error values).

3.2. Stabiliser Preparation

3.2.1. Synthesis of Stabilisers

The LDH-stabilisers were synthesised by a dissolution precipitation method, which is described in Section 2.5.1.2. It was decided that two different mixed metal LDH's would be synthesised, a calcium aluminium LDH as well as a magnesium aluminium LDH. The process for the synthesis of these two LDH was identical, only differing in the reagents used. The reagents used for the MgAl LDH were MgO, $Al(OH)_3$ and $NaHCO_3$, the only difference for the CaAl LDH was the substitution of CaO for MgO.

The mixed metal oxides/hydroxides were added to distilled water in the correct stoichiometric amounts and at a solids concentration of approximately 20%. The mixed metal oxides/ hydroxides were mixed at 160 °C for 5 hours, cooled and the sodium bicarbonate was added as a carbonate source. The mixture was then stirred for a further 2 days at ambient conditions. The exact quantities of reagents used can be found in Appendix 1.

3.2.2. Milling of Stabilisers

The LDH stabilisers were milled in a Netzsch LME1 horizontal disk mill. The operating parameters on the mill were varied to ensure that the required particle size and particle size distributions were achieved. The operating parameters that were varied included the flow rate of the milled sample, the RPM of the mill's internal rotor as well as the amount of time that the sample was milled. A milling curve was generated using magnesium hydroxide (brucite), to determine these factors. The amount of time spent in the mill was decided by the number of passes that the sample made through the mill.

It was found that for the required particle size and particle size distributions the ideal operating conditions were as follows:. The sample flow rate was 2.15 $l.min^{-1}$, the internal rotor speed was 750 RPM and the samples were milled for 0, 1, 2 and 6 passes to achieve 4 separate particle size and particle size distributions. One pass through the mill lasted approximately 90 seconds. The solids concentration was kept constant between 10 and 20 %.

3.2.3. Sample Drying

All the LDH stabiliser samples were filtered in a Buchner type funnel and a pump. Once the filter cakes had formed they were washed three times with water at a ratio of 2:1 (water was added to twice the height of the stabiliser filter cake). This amounted to approximately 750 ml of water being used per wash, a total of 2250 ml being used to wash the sample. The cakes were then dried in an oven at 40 °C overnight.

The dried samples were then broken down to their primary particle size again by using a Kenwood kitchen mixer to break up the filtered sample cake.

3.3. PVC Preparation

3.3.1. PVC Dry Blend Preparation

A PVC dry blend was formulated using the compounds shown in Table 3.1. PVC dry blends were made in 8 kg batches. The PVC was kindly donated by Sasol Polymers, the DINP by Isegen South Africa, the calcium carbonate by Idwala Industrial Holdings Limited and the Ca/ Zn Stabiliser and Plastaid T by Synetica Pty Ltd.

Table 3.1: Formulation of the PVC dry blend.

Component	Grade	Quantity (PHR)	Mass (kg)
PVC	Sasol S7106	100	3.920
Plasticiser	DINP	70	2.740
Filler ($CaCO_3$)	Kulucote-2	30	1.180
Ca/ Zn Stabiliser	Instabex 990	3	0.118
Internal Lubricant	Plastaid T	0.5	0.020
Extra Lubricant	Stearic Acid	0.5	0.020

This PVC dry blend was mixed using a Jones High Speed Mixer. The mixer was filled to approximately two thirds and the dry blend was mixed for 8 minutes. The dry blend reached 70 °C after 4 minutes. It was then blended for a further 4 minutes and the blend reached 80 °C.

3.3.2. LDH Stabiliser Addition

The PVC dry blend was separated into 600 gram batches and the LDH stabilisers were added to the PVC dry blend. This blend was then mixed in a Phillips kitchen blender to ensure that sufficient mixing between the PVC dry blend and LDH stabiliser was achieved. The two components were mixed on the high setting (2) of the blender for 90 seconds. This was repeated at three different loadings of LDH stabiliser, the loadings were 1, 2 and 5 PHR. Appendix 2 shows the sample names, concentrations and quantities of stabiliser added for each sample.

3.3.3. PVC Extrusion

The PVC + LDH stabiliser blend was extruded on a CFam TX 28-P lab extruder, which has four different heating stages. The feed temperature was set to 150 °C, stage two and three were set to 160 °C and 170 °C respectively. The die temperature was set to 180 °C. The extruder speed was set to approximately 130 RPM. The feed speed was set to 4.5 on the dial (maximum of 10). The extruded plastic was then pelletised using a chipper.

3.3.4. PVC Pressing

The pelletised PVC was pressed using a Vertex Press. Experiments were run to find the best conditions for pressing. It was important to optimise these conditions to ensure that the mixing was maximised whilst minimising the amount of thermal degradation. The pellets were placed inside a mould, which measured 100 x 100 x 3 mm and the then placed in the vertex press and pressed for various times, pressures and temperatures. The type of cooling of the mould was also varied. The final operating procedure used was as follows. The PVC was pre-pressed at a pressure of 2 MPa for one minute and then pressed at a pressure of 20 MPa for a further two

minutes. This was done at a temperature of 210 °C and the mould was then force cooled by being clamped between two plates which had cold water circulating through them.

3.4. Analytical Methods

3.4.1. X-ray Diffraction (XRD)

XRD was done on the LDH stabilisers to ensure that the LDH samples had formed correctly and had the correct crystal structure. XRD was also done on the milled samples to ensure that milling did not affect the crystal structure of the stabilisers.
XRD was performed on a PANalytical X-pert Pro powder diffractometer fitted with an X'celerator detector using Fe filtered CoKα radiation (0.17901 nm). The instrument featured variable divergence and receiving slits. The X'Pert High Score Plus software was used for phase identification.

3.4.2. Particle Size Analysis

3.4.2.1. Particle Size Analysis (Wet Samples)

Particle size analysis (PSA) was done on the wet samples after milling to ensure that the correct particle size and particle size distributions were achieved. This was done on a Malvern Mastersizer 3000. The Malvern large volume wet unit was used for PSA. The stirrer speed of the Mastersizer was set to 2000 RPM and no ultrasound was used. Ultrasound was not required as it was expected that very few conglomerates would form whilst the stabilisers were still wet and dispersed in an aqueous solution.

3.4.2.2. Particle Size Analysis (Dry Samples)

Particle size analysis was again done on the LDH stabiliser samples to ensure that they were broken down back into their primary particle size and to ensure that the distribution of the wet and dry samples remained the same.

Dry samples were rewet in a water solution and tested in the Malvern Mastersizer wet unit again.

The Malvern Mastersizer 3000 was again used to conduct PSA testing and the stirrer speed was again set to 2000 RPM. Ultrasound was used on the dry samples, to minimise any conglomerates that had formed. Ultrasound was used continuously at 100 % for 2 minutes prior to measuring the particle size.

These PSA results were more important as the sizes measured here were expected to be the sizes of the particles in the final PVC matrix. For this reason each sample was measured three times to ensure that the method used was in line with ISO 13320. This states that samples must be measured 3 times and that reproducibility must meet specific guidelines. These guidelines state that the coefficient of variance (COV) for the measurement set must be less than 3 % at the D50 and less than 5 % at the D10 and D90. The COV is calculated as the standard deviation divided by the mean multiplied by 100. These guidelines all double when the D50 of the material is less than 10 µm (the LDH samples were all beneath this size).

3.4.3. Brunauer-Emmett-Teller (BET) Surface Area Analysis

BET analysis was done on the LDH stabilisers to determine the surface area of the stabilisers.

BET was done on a Micrometrics Tristar II system and a Micrometrics VacPrep 061 system was used to degas the samples. Nitrogen was used as the adsorptive gas and liquid nitrogen was used as the analysis bath liquid.

3.4.4. Scanning Electron Microscopy (SEM)

SEM was done on the LDH stabilisers to ensure that the initial samples morphology was as expected. The milled samples were also placed under SEM to view how the milling altered the morphology of the stabiliser samples.

The stabiliser samples were stuck to an aluminium sample holder using double sided carbon tape. Any excess stabiliser was removed using compressed air. These sample holders were then placed in the Polaron Equipment E5200 SEM auto-coating sputter system to coat the samples with carbon. The samples were coated twice in two separate directions resulting in a total of 4 coatings.

The samples were then viewed on a Zeiss Ultra plus FEG SEM scanning electron microscope and any interesting images were captured and saved.

3.4.5. Acid Reactivity Tests

A set of acid reactivity tests were devised to observe the rate of reaction of the LDH's with a weak acid. Acetic acid was used as a weak acid. The acids were added to distilled water to a molar concentration of 0.4 M. 2 g of the LDH's were wet with 10 ml of distilled water and 90 ml of the acid solution was then added. The pH was logged for 15 minutes or until the pH was changing by less than 0.01 unit per minute. A few data points were taken at a longer time period to ensure that the reaction had run to completion.

Another 2 g sample of each LDH was also mixed in 100 ml of distilled water to note the pH of the LDH's.

3.5. Thermal Analysis

3.5.1. Hydrochloric Acid Evolution Testing

Hydrochloric Acid Evolution testing was done on a Metrohm 895 Professional PVC Thermomat. The method used followed the guidelines specified by ISO 182 part 3. This reason this method is used is as follows. PVC releases hydrochloric acid when it decomposes at an elevated temperature; this HCl is then flushed from the PVC surface by nitrogen and passed into a measuring vessel where it is bubbled through deionised water. The conductivity of the deionised water changes and is measured. The performance of the PVC is measured by two things, firstly the amount of time

taken for the conductivity curve to start changing (induction time) and secondly the amount of time taken for the conductivity of the water to change by 50 $\mu S.cm^{-1}$ (stability time).

The PVC samples are cut up into pieces measuring no larger than 2 mm and 0.5 ± 0.05 g samples are weighed. The Thermomat temperature was set to 200 °C, the flow of Nitrogen was set to 7 $l.h^{-1}$ and 60 ml of deionised water was used.

3.5.2. Static Thermal Stability Testing

3.5.2.1. Thermal Testing

The static thermal stability testing was done in a Metrastat testing oven. The method used in this test follows ISO 305. The strips were placed in the oven, which was set to 200 °C. The strips are then removed from the oven at a rate of 180 min per 300 mm. Air is constantly circulated in the oven to remove any excess hydrochloric acid, this was circulated at 20 $NI.hr^{-1}$.

3.5.2.2. Photographing Degraded Strips

Degraded PVC strips were then photographed under very specific and constant conditions. A Nikon D60 camera was used, and photos were taken at an exposure time of 1/50 second, f-stop of f5 and an iso speed of 100. The white balance of the camera was set to daylight. The colour space of the camera was set to sRGB. A rig was used to keep the camera at an identical height and two lights were used to light the sample from the sides at an approximately 45 ° angle. Figure 3.1 shows the rig used for the photographs. The light bulbs used were the Phillips MASTER TL-D 90 De Luxe 18W/965 1SL. These bulbs had a colour rendering index of 93 % and had a colour temperature of 6500 K. They are used as standard D65 illuminants.

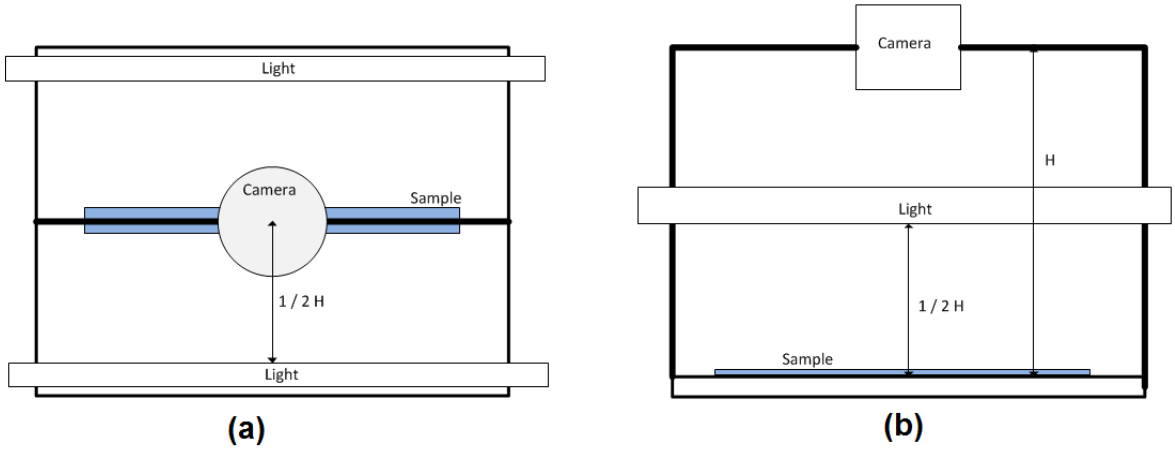

Figure 3.1: Rig used for photographing the samples (a) top view (b) front view.

3.5.2.3. Analysing Photographs

Custom software was developed to analyse the photos of the strips. The software found the red, green and blue (RGB) colour channels of the photos and used those to analyse colour change. Since the white balance of the photos were known and the bulbs used were standard D65 illuminant bulbs, it was possible to convert from the RGB colour space to the CIE-lab colour space. The CIE-lab colour space could then be used to find the yellowing index (YI) of the sample in accordance to ASTM E313. Important points in the YI were found and recorded. The rate of increase of YI was also found and recorded. Figure 3.2 shows the important points that were found in the YI data.

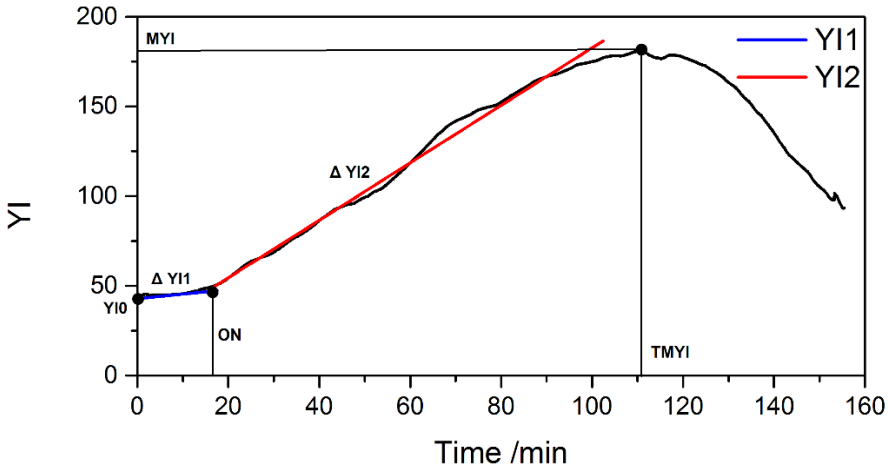

Figure 3.2: Important points in the YI data.

These important points are YI0 (The yellowing index before being placed in the oven), Δ YI1 (the gradient of the first straight line fitted), ON (the onset of degradation), ΔYI2 (the gradient of the second straight line fitted), MYI (the maximum yellowing index and TMYI (the time of the maximum yellowing index).

3.5.3. Dynamic Thermal Stability Testing

Dynamic thermal stability testing was done on a Haake Polylab OS Rheomix torque rheometer, and the method used followed ASTM D 2538-02. The Rheomix rheometer heats a PVC sample to a specified temperature whilst two rotors turn at constant RPM. The torque required to keep the rotors turning at the specified RPM is measured. It is possible to quantify the degradation of PVC using this torque over time data.

The Rheomix torque rheometer had the roller rotors 600 installed, the temperature of the apparatus was set to 200 °C and the rotor speed was set to 50 RPM. 63 g of sample was used. This meant that the loading of the rheometer was 70 %.

The torque curves were then measured and plotted. The torque data was measured and the data was plotted. Important points in the torque data, specified by Jährling (2009) as well as the points specified in ASTM D 2538-02 were found and used to analyse the torque data. These important points in the torque curve are shown in Figure 3.3. The important points are the SP (start point of plateau), ON (onset of degradation), ST (stability time), MT (max torque), TMT (time of max torque), SSP (start of secondary plateau) and ESP (end of secondary plateau).

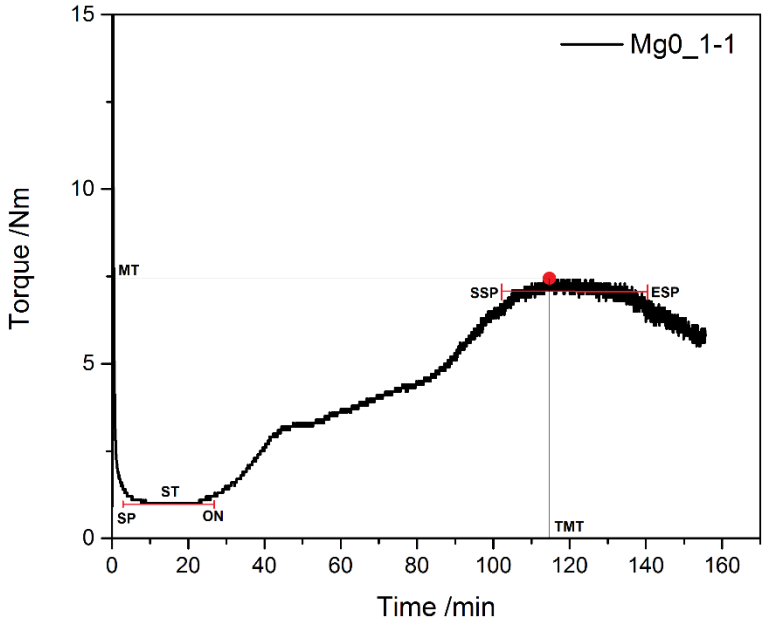

Figure 3.3: Important points found in the Rheomix torque curve.

It is important to note that this method differs from the HCl evolution tests as well as static thermal stability tests in one important aspect. The HCl that evolves in the Rheomix is trapped within the chamber and not removed. The other two tests have methods for removing excess HCl, this is important to note as the presence of HCl can lead to the autocatalytic degradation of PVC.

4. Results

4.1. Analytical Methods

4.1.1. X-ray Diffraction (XRD)

4.1.1.1. Initial Stabiliser XRD

Figure 4.1 shows the X-ray Diffraction patterns for the LDH stabilisers used. The patterns in Figure 4.1 and Figure 4.2 are typical of LDH samples, with tall narrow and symmetrical peaks in the low 2θ range. The d-spacing was then calculated using the XRD peaks. The d-spacing for the MgAl LDH was calculated as 7.61 Å and the CaAl LDH d-spacing was calculated as 7.56 Å. The MgAl LDH did have some unreacted reagents left in the sample, these peaks were identified as $Al(OH)_3$, $MgCO_3$ and $NaAl(CO_3)(OH)_2$ and were only seen in low concentrations. The analysed XRD images can be seen in Appendix 3.

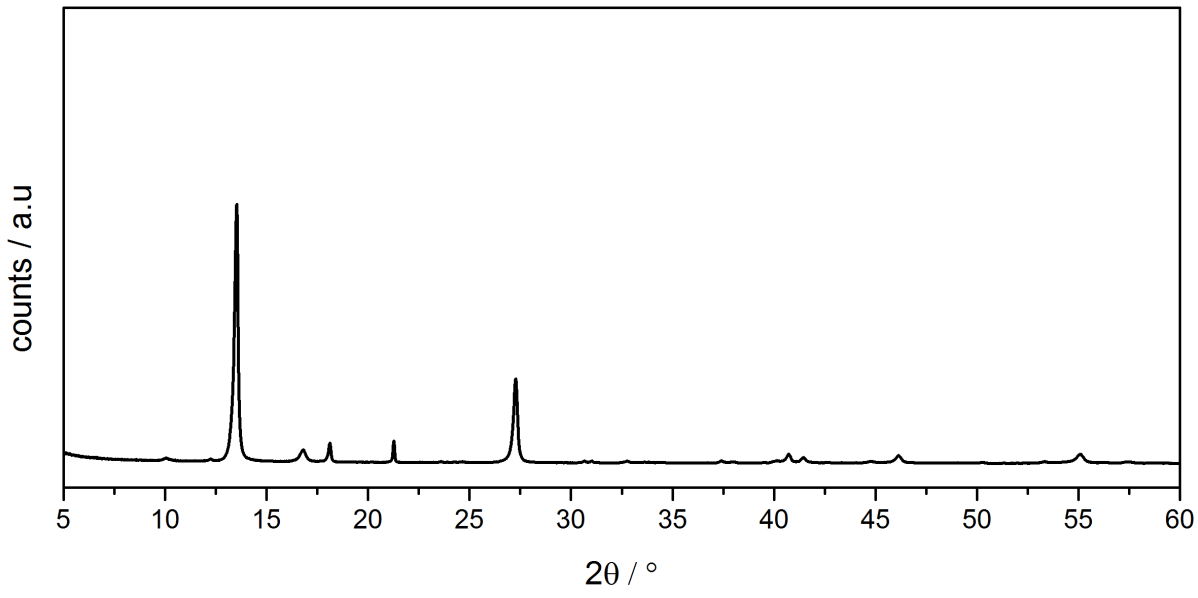

Figure 4.1: XRD patterns for the MgAl LDH stabiliser.

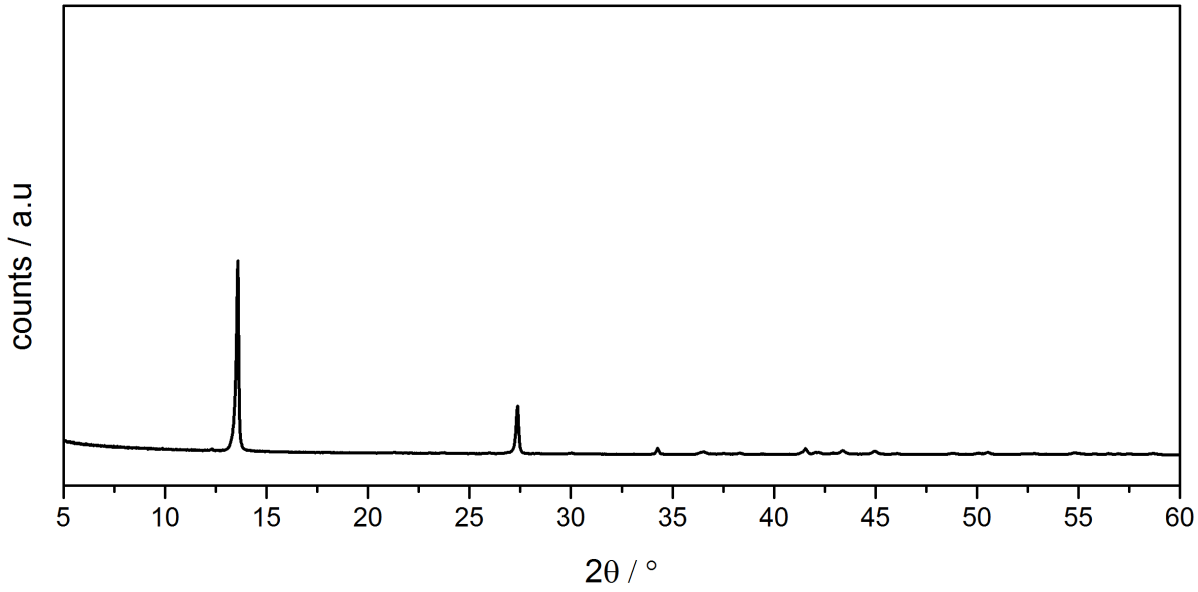

Figure 4.2: XRD patterns for the CaAl LDH stabiliser.

4.1.1.2. XRD on Milled Samples

XRD was also done on the milled samples to ensure that the milling did not damage the crystallised structure of the LDH stabilisers. Figure 4.3 shows the XRD patterns for the milled MgAl samples and Figure 4.4 shows CaAl LDH samples.

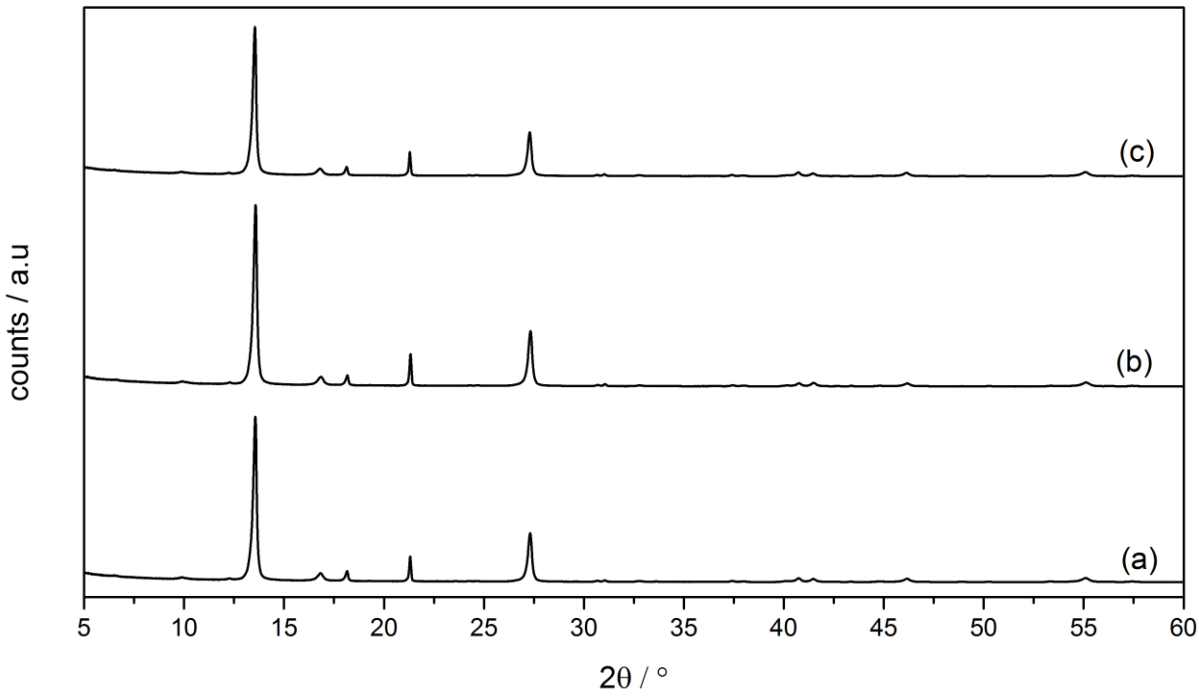

Figure 4.3: XRD patterns for the milled MgAl LDH samples (a) 1 pass through mill (b) 2 passes through the mill (c) 6 passes through the mill.

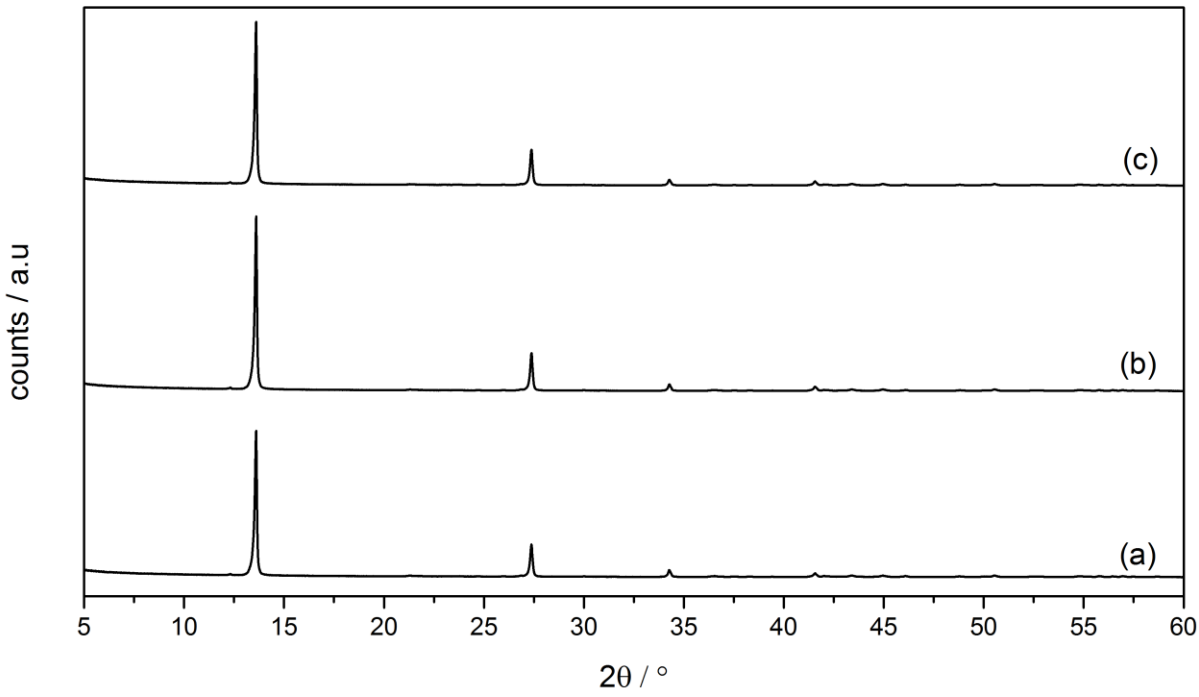

Figure 4.4: XRD patterns for the milled CaAl LDH samples (a) 1 pass through mill (b) 2 passes through the mill (c) 6 passes through the mill.

It is clear that the milled samples are still LDH's as the XRD patterns are very similar, although slight changes in peak heights as well as a few extra peaks were seen. The analysed XRD samples can be seen in Appendix 4. The extra peaks were identified as a zirconium contaminant, which is believed to be from the zirconium oxide beads which were used during milling. This contaminant was seen in low concentrations.

4.1.2. Particle Size Analysis

4.1.2.1. Particle Size Analysis (Wet Samples)

Particle size analysis of the wet samples showed a decrease in particle size with increased milling time as expected. This decrease in particle size can be seen in Figure 4.5 and Figure 4.6. Figure 4.5 shows the decrease in particle size for the MgAl-CO_3 LDH sample and Figure 4.6 shows the decrease in particle size for the CaAL-CO_3 LDH sample.

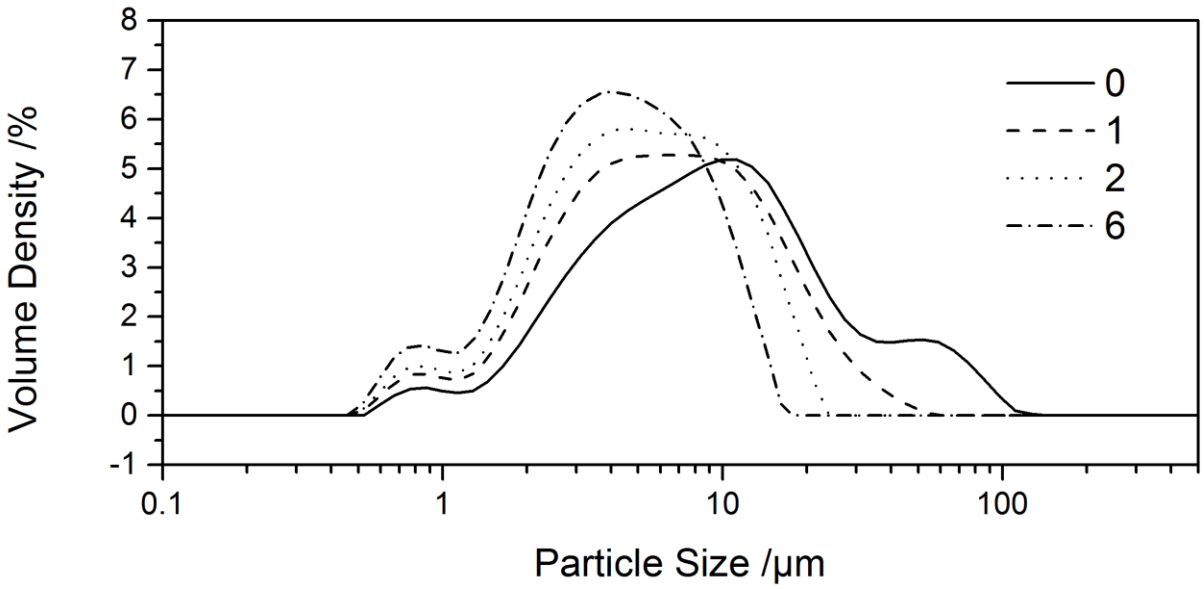

Figure 4.5: Particle size distribution data for the wet MgAl-CO_3 LDH with varying number of passes through the mill.

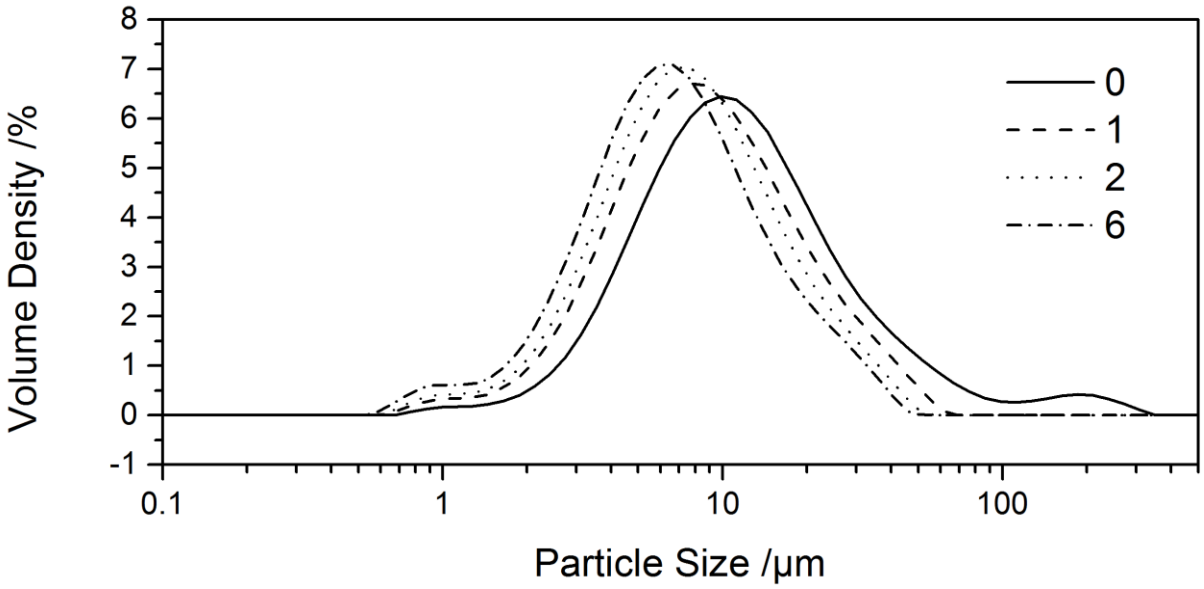

Figure 4.6: Particle size distribution data for the wet CaAl-CO_3 LDH with varying number of passes through the mill.

Table 4.1 shows the D10, D50 and D90 of the LDH samples and analysis of this data makes it clear that the CaAl-CO_3 LDH is mechanically tougher than the MgAl-CO_3 sample, as the CaAl-CO_3 particles are larger even though all the milling conditions were the same for the two samples. It is clear from Figure 4.5, Figure 4.6 and Table

4.1 that the milling process has successfully reduced the particle size of the LDH samples, as the D10, D50 and D90 values have all decreased during milling.

Table 4.1: D10, D50 and D90 values for the LDH samples tested (wet).

Sample	Mill Passes	D10 (µm)	D50 (µm)	D90 (µm)
$MgAlCO_3$	0	2.66	9.4	38.9
	1	2.1	6.5	18.9
	2	1.91	5.49	14
	6	1.54	4.34	10.3
$CaAlCO_3$	0	4.41	11.7	39
	1	3.45	8.98	25.2
	2	3.15	8	21.4
	6	2.7	6.97	19.1

4.1.2.2. Particle Size Analysis (Dry Samples)

Particle size analysis of the dry samples showed a decrease in particle size with increased milling time as expected. It was also noted that some agglomeration had occurred as all the particle sizes had increased. The average particle size distribution for the LDH samples can be seen in Figure 4.7 and Figure 4.8. These figures are for the MgAl-CO_3 LDH sample and the CaAL-CO_3 LDH sample respectively.

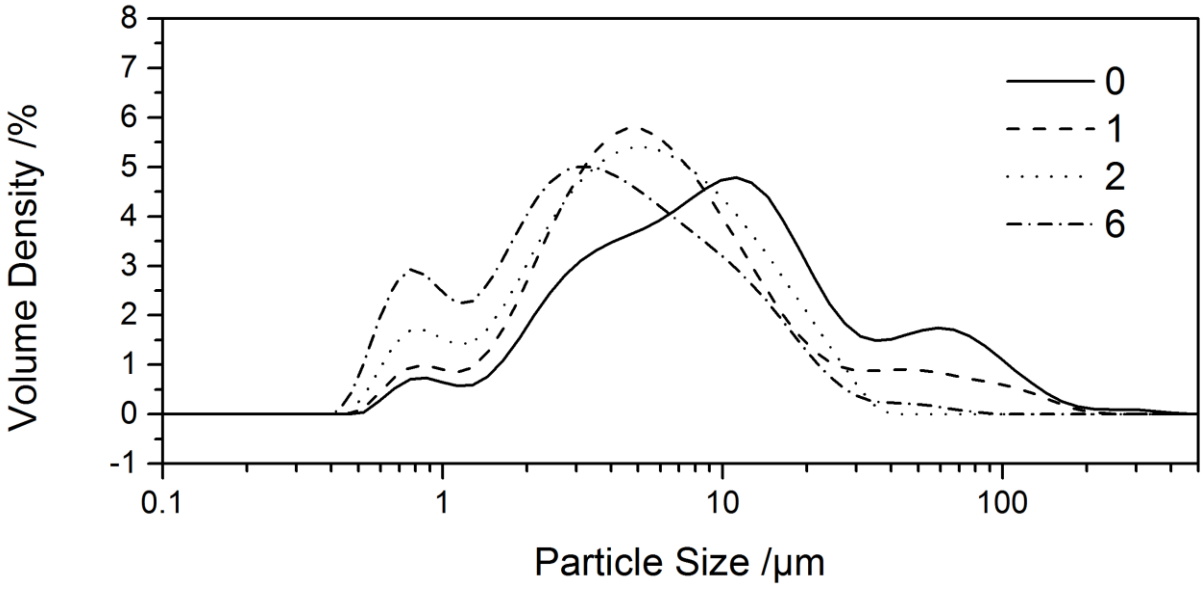

Figure 4.7: Average particle size distribution data for the dry MgAl-CO_3 LDH with varying number of passes through the mill.

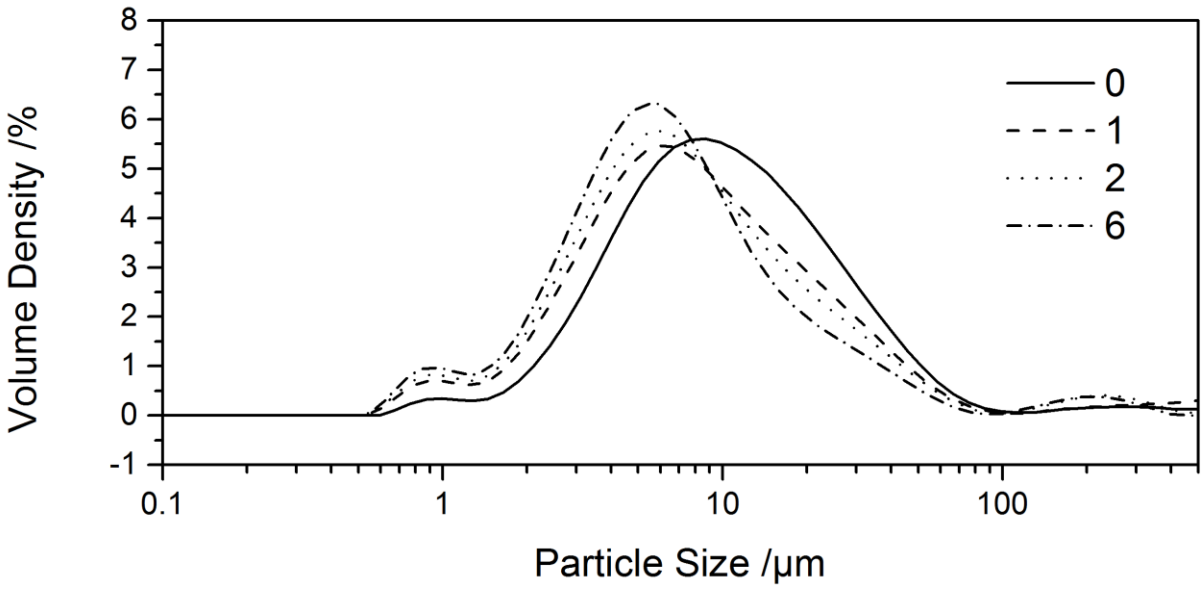

Figure 4.8: Average particle size distribution data for the dry CaAl-CO_3 LDH with varying number of passes through the mill.

It was mentioned in Section 3.4.2.2 that the method used for PSA of the dry samples was slightly different to ensure that ISO standards for laser diffraction particle size analysis methods was met. Table 4.2 shows the mean D10, D50 and D90. The standard deviation as well as the coefficient of variance data can be found in Appendix 5. It is again evident that the particle sizes have decreased with increased milling as D10, D50 and D90 have all changed. It is again evident that the CaAl-CO_3 LDH is mechanically harder than the MgAl-CO_3 LDH. The raw data from the PSA dry runs can be found in Appendix 6.

Table 4.2: D10, D50 and D90 values for the LDH samples tested (dry).

Sample	Mill Passes	D10 (µm)	D50 (µm)	D90 (µm)
$MgAlCO_3$	0	2.48	10.15	60
	1	1.98	5.92	29.9
	2	1.40	5.31	16.4
	6	0.92	3.82	14.3
$CaAlCO_3$	0	3.75	10.53	36.6
	1	2.66	8.27	36.9
	2	2.47	7.47	32.7
	6	2.25	6.53	25.6

4.1.3. Brunauer-Emmett-Teller (BET) Surface Area Analysis

BET analysis of the LDH stabilisers was done and is shown in Table 4.3. This data shows that the milling of the MgAl LDH did not increase its surface area, instead the surface area decreased slightly. The CaAl sample however showed a general increase in surface area with an increase in milling time.

Table 4.3: BET analysis for the LDH stabilisers

Sample	Mill Passes	Surface Area $m^2 . g^{-1}$
$MgAlCO_3$	0	14.6371
	1	14.6038
	2	12.1328
	6	13.7688
$CaAlCO_3$	0	1.93
	1	3.67
	2	3.009
	6	4.413

4.1.4. Scanning Electron Microscopy (SEM)

Scanning Electron microscopy was done on the unmilled and milled LDH stabilisers. For comparative analyses of the milled samples, an overview photo was taken of all samples at 2500 magnification. However this was not sufficient as the primary particle size of the MgAl and CaAl varied significantly. It was therefore necessary to take an additional photo at 8000 magnification. Figure 4.9 shows the CaAl samples at 2500 magnification and Figure 4.10 shows the same samples at 8000 magnification. Figure 4.11 shows the MgAl samples at 2500 magnification and Figure 4.12 shows the same sample at 8000 magnification.

From Figure 4.9 and Figure 4.10 we can see that the particle size of the CaAl LDH has been reduced. At both 2500 and 8000 magnification we can see that average particle size has been reduced. We also notice that there is a lot of small milled particulate matter in the samples that had been milled 2 and 6 times. There was also a reduction in the number of agglomerates in the milled samples. The agglomerates that were still seen, were much smaller and the particles in the agglomerates were much smaller. The MgAl samples also showed a reduction in particle size as well as

a reduction in the number of agglomerates in the sample. This is evident in Figure 4.11 and Figure 4.12

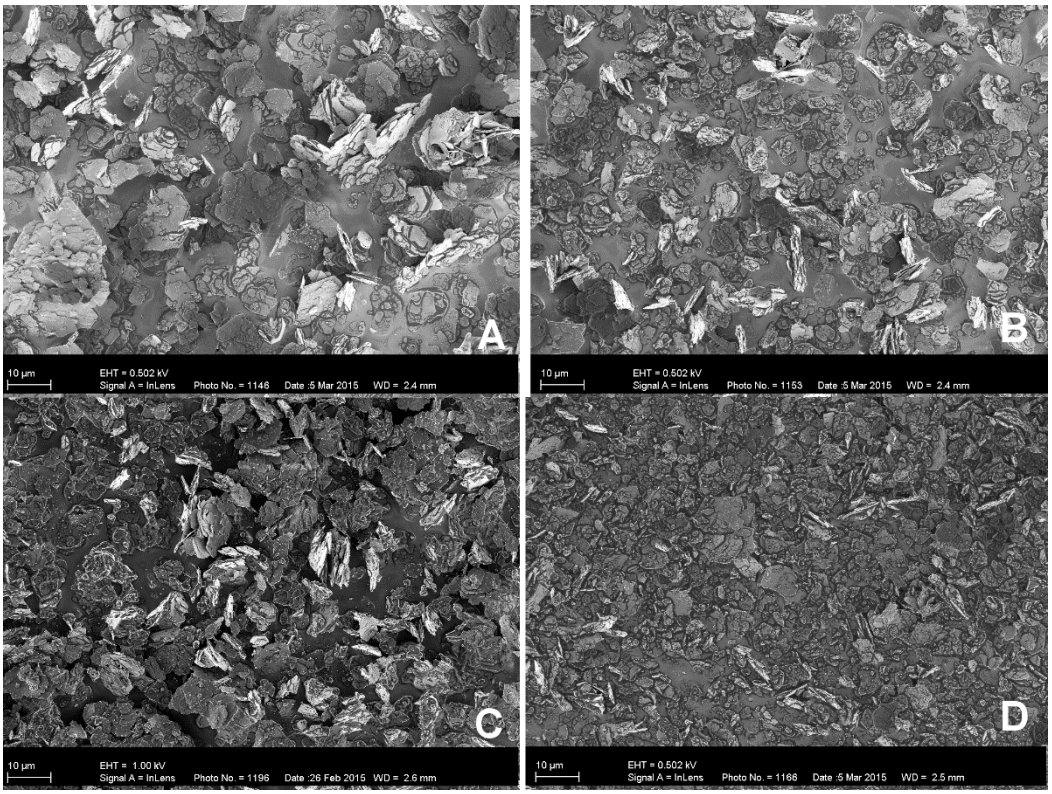

Figure 4.9: SEM images of the CaAl LDH, at 2500 times magnification and different number of mill passes. (A) 0 mill passes, (B) 1 mill pass, (C) 2 mill passes and (D) 6 mill passes

Figure 4.13 shows an example of one of the larger agglomerations in the CaAl unmilled sample. It also shows some of the larger particles that were formed. These large CaAl particles were up to 60 micron in size. Once milled the number of large particles was reduced and few were seen after 6 runs through the mill.

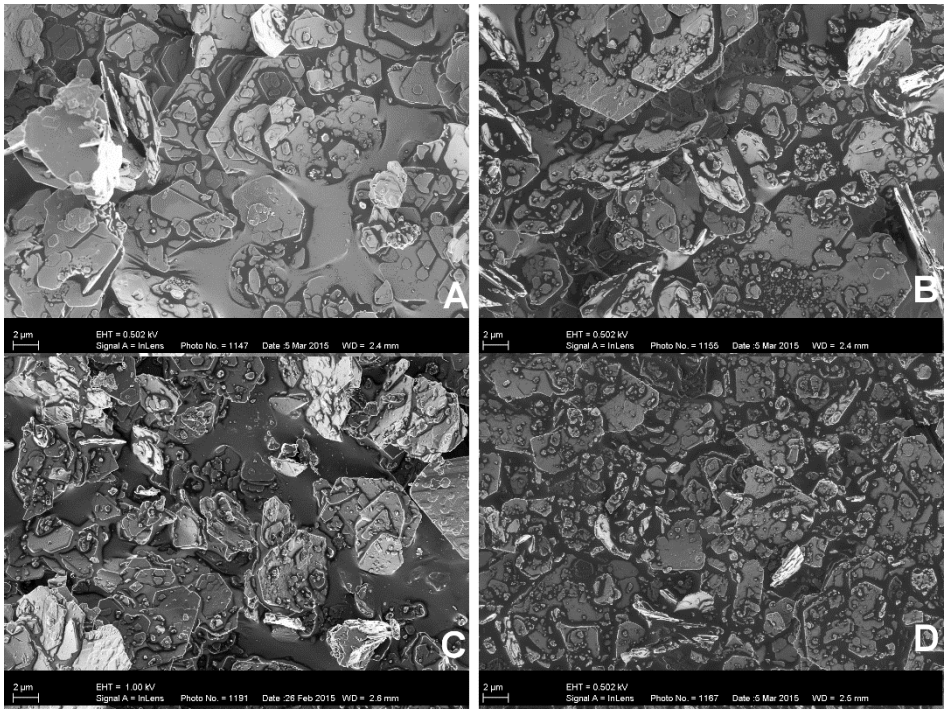

Figure 4.10: SEM images of the CaAl LDH, at 8000 times magnification and different number of mill passes. (A) 0 mill passes, (B) 1 mill pass, (C) 2 mill passes and (D) 6 mill passes.

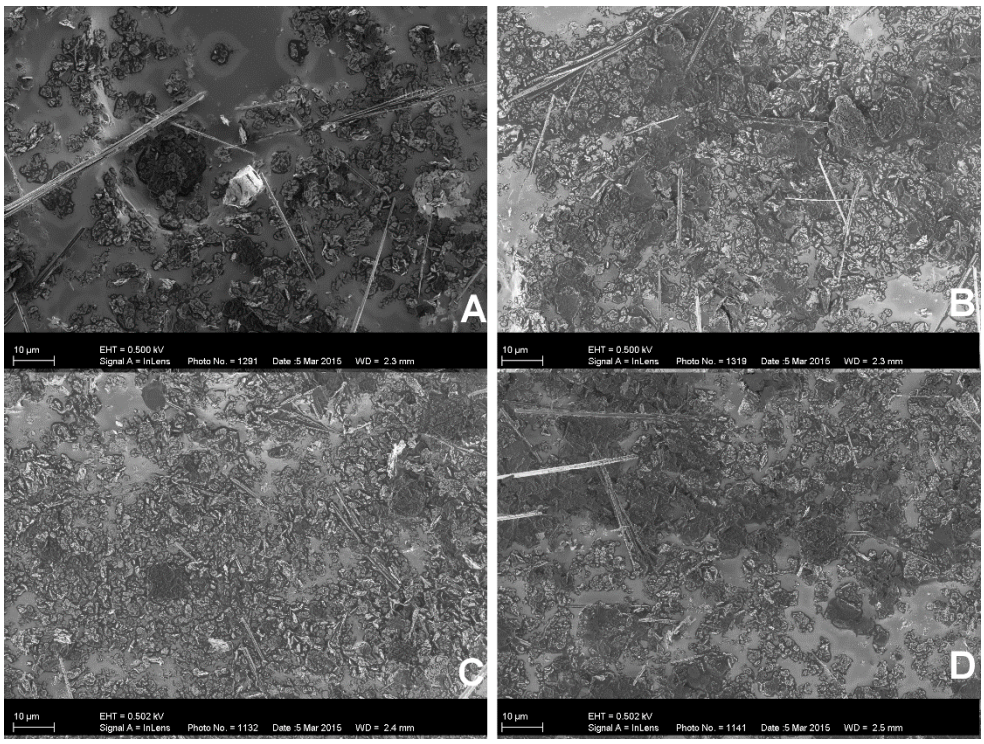

Figure 4.11: SEM images of the MgAl LDH, at 2500 times magnification and different number of mill passes. (A) 0 mill passes, (B) 1 mill pass, (C) 2 mill passes and (D) 6 mill passes.

The SEM images of the MgAl LDH showed that there were also agglomerations, however these were more ordered. This can be seen in Figure 4.14. The SEM images also showed that there were some contaminants in the MgAl samples. The major contaminant was a needle like structure, there were also solid particle contaminants. These contaminants can be seen in the 2500 magnification as well as 8000 magnification photos. A photo was also taken to highlight these contaminants. This can be seen in Figure 4.14

It was also noted that two different configurations of MgAL LDH was formed. The first is the more expected hexagonal platelet shape and the second was a longer thinner platelet shape. These two configurations can be seen in Figure 4.15.

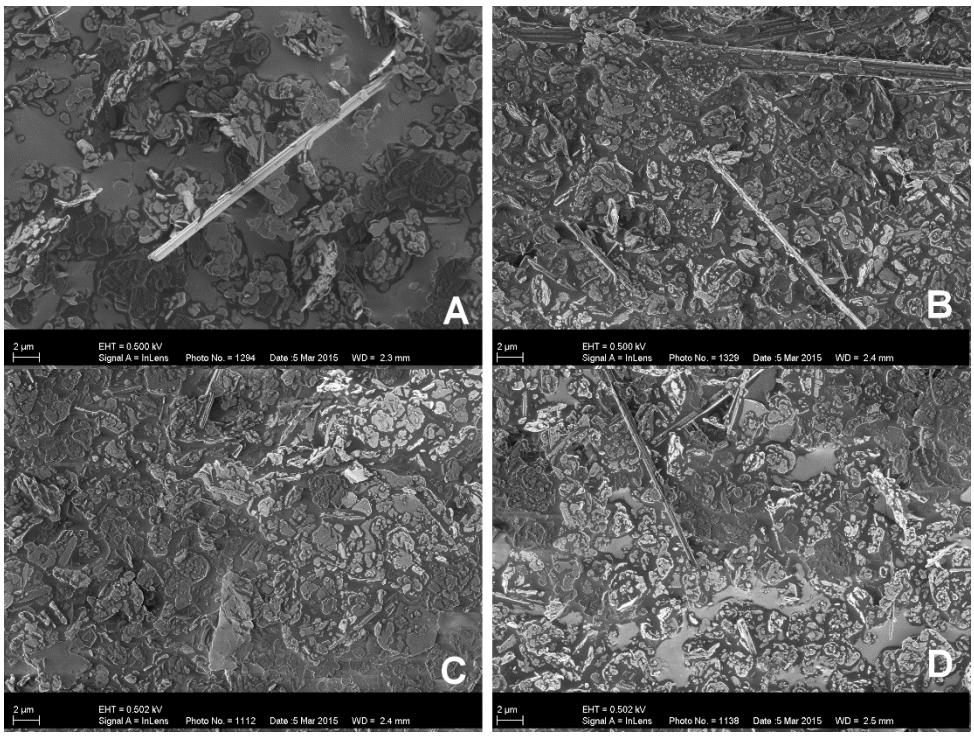

Figure 4.12: SEM images of the MgAl LDH, at 8000 times magnification and different number of mill passes. (A) 0 mill passes, (B) 1 mill pass, (C) 2 mill passes and (D) 6 mill passes.

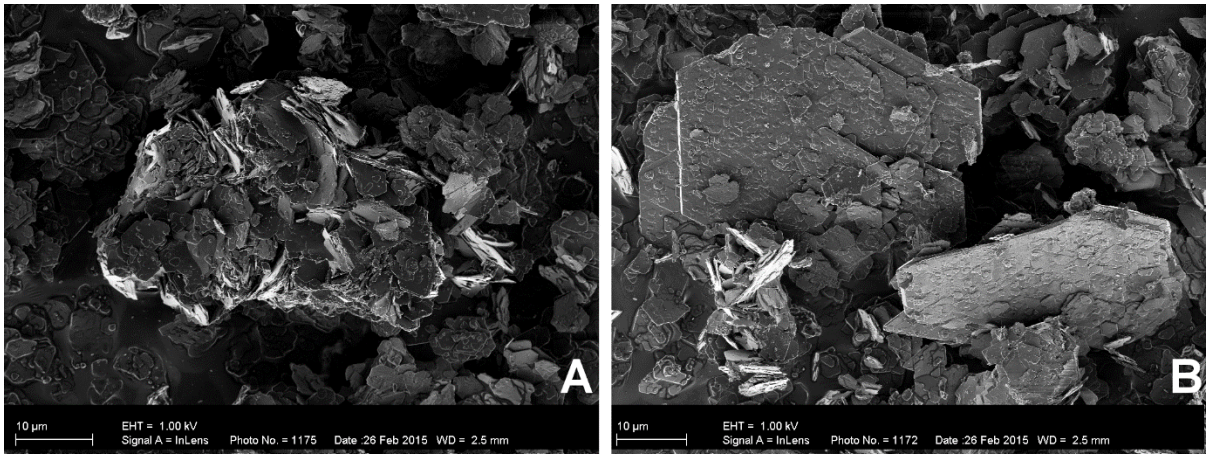

Figure 4.13: SEM images of the CaAl LDH, (A) showing agglomeration of small platelets in and (B) the size of larger platelets.

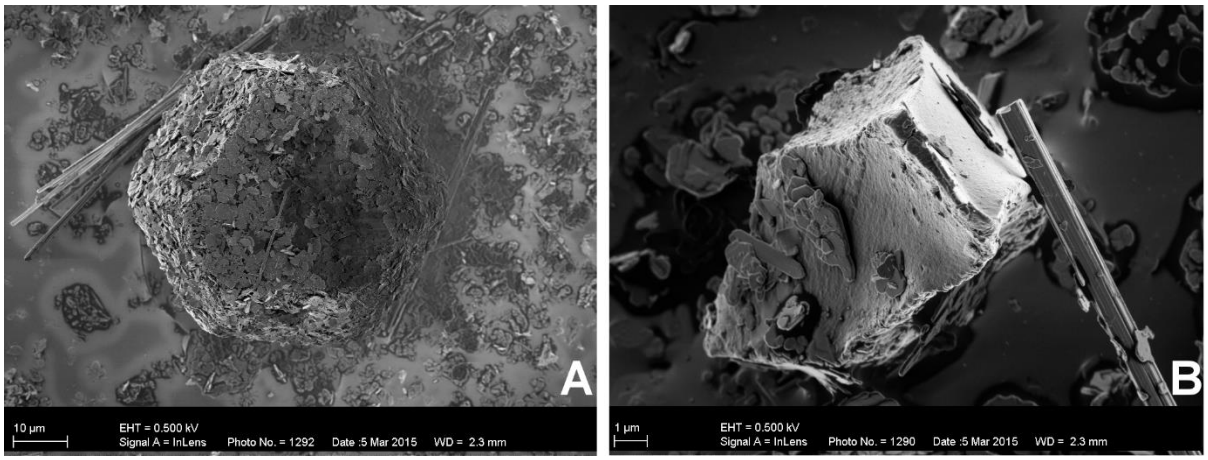

Figure 4.14: SEM images of the MgAl LDH, showing the conglomeration of small particles in (A) as well as some contaminants in (B).

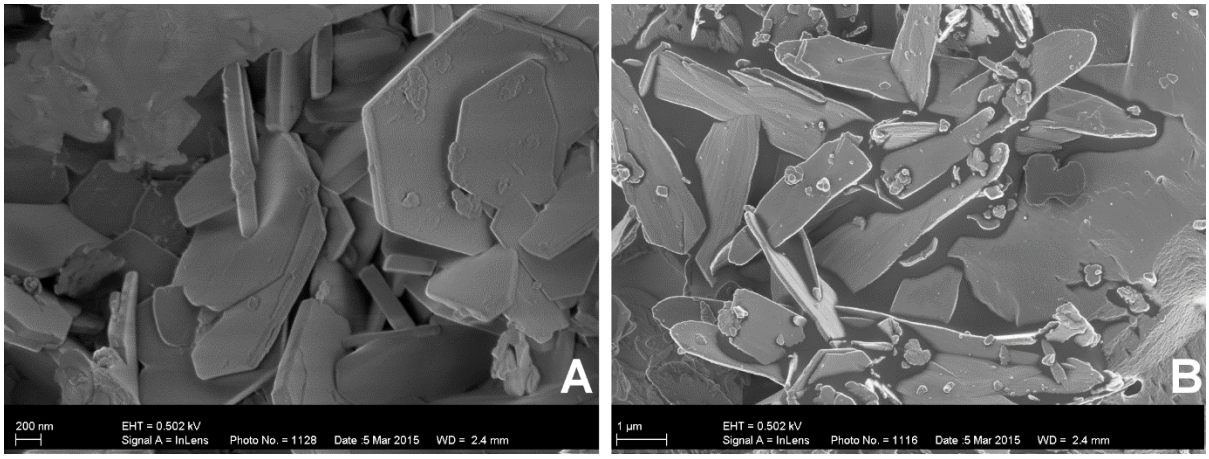

Figure 4.15: SEM images of the MgAl LDH, the formation of two configurations of the MgAl LDH, (A) shows the expected hexagonal platelet structure while (B) shows a long thin platelet.

4.1.5. Acid Reactivity Tests

4.1.5.1. Saturation pH of the LDH's

The saturation pHs for the LDH's in water are shown in Table 4.4. Both the LDH's show a slight increase with pH as the number of mill passes are increased. The CaAl stabiliser also has a much higher pH than the MgAl stabiliser.

Table 4.4: Saturation pH of the LDH's

Stabiliser	Mill Passes	Saturation pH
MgAl	0	9.2
MgAl	1	9.35
MgAl	2	9.48
MgAl	6	9.45
CaAl	0	11.22
CaAl	1	11.37
CaAl	2	11.37
CaAl	6	11.38

4.1.5.2. Weak Acid Reactivity Tests

The weak acid reactivity tests were done with acetic acid. The pH was logged and the results plotted. The plot of the pH can be seen in Appendix 7. It was assumed that the reaction was complete when the pH changed by less than 0.01 per minute. The time

until completion of the reaction is given in Figure 4.16. From this we can note that the CaAl LDH reacted quicker than the MgAl LDH, also that milling slightly reduced the reaction time. The final pH for the weak acid tests is given in Figure 4.17.

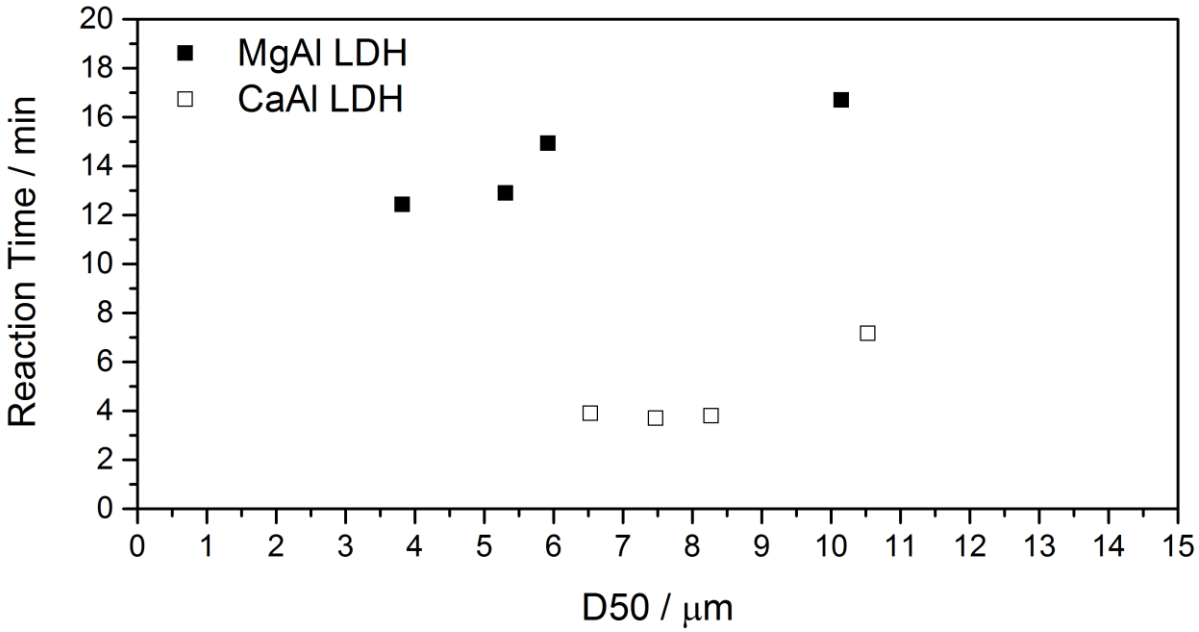

Figure 4.16: Reaction times for the weak acid reactivity tests.

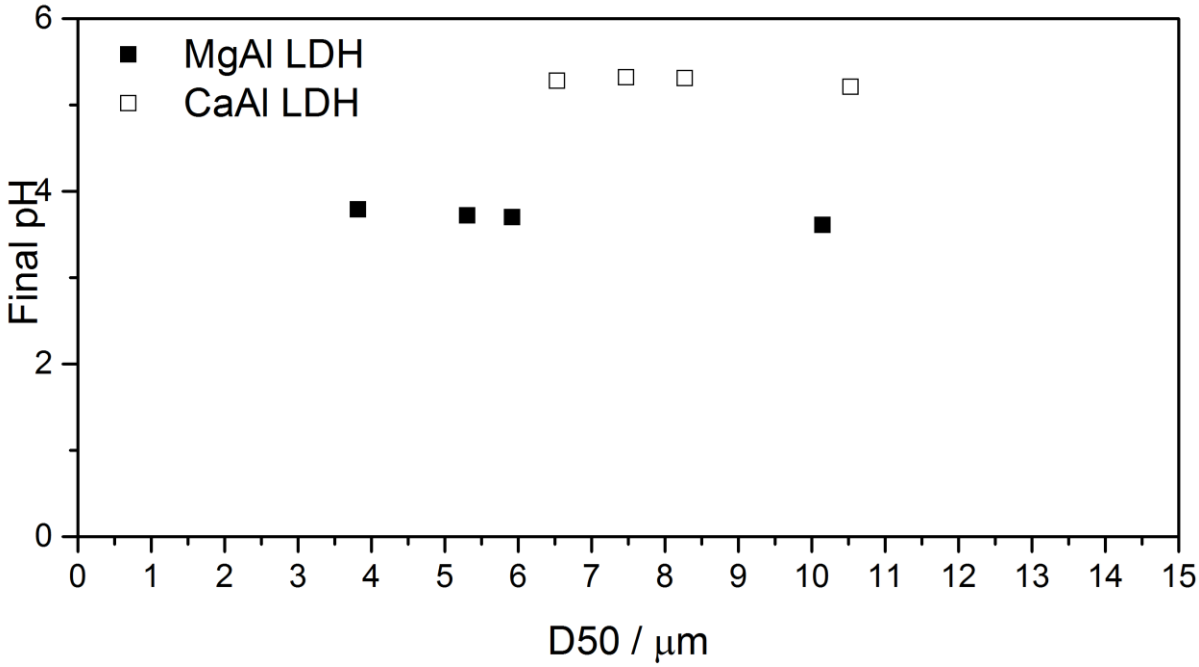

Figure 4.17: Final pH of solution after weak acid reactivity tests.

4.2. Experimental Operating Parameter Determination

4.2.1. Hydraulic Mill

$Mg(OH)_2$ was used to find the correct operating parameters for the hydraulic mill. It was used as it is a similar hardness to the LDH clays that were used. During initial tests the sample flow rate was 2.15 $l.min^{-1}$ and the internal rotor speed was 750 RPM. The samples were passed through the mill 0,1,2,4,8,16 and 16+ (rotor speed increased to 2000 RPM and milled for a further 5 minutes) times. Figure 4.18 shows the particle size distribution for the $Mg(OH)_2$ after variable passes through the mill. From Figure 4.18 we can see that under these milling conditions the $Mg(OH)_2$ was efficiently milled. It was therefore decided to use these operating parameters for milling.

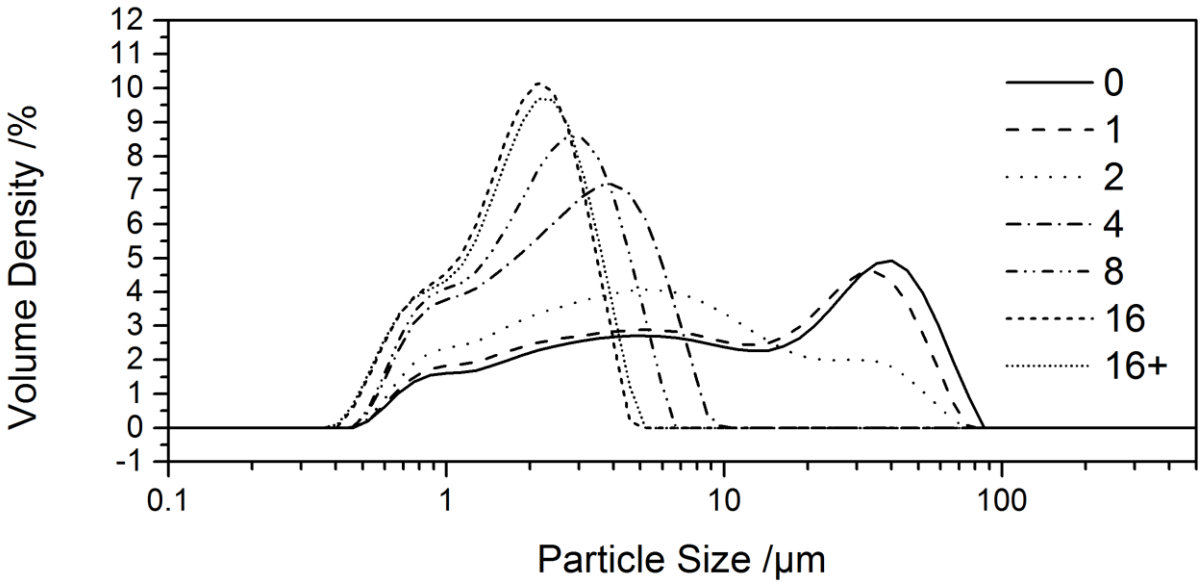

Figure 4.18: Particle size distributions for the milled $Mg(OH)_2$ used for finding operating parameters.

It was also necessary to determine how many passes should be done to ensure a wide range of particle size distributions. Figure 4.19 shows the D50 for the milled $Mg(OH)_2$.

From Figure 4.19 it is clear that the majority of particle reduction occurred between 1 and 6 passes through the mill, for this reason 6 passes through the mill was chosen

as a maximum. An unmilled sample was used as the largest particles. A range of particle sizes was required, to achieve this 1 pass and 2 passes through the mill were chosen. Therefore the number of passes through the mill used for all LDH stabilisers was 0, 1, 2 and 6.

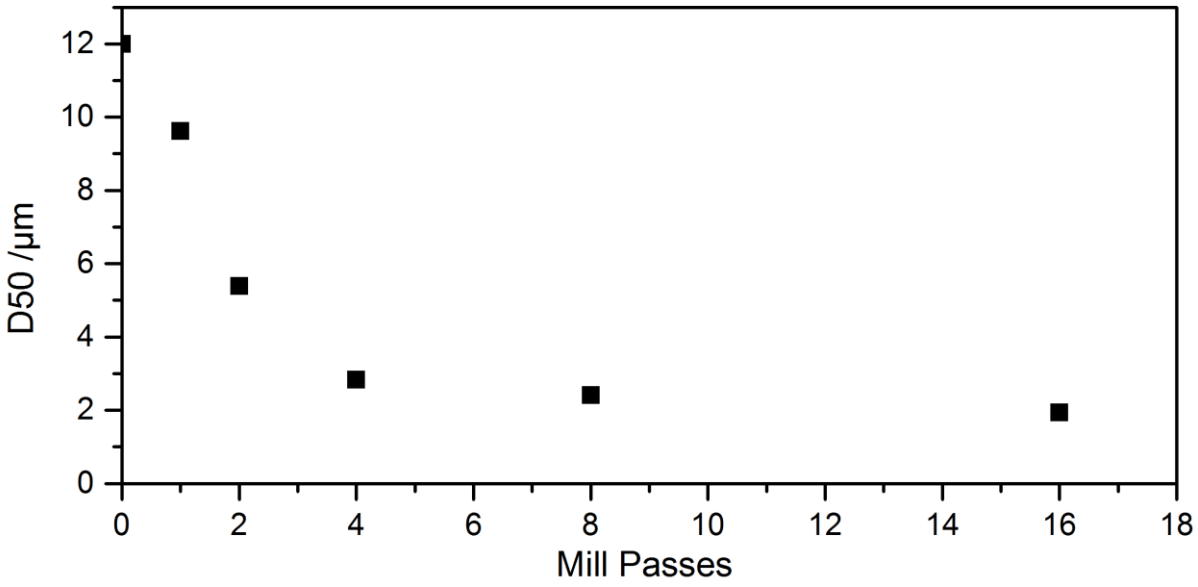

Figure 4.19: D50 for the milled Mg(OH)2 samples used to determine the number of mill passes needed.

4.2.2. Vertical Press

Operating parameters for the Vertex Press also needed to be determined. It was necessary to achieve sufficient mixing without degrading the PVC sample. Several operating parameters were varied to achieve an ideal set of operating parameters. These included the pressing temperature, press pressure, time pressed as well as the cooling method. Table 4.5 shows the set of experiments run, as well as operating conditions for each run, used to find the ideal operating parameters of the press.

Table 4.5: Experimental conditions used to determine press operating parameters.

Sample Name	Press Temperature (°C)	Pre Pressing Conditions	Pressing Conditions	Cooling Method
N1-1	180	2 mPa for 30 sec	20 mPa for 150 sec	Ambient
N1-2	180	2 mPa for 45 sec	20 mPa for 300 sec	Ambient
N1-3	190	2 mPa for 30 sec	20 mPa for 180 sec	Ambient
N1-4	190	2 mPa for 30 sec	20 mPa for 300 sec	Ambient
N1-5	200	2 mPa for 30 sec	20 mPa for 180 sec	Ambient
N1-6	200	2 mPa for 30 sec	20 mPa for 180 sec	Forced
N1-7	210	2 mPa for 30 sec	20 mPa for 180 sec	Forced
N1-8	210	2 mPa for 30 sec	20 mPa for 90 sec	Forced

Figure 4.20 shows the pressed samples used to find the ideal operating parameters for the vertex press. From Figure 4.20 we can see that sample N1-7 is the best mixed of all the samples. It has degraded slightly more than the other samples due to the higher pressing temperature. Sample N1-8 was pressed under the same conditions but for a shorter time period, we can see that it is not as well mixed as the pellet boundary is more visible. The conditions used for N1-7 was therefore used for the pressing of samples. The pre pressing time was however increased to one minute and the main pressing was reduced to two minutes. This proved to be an effective set of parameters as pressed samples proved to be well mixed and only slightly degraded.

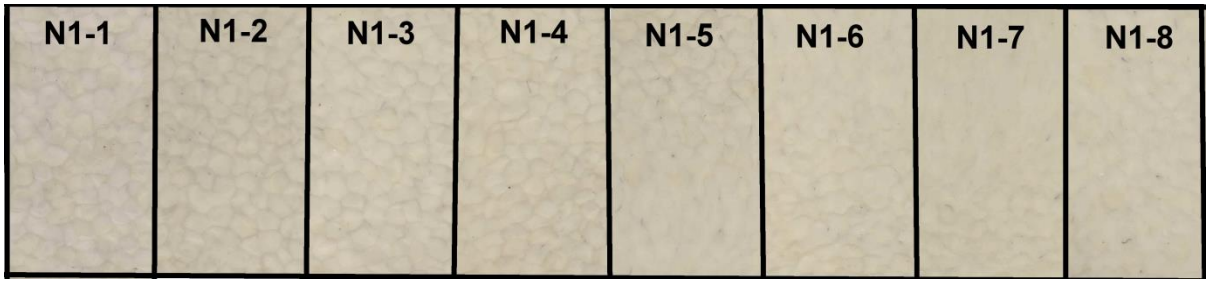

Figure 4.20: Images of the different samples used to determine the ideal parameters for pressing.

4.3. Thermal Analysis

4.3.1. Thermal Degradation during Processing

The different stabilisers degraded with significant differences during processing. The colour change of the MgAl LDH stabilised PVC is shown in Figure 4.21 and the colour change of the CaAl LDH stabilised PVC is shown in Figure 4.22. These figures also give the yellowing index of the sample after processing. The MgAl stabilised PVC showed very little difference in degradation when loading or number of mill passes was varied, however the CaAl LDH stabilised samples showed major variations in degradation.

The colour of the PVC without a LDH stabiliser is shown in Figure 4.23. Addition of any LDH has increased the YI to some extent.

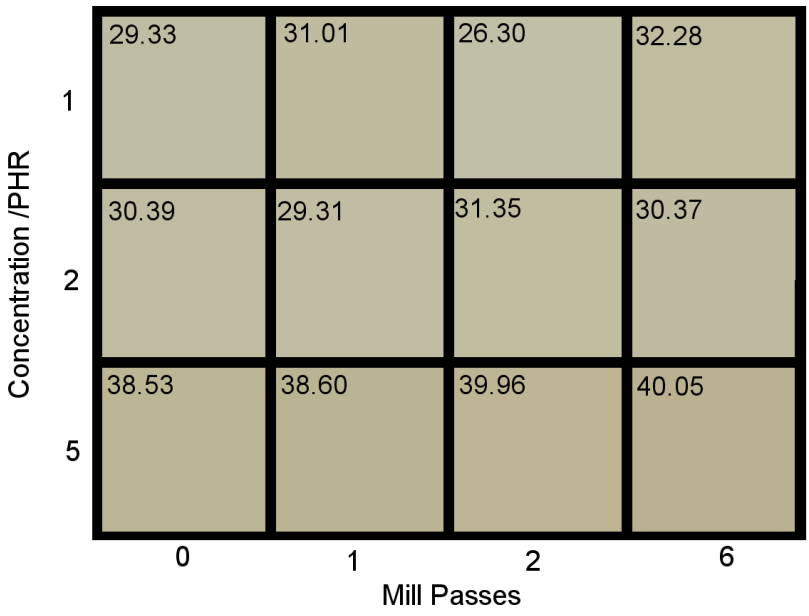

Figure 4.21: Colour of the PVC stabilised with MgAl LDH after processing.

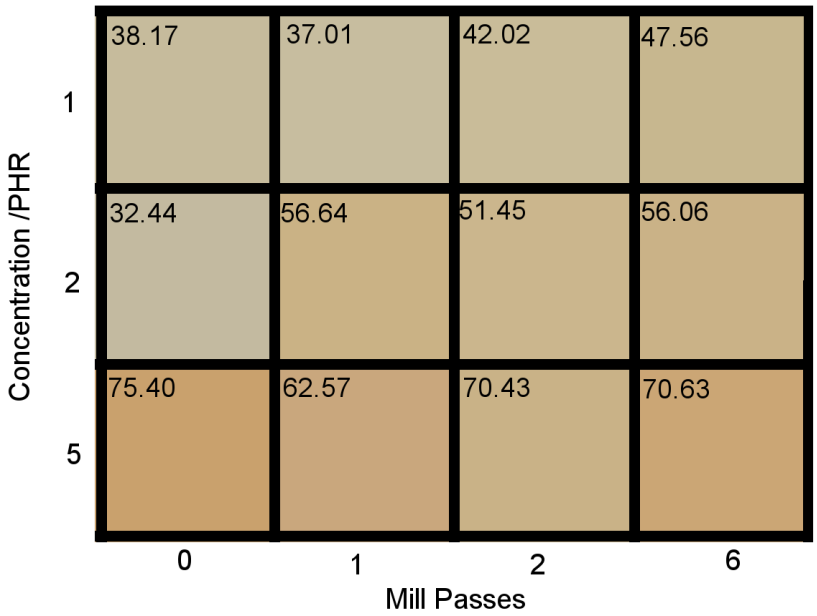

Figure 4.22: Colour of the PVC stabilised with CaAl LDH after processing.

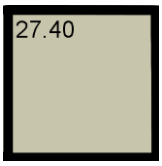

Figure 4.23: Colour of the PVC with no LDH stabiliser.

4.3.2. Hydrochloric Acid Evolution Testing

The hydrochloric acid evolution tests were done on the Metrohm 895 Professional PVC Thermomat (Rancimat). The degradation time of PVC can be found by the amount of time required for the conductivity to change by 50 $\mu s.cm^{-1}$. This change of conductivity can be plotted and this can be seen in Figure 4.24 which shows the change of conductivity of the MgAl stabiliser , loaded at 1 PHR , at different number of mill passes. The remaining graphs of the conductivity can be seen in Appendix 8.

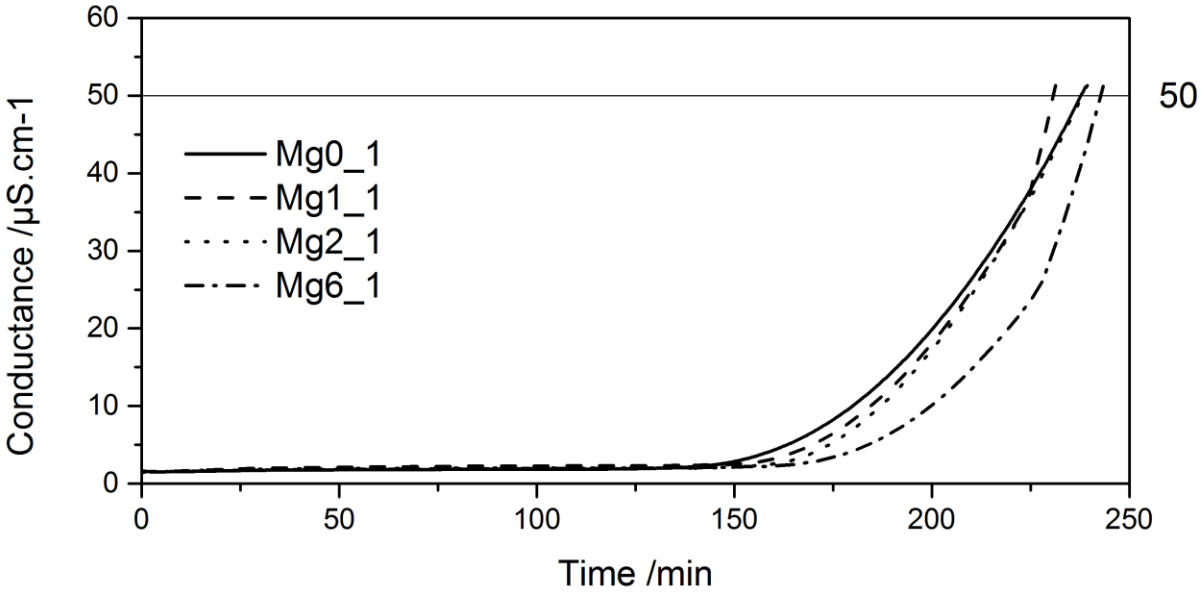

Figure 4.24: Conductivity graphs for the MgAl LDH stabiliser at a loading of 1 PHR at different number of mill passes.

The most important information that can be extracted from the conductivity curves shown in Figure 4.24 is the degradation time. Figure 4.25, Figure 4.26 and Figure 4.27, shows the degradation times at different particle sizes for the two LDH stabilisers at 1, 2 and 5 PHR respectively. The particle sizes shown in the below figures are for the D50 of the samples.

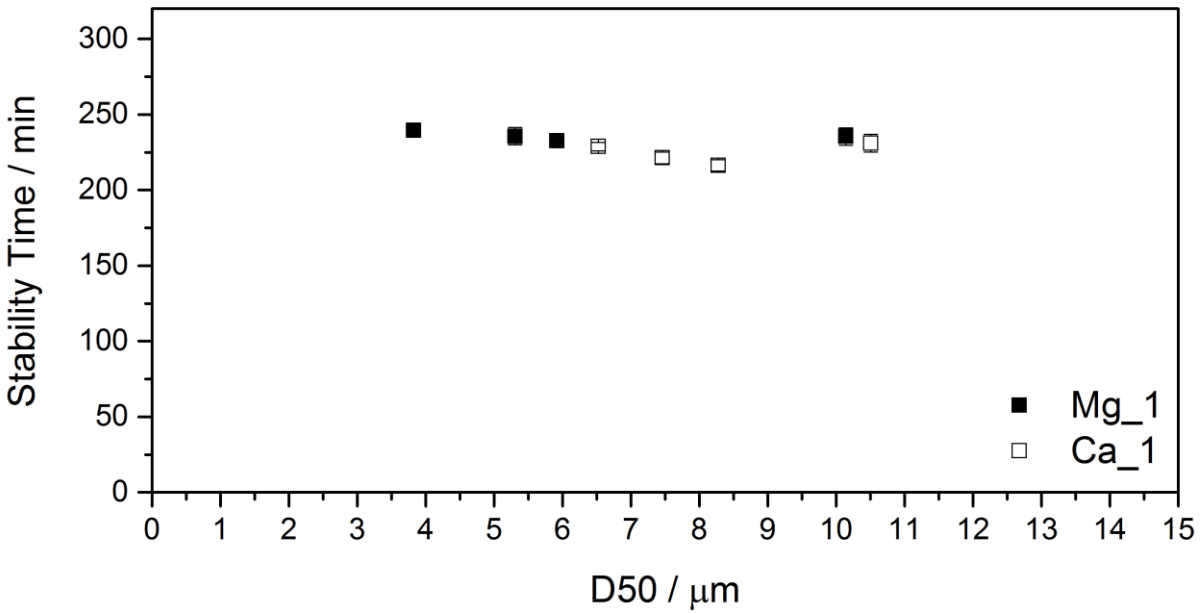

Figure 4.25: Rancimat degradation times for different particles sizes of the two LDH stabilisers, above results are for 1 PHR of stabiliser.

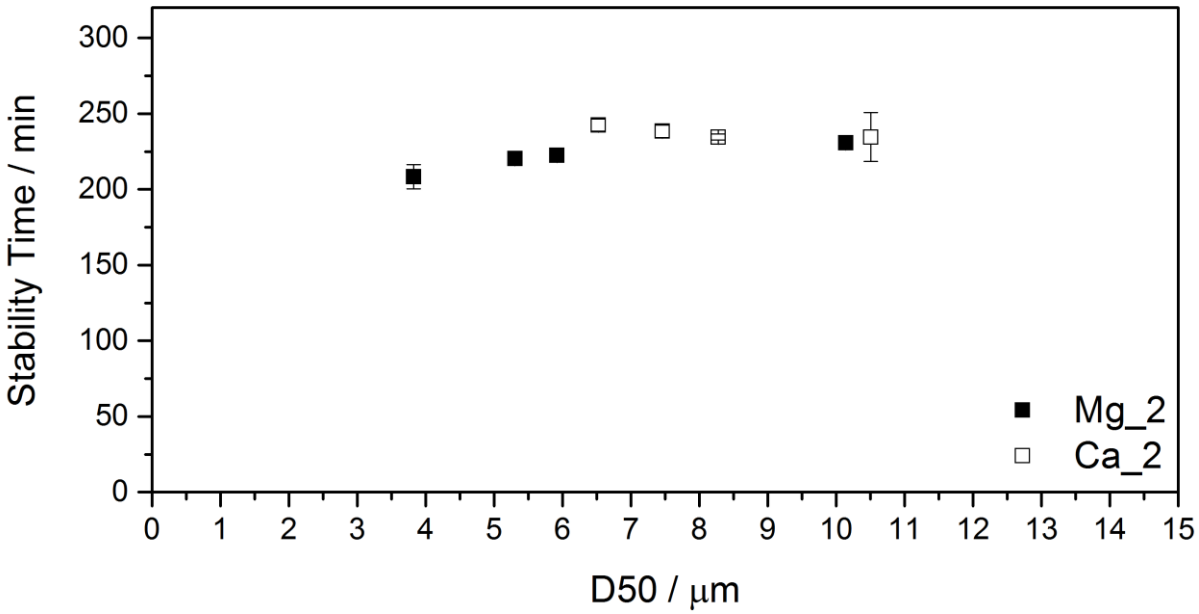

Figure 4.26: Rancimat degradation times for different particles sizes of the two LDH stabilisers, above results are for 2 PHR of stabiliser.

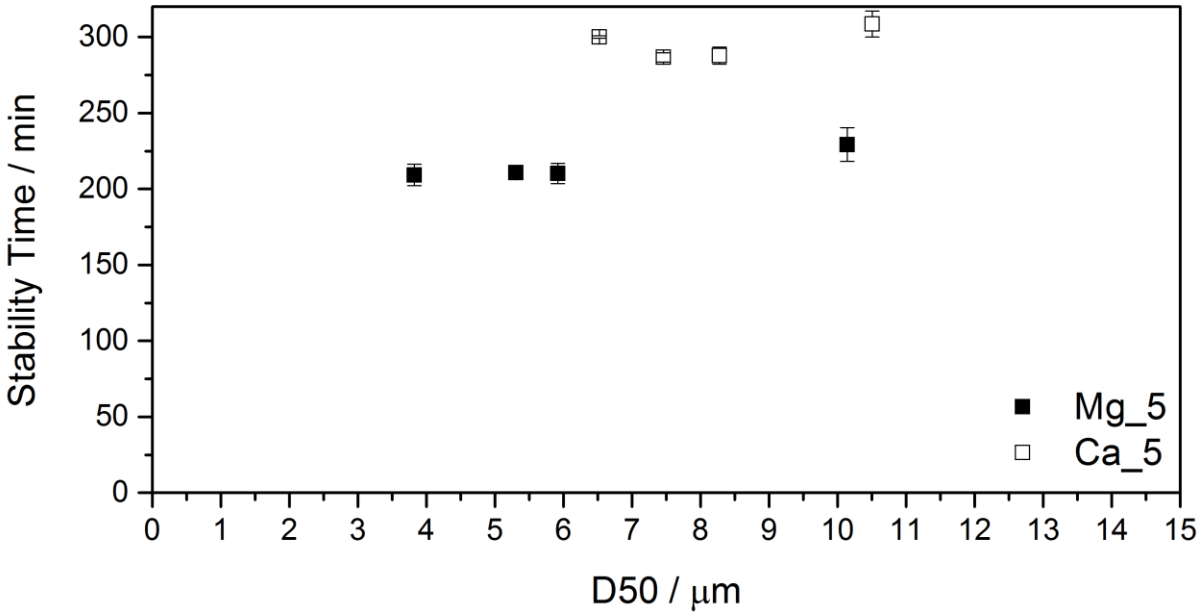

Figure 4.27: Rancimat degradation times for different particles sizes of the two LDH stabilisers, above results are for 5 PHR of stabiliser.

From Figure 4.25, Figure 4.26 and Figure 4.27 we can see that the milling of the LDH stabilisers did not increase the degradation time. The general trend that can be noted is that the degradation time decreased when the sample was milled, however amongst

the milled samples, the smallest sample did best. The smallest milled stabiliser was often comparable in stability time to the unmilled stabiliser.

We can also note that the degradation time for the CaAl LDH increased with an increase in concentration, whilst for the MgAl LDH, the degradation time remained approximately constant (slight decrease) as the concentration was increased. This result is confirmed in Figure 4.28 which shows the Rancimat degradation times in minutes for the two LDH stabilisers (unmilled) at different concentrations. Figure 4.28 also shows the stability time for the PVC with no LDH in the polymer matrix. It is evident from Figure 4.28 that both the MgAl LDH and the CaAl LDH drastically outperformed the polymer with no LDH.

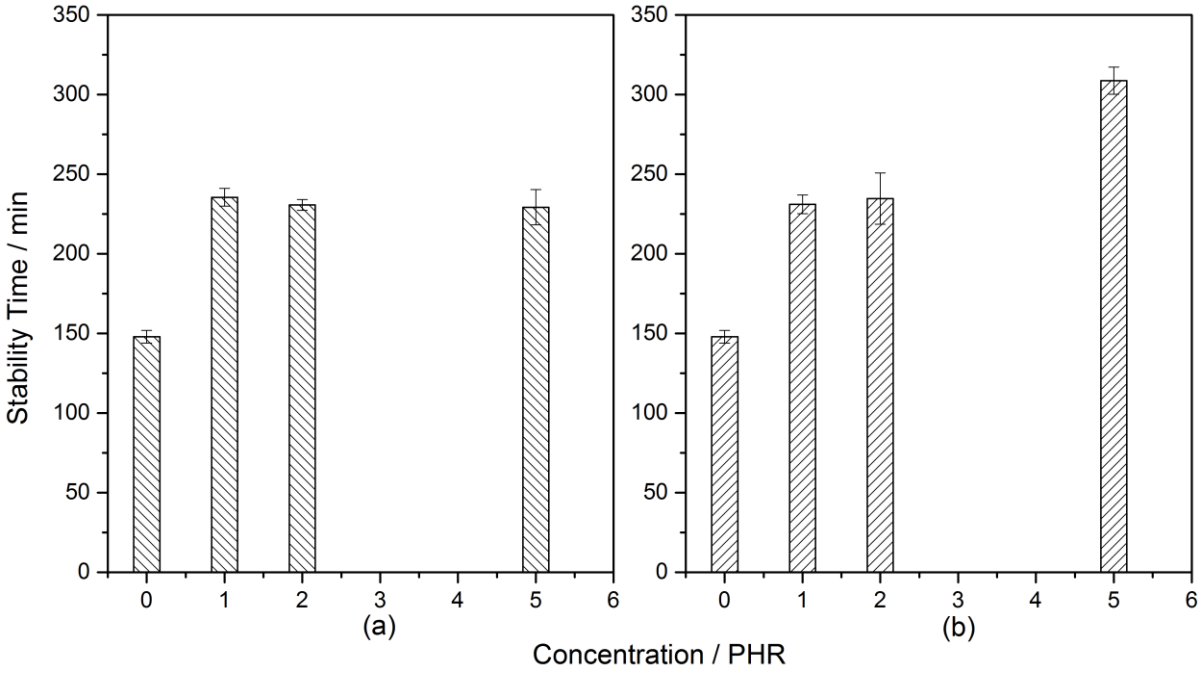

Figure 4.28: Rancimat degradation times for the unmilled LDH stabilisers at different concentrations for (a) MgAl LDH and (b) CaAl LDH.

4.3.3. Static Thermal Stability Testing

Static thermal stability was done in a Metrastat testing oven. Section 3.5.2.3 shows all the points and data that was analysed using custom software. Of this data, the most important points are the onset of degradation (taken as the stability time) and the time of the maximum yellowing index (taken as the degradation time). Figure 4.29, Figure

4.30 and Figure 4.31 show the stabilisation times at different particle sizes for the two LDH stabilisers at 1, 2 and 5 PHR respectively.

Images of the burned strips can be found in Appendix 9.

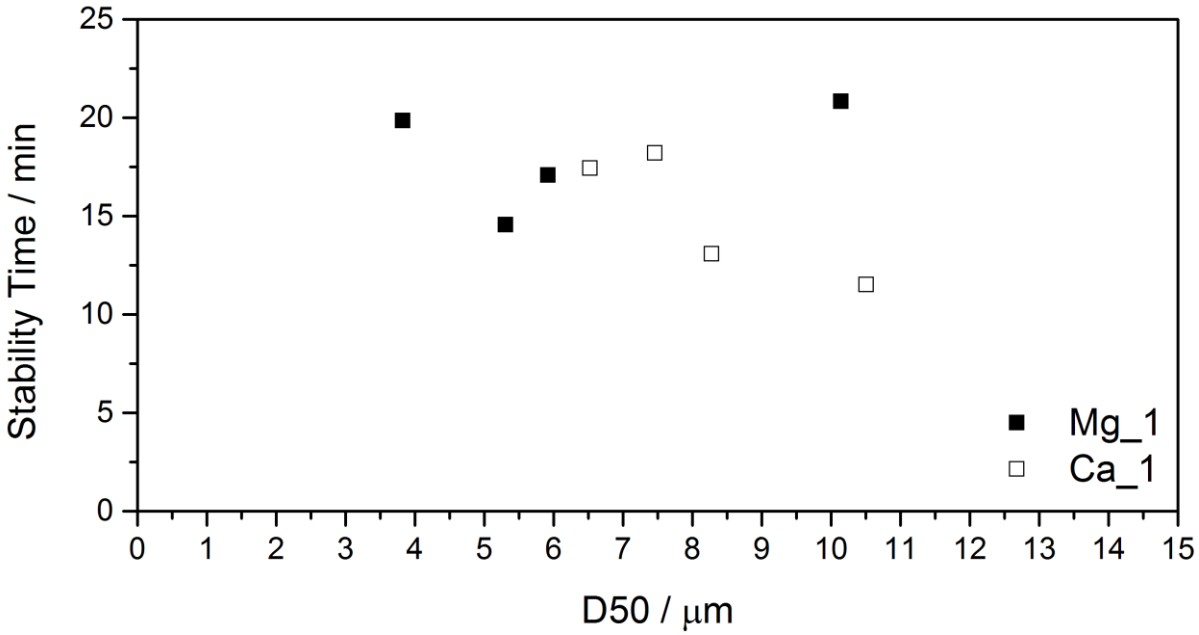

Figure 4.29: Metrastat stability times for different particles sizes of the two LDH stabilisers, above results are for 1 PHR of stabiliser.

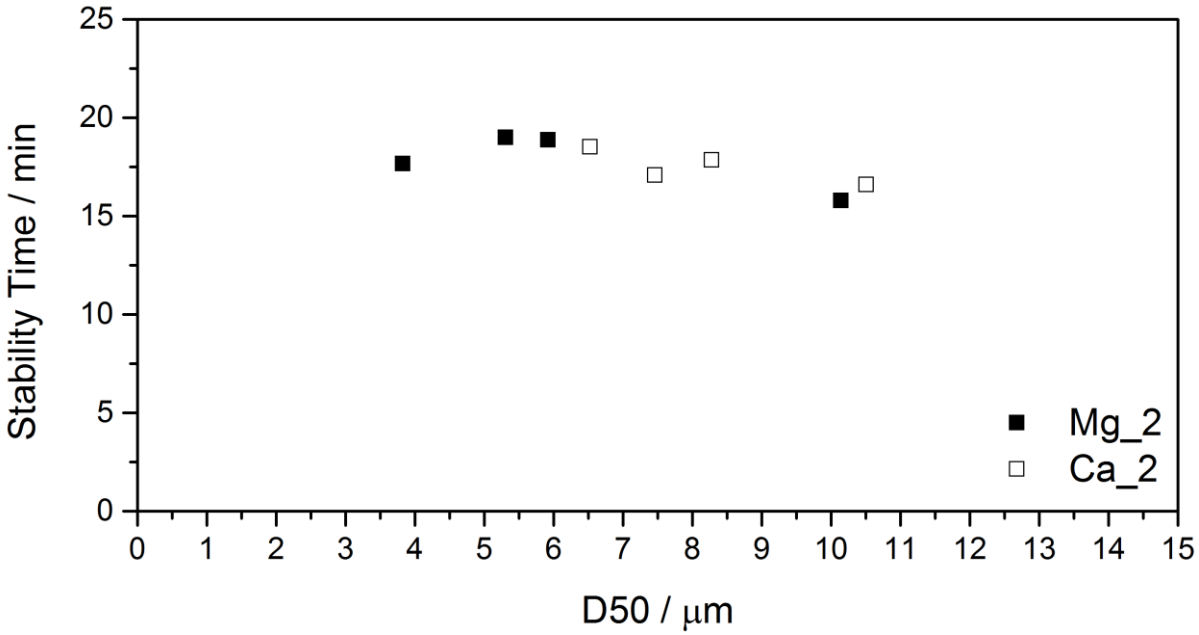

Figure 4.30: Metrastat stability times for different particles sizes of the two LDH stabilisers, above results are for 1 PHR of stabiliser.

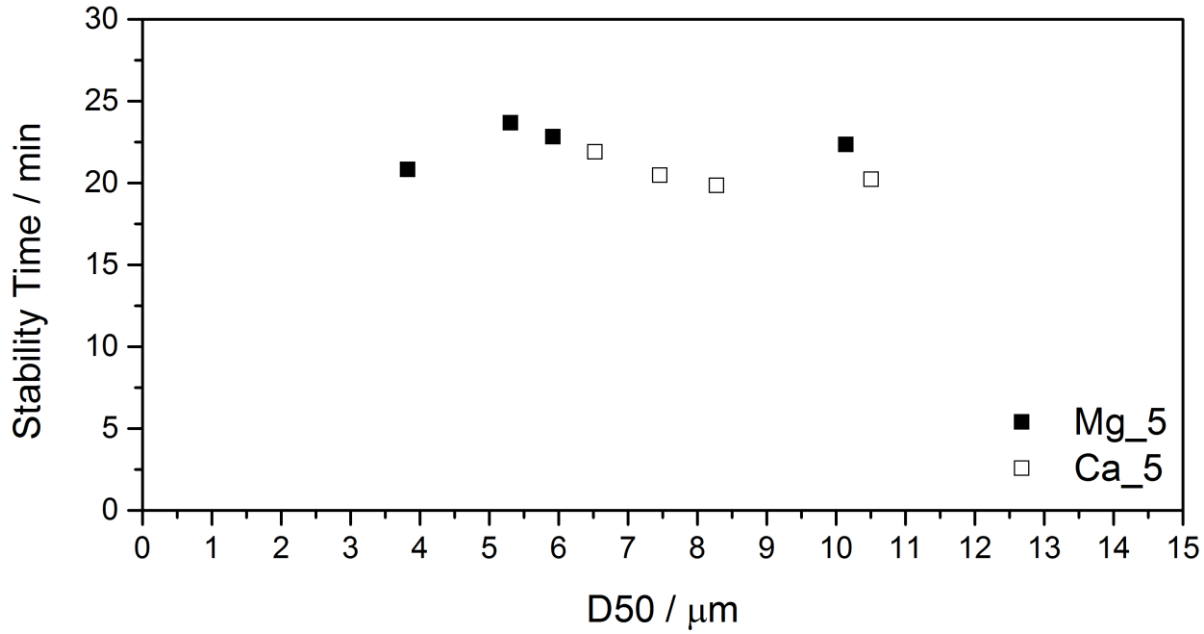

Figure 4.31: Metrastat stability times for different particles sizes of the two LDH stabilisers, above results are for 5 PHR of stabiliser.

From Figure 4.29, Figure 4.30 and Figure 4.31 there appears to be no trend in how the particle size effects the stability time of the PVC. The MgAl LDH slightly out performs the CaAl LDH with regards to stability time in the Metrastat testing oven. The Metrastat tests showed great variability with regards to stability time. For this reason the raw data was averaged for the three runs and then analysed using custom software to find the important points. This smoothed the data out and is the reason for no error bars. Large variability in results may be due to uneven heating in the oven. Figure 4.32 shows the variability between three runs.

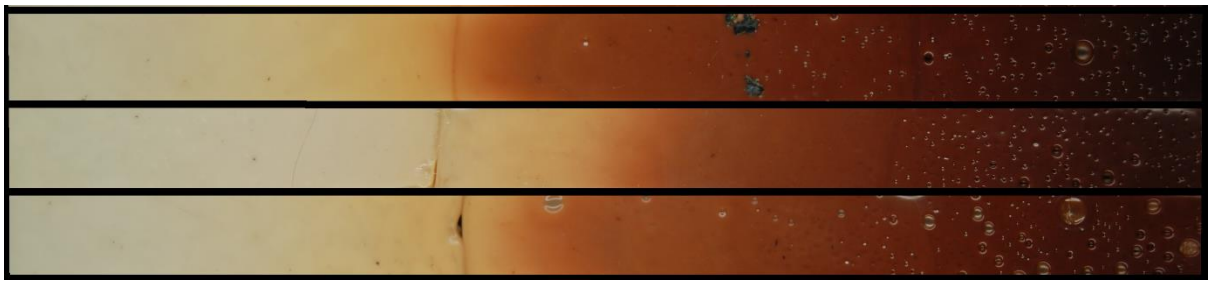

Figure 4.32: Metrastat burn strip, showing the variance between three runs of an identical sample.

Although there was no significant difference due to particle size, loading did play an important role in the thermal stability of the PVC. Figure 4.33 shows the stability time for the PVC with no LDH in the polymer matrix as well as the stability for the unmilled samples at different concentrations. It is evident from Figure 4.33 that both the MgAl LDH and the CaAl LDH outperformed the polymer with no LDH.

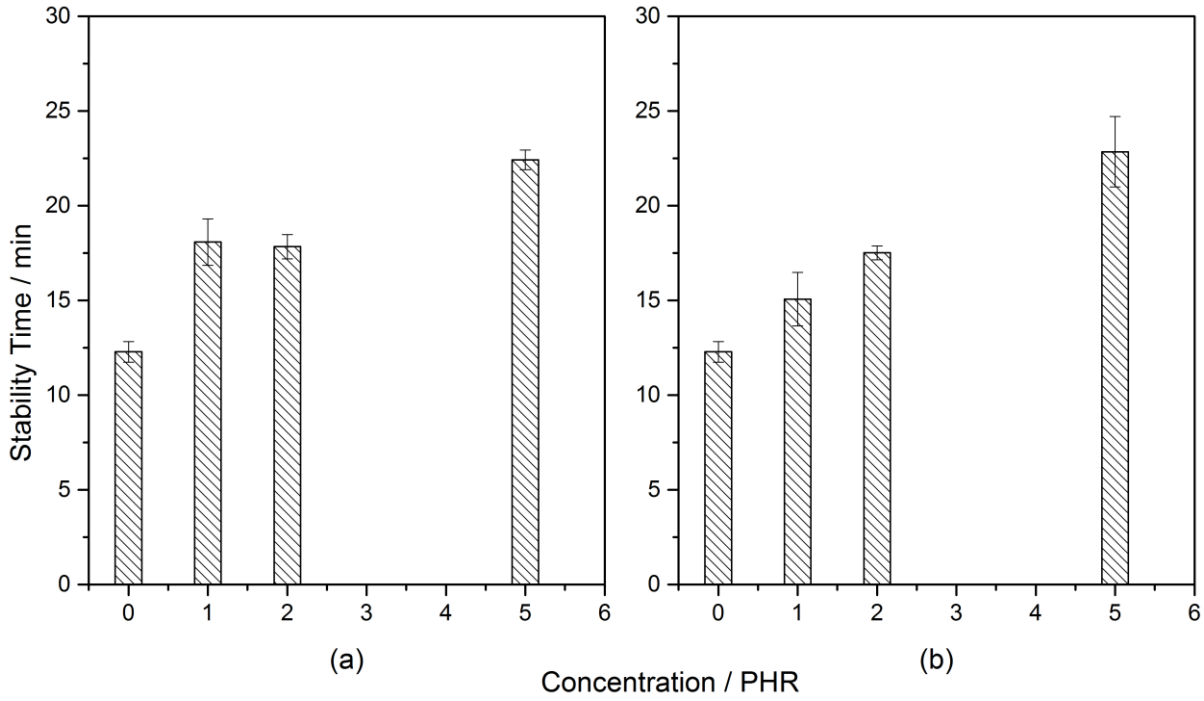

Figure 4.33: Metrastat stability times for the unmilled LDH stabilisers at different concentrations for (a) MgAl LDH and (b) CaAl LDH.

Figure 4.34, Figure 4.35 and Figure 4.36 show the degradation time for the PVC degraded in the Metrastat testing oven. From these figures it is clear that particle size had little influence on the final degradation time of the PVC. It also shows that the MgAl and CaAl LDH's performed almost identically.

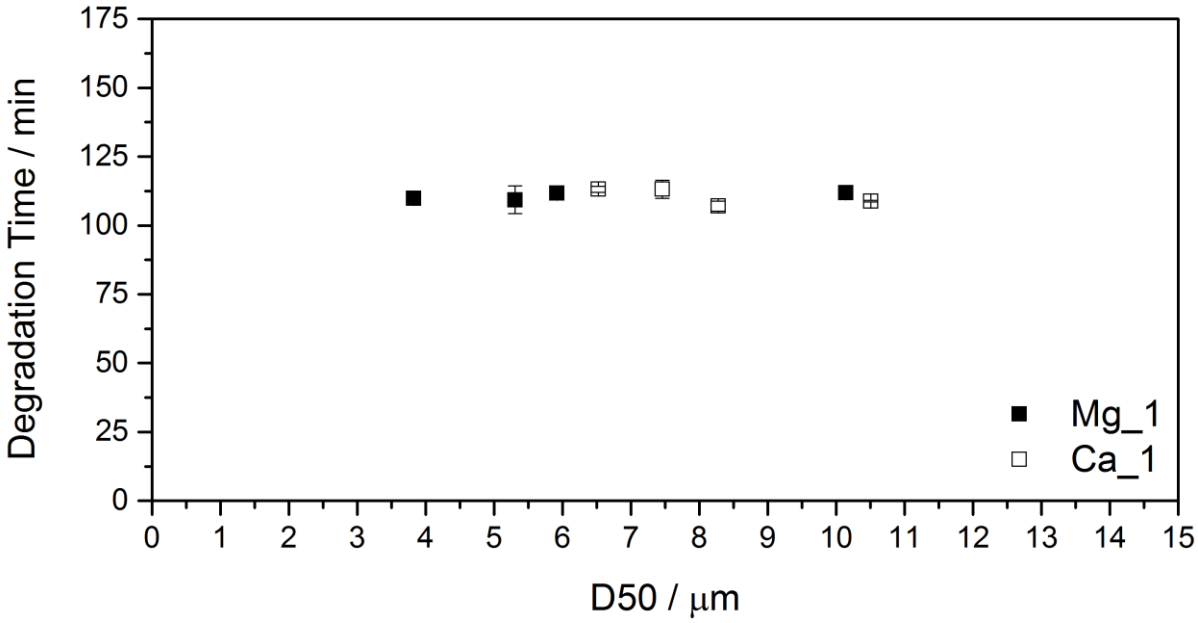

Figure 4.34: Metrastat degradation times for different particles sizes of the two LDH stabilisers, above results are for 1 PHR of stabiliser.

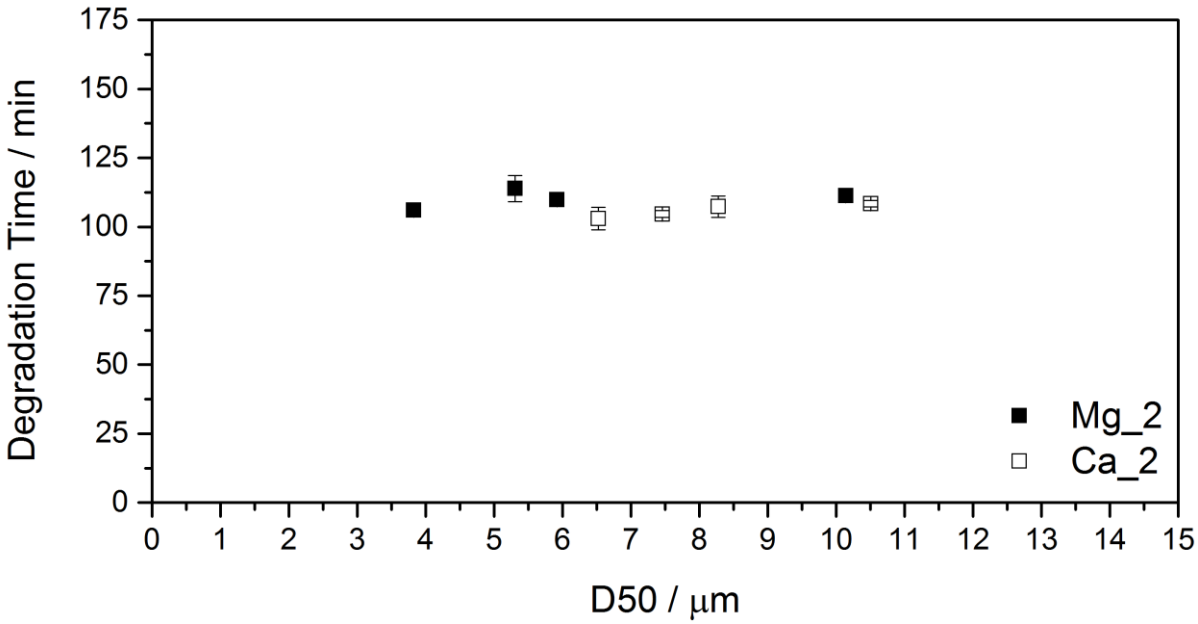

Figure 4.35: Metrastat degradation times for different particles sizes of the two LDH stabilisers, above results are for 2 PHR of stabiliser.

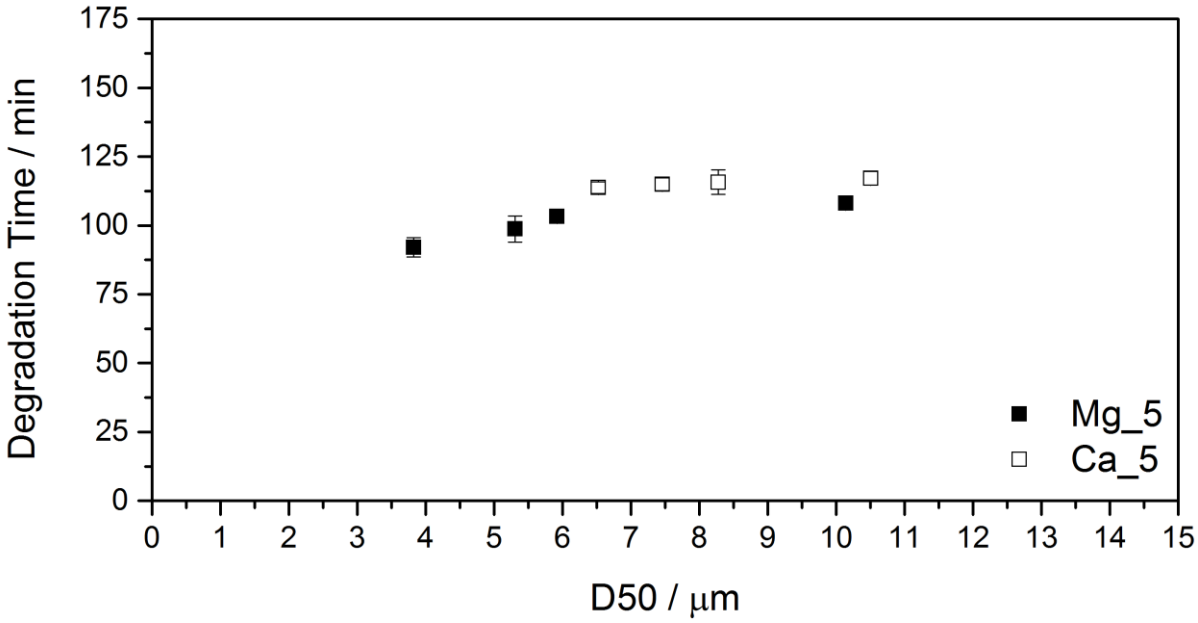

Figure 4.36: Metrastat degradation times for different particles sizes of the two LDH stabilisers, above results are for 5 PHR of stabiliser.

Figure 4.37 shows how loading of the LDH's affected the degradation time of the PVC. The addition of an LDH improves the final degradation time slightly, however the loading seems to have little effect on the final degradation time.

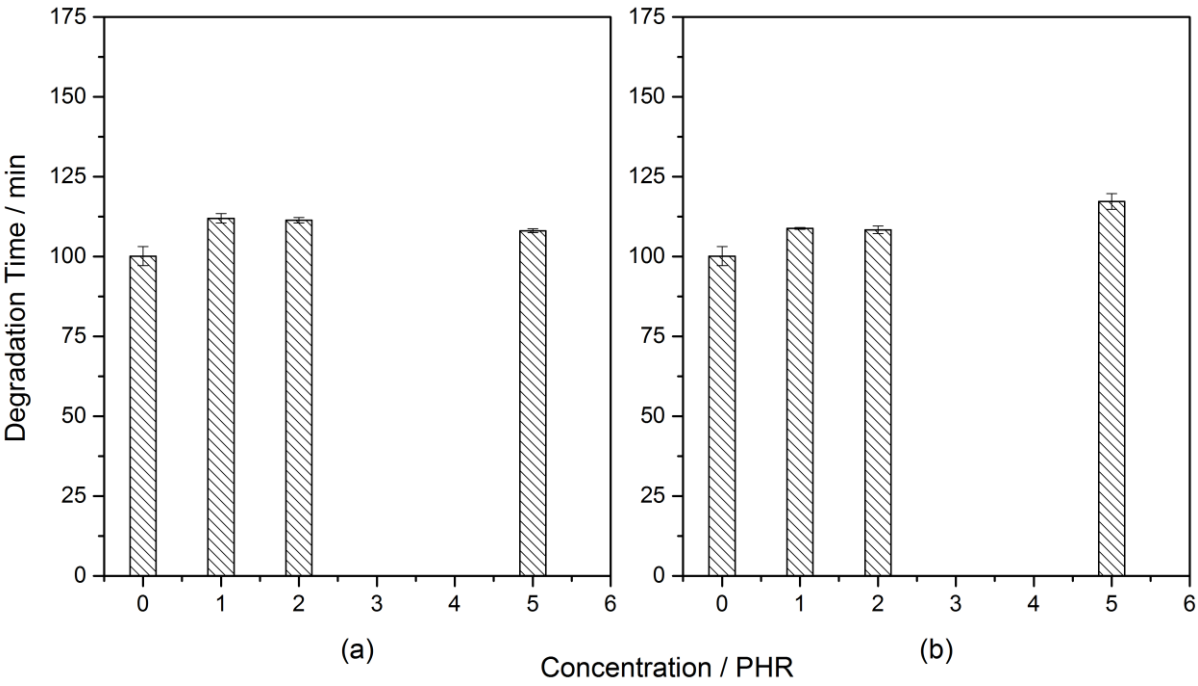

Figure 4.37: Metrastat degradation times for the unmilled LDH stabilisers at different concentrations for (a) MgAl LDH and (b) CaAl LDH.

4.3.4. Dynamic Thermal Stability Testing

Dynamic tests were done on the Haake Polylab OS Rheomix torque rheometer. The most important data that is generated by this method is the stability time, as well as the time taken to reach final degradation. Figure 4.38, Figure 4.39 and Figure 4.40 shows the stabilisation times at different particle sizes for the two LDH stabilisers at 1, 2 and 5 PHR respectively. The raw data for the Rheomix tests can be found in Appendix 10.

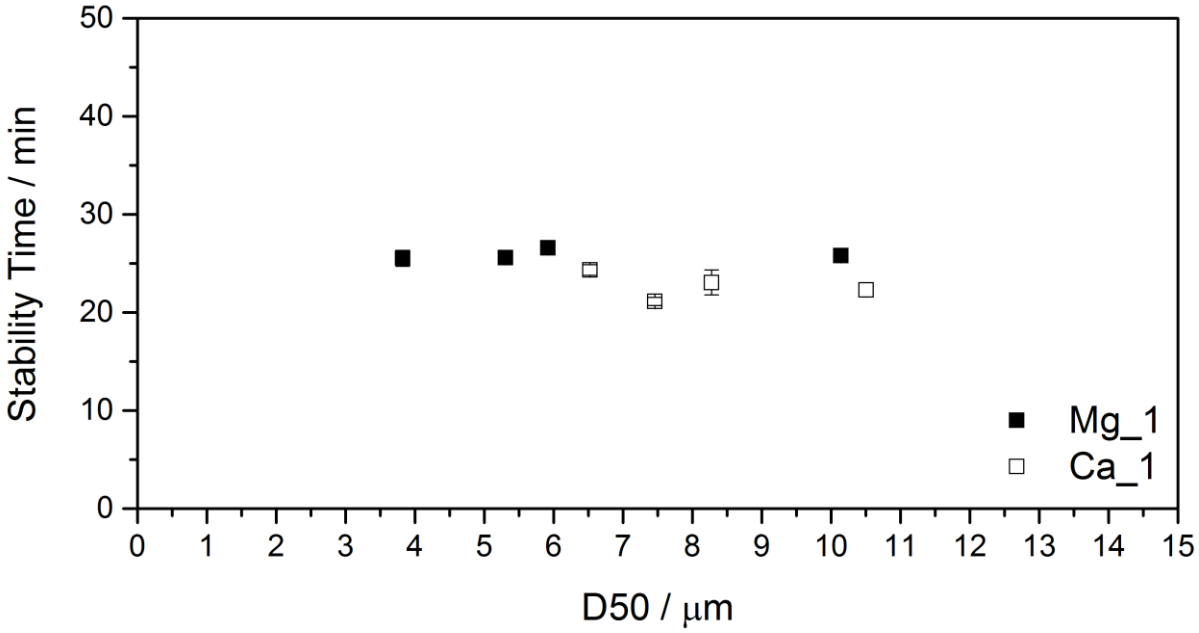

Figure 4.38: Rheomix stability times for different particles sizes of the two LDH stabilisers, above results are for 1 PHR of stabiliser.

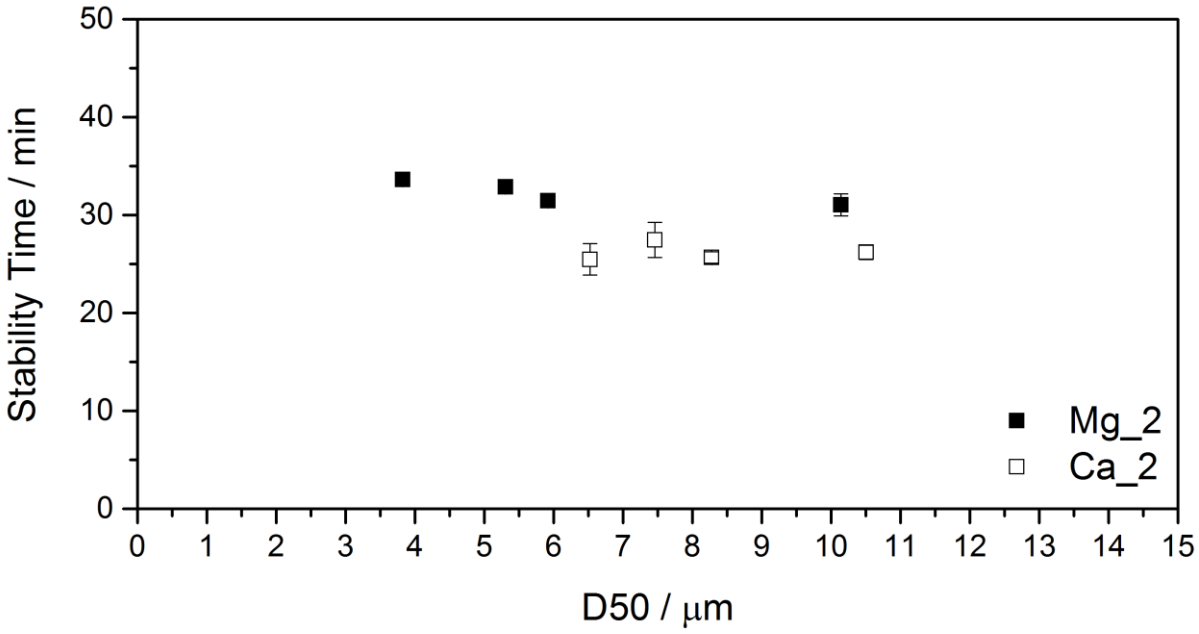

Figure 4.39: Rheomix stability times for different particles sizes of the two LDH stabilisers, above results are for 2 PHR of stabiliser.

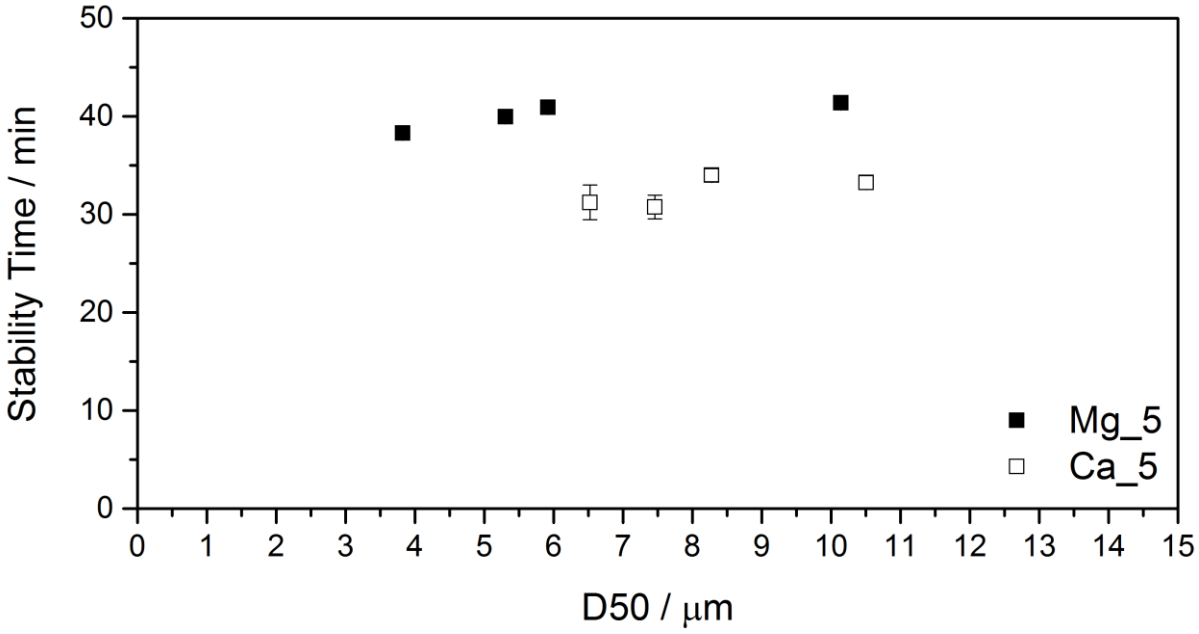

Figure 4.40: Rheomix stability times for different particles sizes of the two LDH stabilisers, above results are for 5 PHR of stabiliser.

From Figure 4.38, Figure 4.39 and Figure 4.40 we can see that milling the LDH samples had very little effect on the stability of the PVC. We can also notice that the stability time did increase with an increase in stabiliser loading, this was true for both

the MgAl LDH as well as the CaAl LDH. We can also note that at all three loadings the MgAl LDH outperformed the CaAl LDH.

This result is confirmed in Figure 4.41 which shows the Rheomix stability times in minutes for the two LDH stabilisers (unmilled) at different concentrations. Figure 4.41 also shows the stability time for the PVC with no LDH in the polymer matrix. It is evident from Figure 4.41 that both the MgAl LDH and the CaAl LDH outperformed the polymer with no LDH.

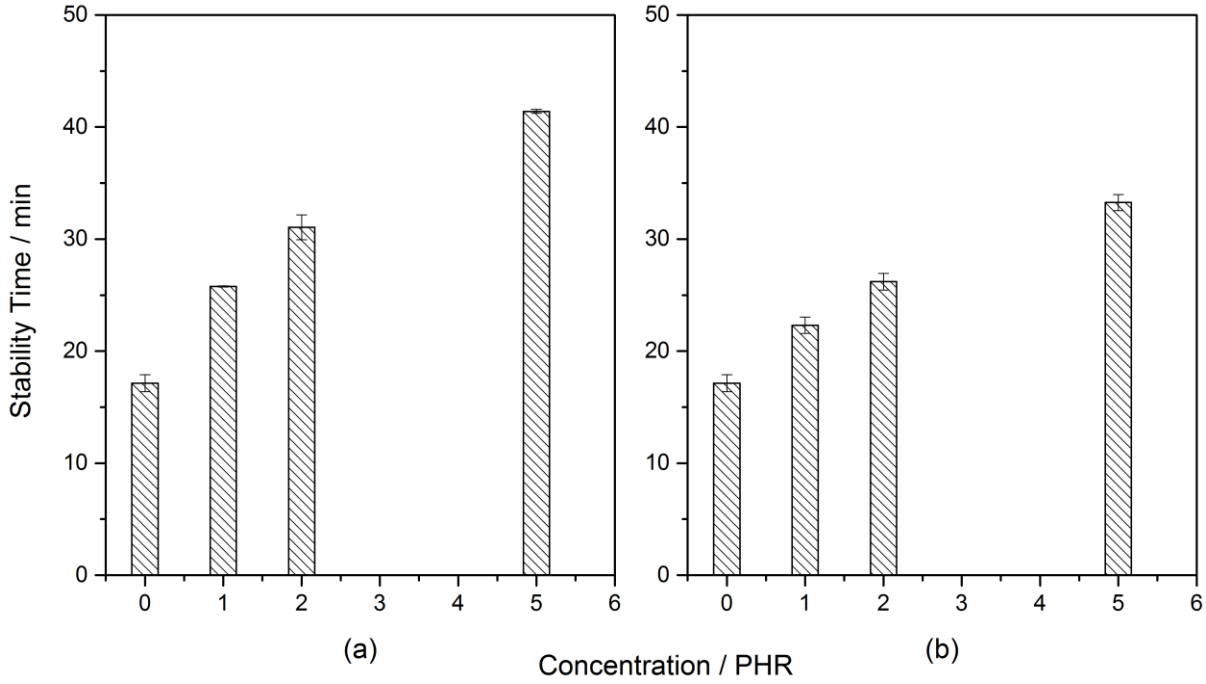

Figure 4.41: Rheomix stability times for the unmilled LDH stabilisers at different concentrations for (a) MgAl LDH and (b) CaAl LDH.

The final degradation times of the PVC at different particle sizes for the two LDH stabilisers at the three concentrations are shown in Figure 4.42, Figure 4.43 and Figure 4.44.

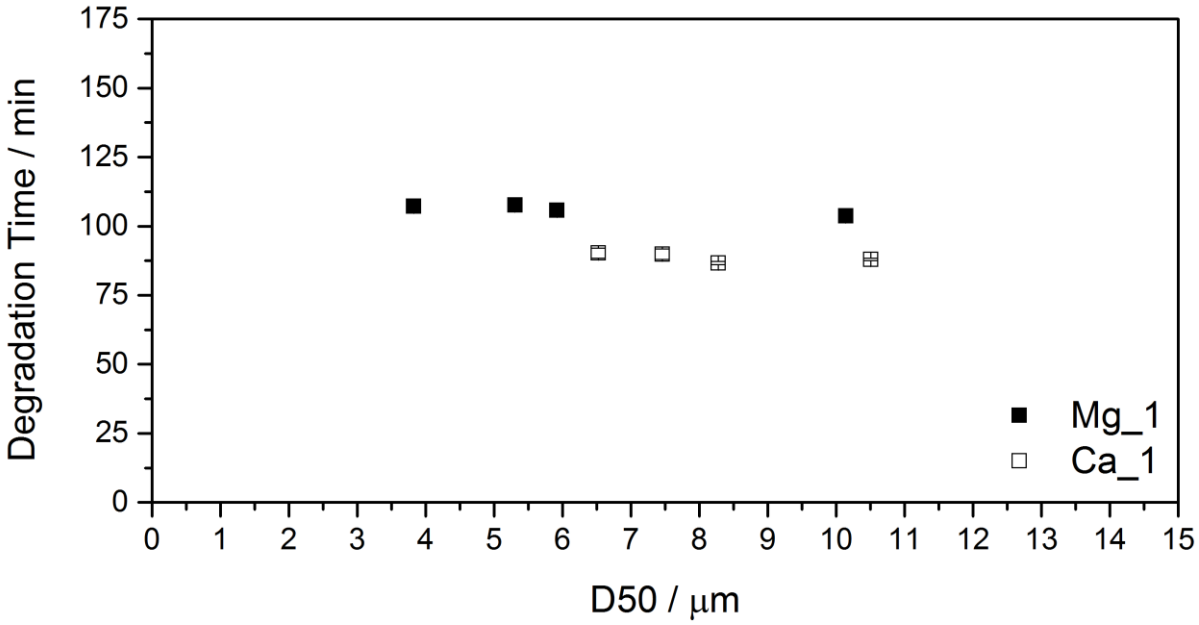

Figure 4.42: Rheomix degradation times for different particles sizes of the two LDH stabilisers, above results are for 1 PHR of stabiliser.

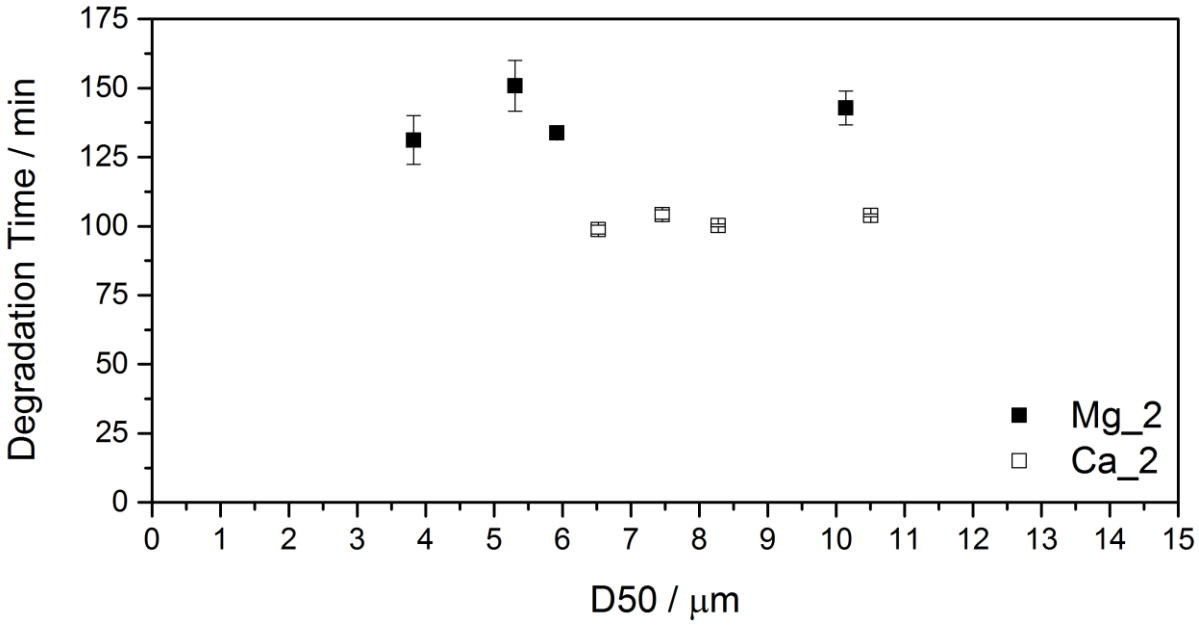

Figure 4.43: Rheomix degradation times for different particles sizes of the two LDH stabilisers, above results are for 2 PHR of stabiliser.

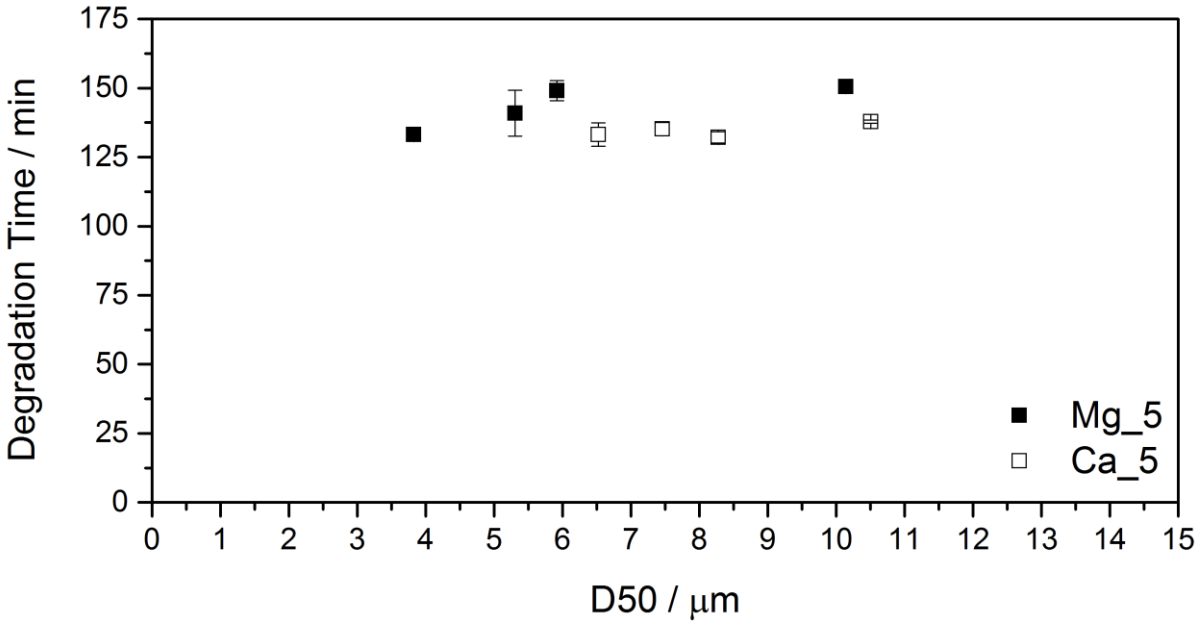

Figure 4.44: Rheomix degradation times for different particles sizes of the two LDH stabilisers, above results are for 5 PHR of stabiliser.

Once again from Figure 4.42, Figure 4.43 and Figure 4.44 it appears that milling the LDH sample had very little effect on the degradation times. These results are again confirmed in Figure 4.45 which shows the Rheomix degradation times in minutes for the two LDH stabilisers (unmilled) at different concentrations. We again see that both the MgAl LDH and CaAl LDH outperform the PVC with no LDH stabiliser.

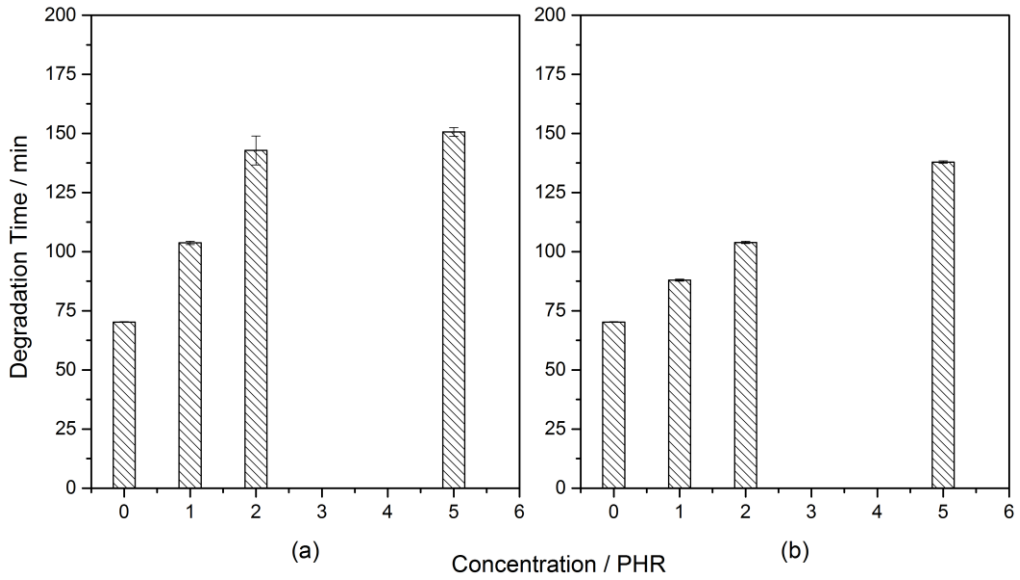

Figure 4.45: Rheomix degradation times for the unmilled LDH stabilisers at different concentrations for (a) MgAl LDH and (b) CaAl LDH.

5. Discussion of Results

5.1. Analytical Methods

XRD results showed that synthesis of an MgAl LDH as well as a CaAl LDH were successful, having the correct peaks as well as very few other peaks. This indicates that the LDH samples were pure in nature. The d-spacing of the LDH's were also calculated from the XRD data. The d-spacing of the MgAl LDH and the CaAl LDH were very similar.

PSA proved that the milling of the LDH's was effective, as both had reduction in particle size with an increase in milling time. It was also interesting to note that the CaAl LDH was a mechanically harder particle, as milling was less effective for this sample. There was also so conglomeration of particles which was noticeable on the PSA data. The milling of the particles appeared to have little effect on the surface area of the particles. This may be due to the conglomeration that was noted from the PSA data, as a reduction in particle size should increase the surface area.

SEM imaging gave a better understanding to the particles and their morphology. The SEM images showed that both the MgAl and CaAl LDH were hexagonal platelets, although the MgAl samples had some particles which showed a different configuration, with a long thin platelet. The images also showed the conglomeration of small particles and the reduction of particle size with increased milling time.

The pH of the saturated clays was measured and the CaAl LDH showed a much higher pH than the MgAl LDH. Acid reactivity tests were then done with the samples and the CaAl LDH reacted much quicker than the MgAl LDH. This may be due to the fact that it had a higher pH and therefore acted as a stronger base in the reaction. This may be an important fact in explaining the uptake of hydrochloric acid in the degradation of PVC. Particle size seemed to play no role in the pH of the saturated solution or the rate at which the acid reaction proceeded.

5.2. Thermal Degradation

5.2.1. Degradation during processing

Degradation during processing was quantified by a change in the colour of the pressed sheets. There was a colour change in both the MgAl LDH as well as the CaAl LDH. The degradation of the CaAl LDH was severe whereas the MgAL LDH was minor. The degradation of both LDH stabilised PVC samples increased with an increase in concentration. The CaAl LDH degraded significantly more with the increase in concentration of the stabiliser.

5.2.2. Thermal Degradation Tests

5.2.2.1. Effect of Particle size

All evidence from the thermal degradation tests indicate that particle size of the LDH stabilisers had very little, if any effect on the stability of the PVC. This may be due to the agglomeration that was seen in the images. This agglomeration may have also occurred in the PVC matrix. Use of a surface coating may have helped the dispersion of the stabilisers into the matrix, however it was thought that a surface coating may have affected other properties, such as lubrication and BET surface area.

5.2.2.2. Effect of concentration

The thermal testing suggested in general that an increase in concentration increased the stabilising effect of the LDH's, however some of the tests did not show this trend and this needs to be addressed.

The colour change during the Metrastat tests showed very little increase in stability or degradation times with an increase of concentration. This can be seen in Figure 5.1 and Figure 5.2, which show the stability and degradation times for the three tests respectively. The fact that very little increase in stability is noted, can be attributed to the fact that these LDH's are unmodified and therefore only act as secondary

stabilisers. They only scavenge HCl, and colour change is an effect which occurs due to the formation of double bonds. This implies that LDH stabilisers should have little effect on colour change.

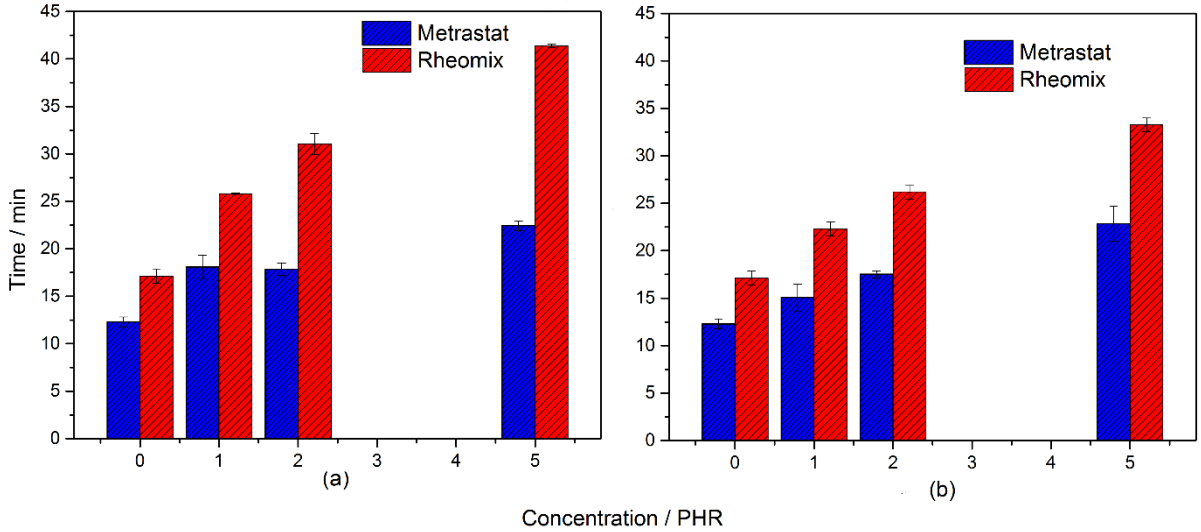

Figure 5.1: Stability times for the different thermal degradation tests for PVC stabilised with (a) MgAl LDH and (b) CaAl LDH.

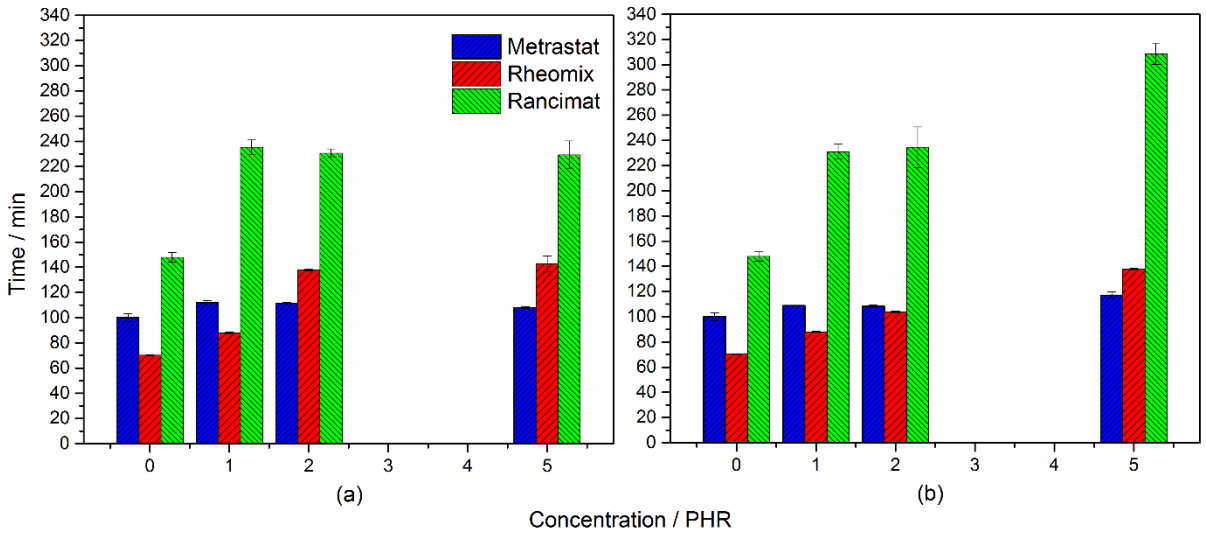

Figure 5.2: Degradation times for the different thermal degradation tests for PVC stabilised with (a) MgAl LDH and (b) CaAl LDH.

The other test which showed very little increase in degradation time with an increase in stabiliser concentration was the Rancimat test for HCl evolution, specifically for the MgAl LDH. This is a much more unexpected result as the CaAl LDH showed a definite

increase in stability time with an increase in concentration. This can be seen in Figure 5.2. Again since the LDH stabilisers are secondary stabilisers they should absorb HCl and an increase in concentration should increase the stability time. The lack of an increase in effectivity of the MgAl stabiliser may be explained by the fact that the MgAl reacts much slower than the CaAl LDH with an acid, as shown in Section 4.1.5.2. This reduced reaction rate may imply that the MgAl LDH may not be used up but is instead unable to react in time with all the free HCl. Another possible explanation may be that the MgAl LDH had more agglomeration in the PVC matrix, and therefore there were less reactive sites, and the stabiliser was again ineffective. If this was the case, use of a surface coating may have reduced the amount of agglomeration as well as increase the dispersibility of the stabiliser.

Rheomix stability increased with concentration for both the CaAl and MgAl stabiliser samples, and again there was little if any influence from the particle size. The MgAl stabiliser outperformed the CaAl sample at all three concentrations.

Figure 5.1 and Figure 5.2 also show that the LDH stabilisers both improved stability over the use of no LDH stabiliser.

5.2.2.3. Effect of Mixed Metal Layer

The effect of the two different mixed metal layers was also considered. The MgAl outperformed the CaAl stabiliser in the majority of the thermal degradation tests. The CaAl LDH only outperformed the MgAL LDH in the Rancimat HCl evolution tests. This could be explained again by the reaction time of the two stabilisers with an acid as shown in Section 4.1.5.2. The decreased reaction time of the CaAl, means that it would easily be able to scavenge any free HCl available.

This increased reaction rate, may be due to the higher pH of the CaAl LDH. This may also explain why overall the MgAl LDH outperformed the CaAl LDH. This may also explain the large colour change in the processed CaAl stabilised PVC. The high pH of the CaAl LDH may be causing the stabiliser to pull HCl off the PVC backbone and then absorb it. It still gives secondary stabilisation however many more double bonds are formed and the colour changes is more drastic than the MgAl stabilised PVC. The

CaAl therefore still outperforms the neat PVC however does not perform as well as the MgAl stabiliser.

5.3. Interaction Between Degradation Variables

Degradation variables from the three thermal degradation tests were examined, to try find interactions between the variables. Any interactions between the three tests would allow test results to be predicted from another test.

This was done using a scatter plot matrix, which can be seen in Figure 5.3. Examining this graph shows two interesting interactions. The interaction between Initial YI and Rancimat Degradation Time as well as the interaction between Rheomix Stability Time and Rheomix Degradation Time.

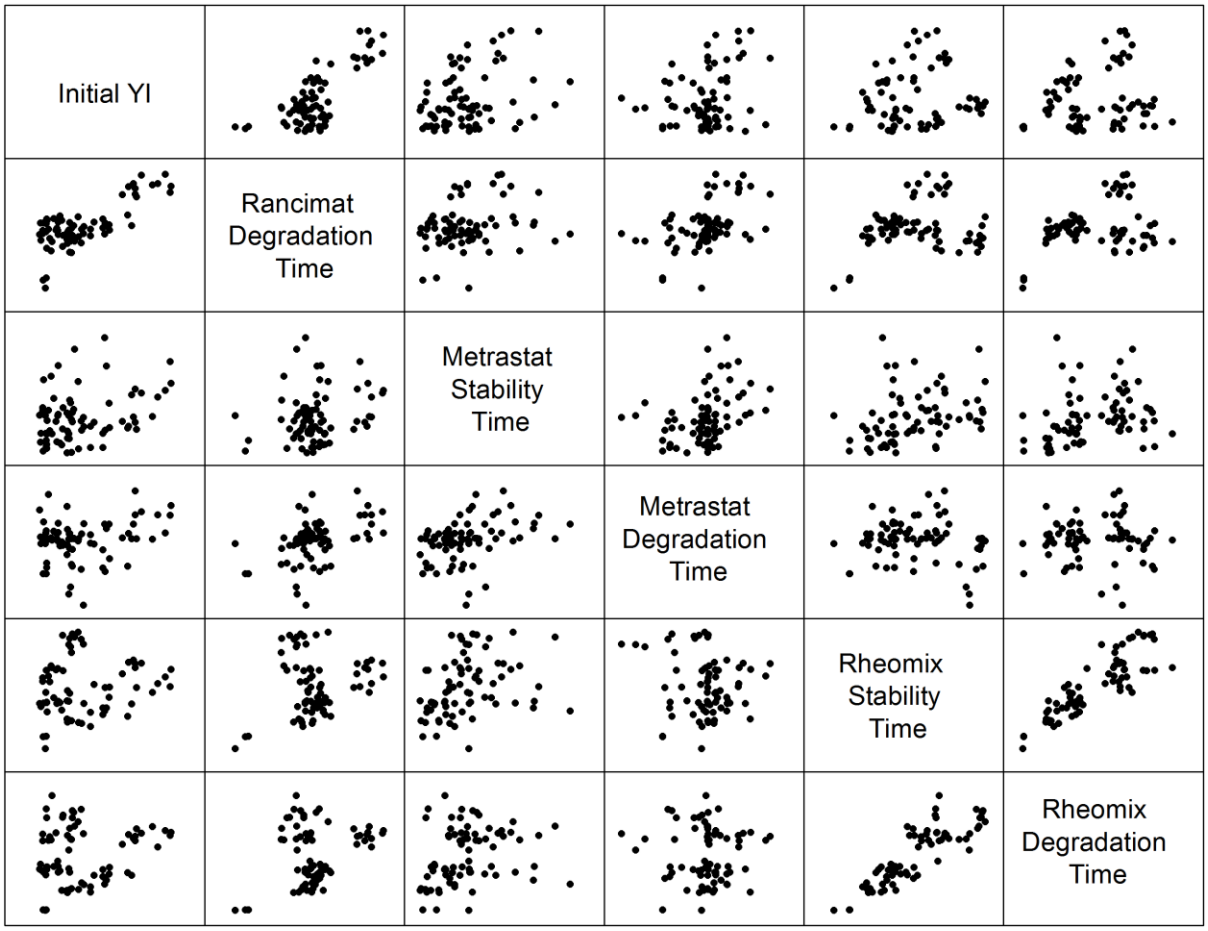

Figure 5.3: Scatter Matrix for the results of thermal degradation tests.

These two interactions were further analysed and a linear fit for the two was plotted, this can be seen in Figure 5.4. The R^2 for the fit is also given in the figure. The R^2 for the YI and Rancimat Degradation Time was 0.55 and the R^2 for the Rheomix Stability Time and Rheomix Degradation Time was 0.75.

The interaction between the Initial YI and Rancimat Degradation Time can be explained by the same principle used in Section 5.2.2.3. This interaction is thought to be due to the stabiliser usage and not an intrinsic interaction between the variables. This is substantiated by the three points at low YI and low degradation time, which appear to be outliers. These points are the PVC with no LDH stabilisers.

The second interaction (Rheomix Stability and Degradation time) seems more promising, with a much higher R^2. This may be an interaction unique to this set of stabilisers, or it may be an intrinsic interaction between the two variables. Further studies need to be done, with a wide range of stabilisers. This interaction is important as experimental time may be saved, if the degradation time can be predicted from the stability time.

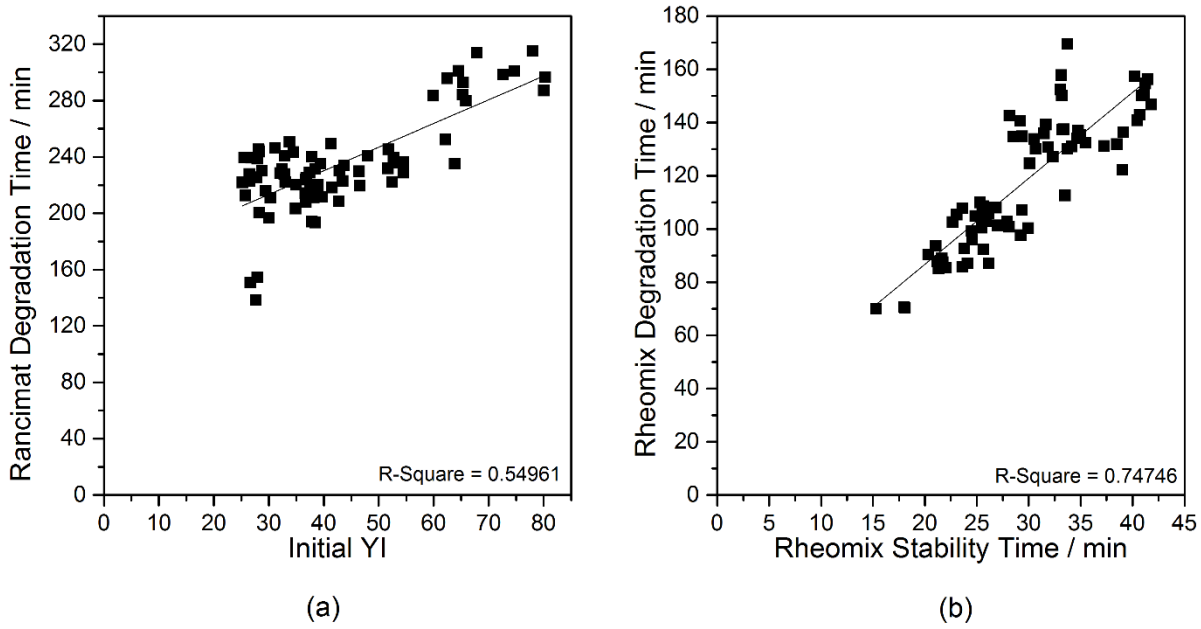

Figure 5.4: Possible interactions between degradation variables. (a) low R^2 interaction (b) high R^2 interaction.

6. Conclusions and Recommendations

An MgAl and CaAl stabiliser were synthesised, and milled to several particle sizes. These stabilisers were characterised by XRD, PSA, SEM, BET and an acid reactivity test. XRD showed that LDH's had indeed been formed. PSA showed a decrease in particle size with an increase in milling time. The LDH's were milled to four different sizes. The d50 for the four MgAl LDH's were: 10.15 µm, 5.92 µm, 5.31 µm and 3.82 µm. The d50 for the four CaAl LDH's were: 10.53 µm, 8.27 µm, 7.47 µm and 6.53 µm. This also proved that the CaAl LDH was harder than the MgAl LDH. SEM showed the morphology of the LDH's as well as some agglomeration. BET showed that particle size had little effect on surface area. Finally acid reactivity tests showed that the CaAl LDH had a higher saturation pH and reacted quicker with a weak acid than the MgAl LDH.

A PVC formulation was extruded and pressed with the LDH stabilisers. The CaAl stabilised PVC showed severe colour change during processing.

PVC thermal degradation tests proved that the decrease in particle size had little to no effect on the thermal stability of the PVC. This is a rather unexpected result and may be due to agglomeration and bad dispersibility. The concentration of the stabiliser generally increased the thermal stability, where this was not the case it was due to expected agglomeration of stabiliser particles or bad dispersibility. It is therefore recommended that further degradation testing is done, however with the coated LDH's to reduce agglomeration and increase the dispersibility of the stabiliser into the polymer matrix.

The MgAl LDH outperformed the CaAl LDH in all thermal degradation tests, except for the Rancimat HCl evolution test. This was due to the CaAl LDH reacting much faster with the acid, due to its higher pH. This also explained the colour change during processing. The high pH stabiliser may have removed HCl from the PVC backbone, increasing the rate of colour change as more double bonds were formed.

Interaction between stability and degradation time of Rheomix stability time was also examined and a linear plot was fitted to this data, with an R^2 of 0.75. This may be due to the set of stabilisers used, however further investigation is required. If this interaction proves to be intrinsic to the thermal stability test, experimental time can be saved, as degradation times could be predicted from stability time.

A final important note is that the testing methods give slightly different results, so depending on the application of the product, different testing methods need to be used.

7. References

Abbas, KB and Sorvik, EM (1980) “Heat Stabilizers for Poly (Vinyl Chloride). I. Synergistic Systems Based on Calcium/Zinc Stearate” *Journal of Vinyl Technology*, 2 (2), 87-94.

Adacho-Pagano, M, Forano, Claude and Besse, JP (2003) “Synthesis of Al-rich hydrotalcite-like compounds by using the urea hydrolysis reaction- control of size and morphology” *Journal of Materials Chemistry*, 13, 1988-1993.

Amer, AR and Shapiro, JS (1980) “Hydrogen Halide-Catalyzed Thermal Decomposition of Poly(vinyl Chloride)” *Journal of Macromolecular Science*, 14 (2), 185-200.

Anon (2007) “PVC additives- What lies ahead?” *Plastic Additives & Compounding*, November/ December, 22-25.

Aramendia, MA, Borau, V, Jimenez, C, Marinas, JM, Ruiz, JR and Urbano, FJ (2002) “Comparitive Study of Mg/M(III) (M= Al, Ga, In) Layered Double Hydroxides Obtained by Coprecipitation and the Sol-Gel Method” *Journal of Solid State Chemistry*, 168, 156-161.

Ari, GA (2010) “Using a torque rheometer to characterize flow in poly(vinyl chloride) composites” *Plastics Research Online*.

Arlman, EJ (1954) “Thermal and Oxidative Decomposition of Polyvinyl Chloride” *Journal of Polymer Science*, 12, 547-558.

Attenberger, P, Hohenadel, R, Kufner, T, Mieden, O and Winter, A (2011) “Polyvinyl Chloride (PVC)” *Kunststoffe*, 10, 7-10.

Bacaloglu, R and Fisch, M (1995) “Degradation and stabilization of poly(vinyl chloride). V. Reaction mechanism of poly(vinyl chloride) degradation” *Polymer Degradation and Stability*, 47, 33-57.

Bacaloglu, R and Fisch, M (2004) *Thermal Degradation and Stabilization of PVC*, Lampertheim, Germany.

Bacaloglu, R and Stewen, U (2001) "Study of PVC Degradation using a Fast Computer Scanning Procedure" *Journal of Vinyl & Additive Technology*, 7(3), 149-155.

Balkose, D, Gokcel, HI and Goktepe, SE (2001) "Synergism of Ca/Zn soaps in poly(vinyl chloride) thermal stability" *European Polymer Journal*, 37, 1191-1197.

Bamford, CH and Fenton, DF (1969) "The Thermal Degradation of Polyvinyl Chloride" *Polymer*, 10, 63-77.

Bao, YZ, Zhi-ming, H, Shen-xing, L and Zhi-xue, W (2008) "Thermal stability, smoke emission and mechanical properties of poly(vinyl chloride)/hydrotalcite nanocomposites" *Polymer Degradation and Stability*, 93(2), 448-455.

Braterman, PS, Xu, ZP and Yarberry F (2004) "Layered Double Hydroxides (LDH's)" *Handbook of Layered Materials*, Auerbach SM, Carrado, KA and Dutta, PK , 1st ed, New York, Marcel Dekker.

Bergaya, F, Theng, BKG and Lagaly, G (2006) *Handbook of Clay Science*, Elsevier, Oxford, UK.

Braun, D (1981) "Thermal degradation of poly (vinyl chloride)" *Development in polymer degradation*, *3*, 173-192.

Braun, D (2001) "PVC – Origin, Growth, and Future" *Journal of Vinyl & Additive Technology*, 7(4), 168 - 176.

Braun, D (2003) "Poly(vinyl chloride) on the Way from the 19th Century to the 21st Century" *Journal of Polymer Science: Part A: Polymer Chemistry*, 42, 578 - 586.

Briggs, G and Wood, NF (1971) "An Investigation of Mechanisms of Synergistic Interactions in PVC Stabilisation" *Journal of Applied Polymer Science*, 15, 25-37.

Brinker, CH and Scherer, GW (1999) *Sol-Gel Science: The Physics and Chemistry of Sol-Gel Processing*, Academic Press inc, San Diago.

Carroll, WF (1996) “Is PVC in House Fires the Great Unknown Source of Dioxin?” *Fire and Materials*, 20, 161-166.

Conroy, G (1999) “New Alternatives for Environmentally friendly Heat Stabilizers” *Plastics Technology*, https://www.plasticstechnology.com/articles/new-alternatives-for-environmentally-friendly-heat-stabilizers [2013/05/10].

Constantino, U, Marmottini, F, Nocchetti, M and Vivani, R (1998) “New Synthetic Routes to Hydrotalcite-Like Compounds – Characterisation and Properties of Obtained Materials”, *European Journal of Inorganic Chemistry*, 1439-1446.

Crepaldi, EL, Pavan, PC and Valim, JB (2000) “Comparitive Study of the Coprecipitation methods for the Preperation of Layered Double Hydroxides” *Journal of the Brazilian Chemical Society*, 11 (1), 64-70.

De Ray, A, Forano, c and Besse, JP (2001) *Layered Double Hydroxides: Past and Present. Chapter 1: Layered Double Hydroide: Synthesis and Post-Synthesis Modification*, Nova Science Publishers.

Dunkelberger, DL (1987) “History of the Development of Processing Aids for Rigid PVC” *Journal of Vinyl Technology*, 9(4), 173-178.

Dworkin, RD (1989) “PVC stabilizers of the Past, Present and Future” *Journal of Vinyl Technology*, 11(1), 15-22.

Duty, SM, Calafat, AM, Silva, MJ, Ryan, L and Hauser, R (2005) “Phthalate exposure and reproductive hormones in adult men” *Human Reproduction*, 20(3), 604-610.

Endo, K (2002) “Synthesis and structure of poly(vinyl chloride)” *Progress in Polymer Science*, 27, 2021-2054.

Ertl, J, Eiben, A, Schellerer, KM and Mieden, O (2010) “Polyvinyl Chloride (PVC)” *Kunststoffe*, 10, 45-48.

Fink, JK (2010) *A concise Introduction to Additives for Thermoplastic Polymers*, Scrivener Publishing, Massachusetts.

Focke, WW, Molefe, D, Labuschagne, FJW and Ramjee, S (2009) "The influence of stearic acid coating on the properties of magnesium hydroxide, hydromagnesite and hydrotalcite powders" *Journal of Material Science*, 44(22), 6100-6109.

Forano, C, Hibino, T, Lerouw, F and Taviot-Guého, C (2006) "Layered double hydroxides", in *Handbook of Clay Science*, Bergaya, F, Theng, BKG and Lagaly, G (Eds.), Elsevier, Amsterdam.

Geddes, WC (1967) "The Thermal Degradation of Polyvinylchloride – III. An investigation of Discolouration" *European Polymer Journal*, 3, 747-765.

Grey, IE and Ragozzini, R (1991) "Formation and Characterization of New Magnesium Aluminium Hydroxycarbonates" *Journal of Solid State Chemistry*, 94, 244-253.

Grzybkowski, W (2002) "Conductometric and Potentiometric Titration" Gsansk.

Gupta, S, Agarwal DD and Banerjee S (2008) "Synthesis and characterisation of hydrotalcites: Potential thermal stabilisers for PVC" *Indian Journal of Chemistry*, 47 (A), 1004-1008.

Guyot, A and Benevise JP (1926) "Sur la Digradation Thermique du Chlorure de Polyvinyle. I. Mithodes Exphrimentales d'Etude Cinhtique " *Journal of Applied Polymer Science*, 19, 98-102.

Hjertberg, T, Martinsson, E and Sorvik, E (1987) "Influence of the Dehydrochlorination Rate on the Degradation Mechanism of Poly(vinyl chloride)" *Macromolecules*, 21(3), 603-609.

Ivan, B, Kelen, T and Tudos, F (1989) "The main elementary events of degradation and stabilization of PVC" *Makromol. Chem., Macromol. Symp.*, 29, 59-72.

Jahrling, M (2009) “Examining the Fusion and Degradation Behavior of PVC Dry Blends with the HAAKE PolyLab QC” Thermo Fischer Scientific, Germany.

Kelen, T, Ivan, B, Nagy, TT, Turcsanyi B, Tudos, F and Kennedy JP (1978) “Reversible Crosslinking during Thermal Degradation of PVC” *Polymer Bulletin*, 1, 79-84.

Labuschagne, FJWJ, Giesekke, EW and van Schalkwyk, JD(2006) “Production of hydrotalcite”, PCT WO 2006/123284 A2.

Labuschagne, FJWJ, Molefe, DM, Focke WW, van der Westhuizen, I, Wright, HC and Royeppen, MD (2015), “Heat stabilising flexible PVC with layered double hydroxide derivatives” *Polymer Degradation and Stability*, 113, 46-54.

Lerke, I and Szymanski, W (1977) “Radiation Yield of Hydrogen Chloride in Gamma-Irradiated Poly(vinyl Chloride) Stabilized by Epoxy Compounds” *Journal of Applied Polymer Science*, 21, 2067-2075.

Lin, Y, Wang, J, Evans, DG and Li, D (2006) “Layered and intercalated hydrotalcite-like materials as thermal stabilizers in PVC resin” *Journal of Physics and Chemistry of Solids*, 67, 998-1001.

Lui, P, Zhao, M, Guo, J (2006) “Thermal Stabilisers of Poly(Vinyl Chloride)/Calcium Carbonate (PVC/$CaCO_3$) composites” *Journal of Macromolecular Science*, Part B, 45(6), 1135-1140.

Lui, ST, Zing, PP, Yan, KK, Zhang, YH, Ye, Y and Chen, XG (2015) “Sb-intercalated layered double hydroxides-poly(vinyl chloride) nanocomposites: Preperation, characterization and thermal stability” *Journal of Applied Polymer Science*, 132, 1-7.

Marongiu, A, Faravelli, T, Bozzano, G, Dente, M and Ranzi, E (2003) “Thermal degradation of poly(vinyl chloride)” *Journal of Analytical and Applied Pyrolysis*, 70, 519-553.

Mascolo, G (1995) “”Synthesis of anionic clays by hydrothermal crystallization of amorphous precursors” *Synthesis and Application of Anionic Clays*, 10 (1-2), 21-30.

McNeill, IC, Memetea, L and Cole WJ (1995) “A study of the products of PVC thermal degradation” *Polymer Degradation and Stabilisation*, 49, 181-191.

McNeill, IC and Neil, D (1969) “Degradation of Polymer Mixtures-III- Poly(Vinyl Chloride/Poly(Methyl Methacrylate) mictures, studied by thermal volatilization analysis and other techniques, the nature of Reaction Products and the Mechanism of Interaction of the Polymer” *European Polymer Journal*, 6, 569-583.

Meikle, JI (1997) *American Plastic: A Cultural history*, Rutgers University Press, New Jersey.

Miyata, S (1983) “Anion-exchange properties of hydrotalcite-like compounds”, *Clays and Clay Minerals*, 31(4), 305-311.

Miyata, S and Nosu, T (1988) “Stabilzed Polyvinyl Chloride resin composition” *US Patent 4,751,261*, assigned to Kyowa Chemical Industry Co., Ltd, Kagawa, Japan.

Mulder, K and Knot, M (2001) “PVC Plastic: a history of systems development and entrenchment” *Technology in Society*, 23, 265 - 286.

Nagy, TT, Kelen, T, Turcsanyi, B and Tudos, F (1980) “The Reinitiation Mechanism of HCI Catalysis in PVC Degradation” *Polymer Bulletin*, 2, 77-82.

Ocskay, GY, Nyitrai, ZS, Varfalvi, F and Wein T (1971) “Investigation of Degradation processes in PVC based on the concomitant colour changes” *European Polymer Journal*, 7, 1135-1145.

Ocskay, GY, Levai, J, Nyitrai, ZS and Varfalyi, F (1974) “The Discolouration of PVC-1. Correlation between the dehydrochlorination and discolouration of PVC” *European Polymer Journal*, 10, 1121-1125.

Owen, ED (1984) *Degrdation and Stabilisation of PVC*, Elsevier Science Publishing co., New York, United States of America.

Palma, G and Carenza, M (1970) “Degradation of poly(vinyl chloride). I. Kinetics of thermal and radiation-induced dehydrochlorination reactions at low temperatures” *Journal of Applied Polymer Science*, 14(7), 1737-1754.

Papino, F (2010) “Synthesis and Modification of Hydrotalcite as a Thermal Stabiliser for Poly(vinylchloride)”, PhD Thesis, Loughborough University, United Kingdom.

Perkin Elmer (2010) “The Analysis of PVC with Different Phthalate Content by TG-MS and TG-GC/MS”

Sauerwein, R (2008) “New mineral additive for heat stabilisation of PVC” *Plastics, Rubber and Composites*, 37 (9-10), 453-458.

Schecter, A, Birnbaum, L, Ryan, JJ and Constable, JD (2005) “Dioxins: An overview” *Environmental Research*, 101, 419-428.

Semon, WL and Stahl ,GH (1982) “History of vinyl chloride polymers” *Journal of Macromolecular Science: Part A - Chemistry*, 15(6), 199 – 214.

Starnes, WH (2005) “Structural Defects in Poly(vinyl chloride)” *Journal of Polymer Science: Part A: Polymer Chemistry*, 43, 2451-2467.

TA Instruments (*s.a.*) “Analysis of Polymer Degradations by TGA-Mass Spectrometry”.

Thermo Fisher Scientific (*s.a.*) “PolyLab System, Torque Rheometer: Rheodrive”.

Titow, WV (1984) *PVC Technology*, Elsevier Science Publishing Co., New York, United States of America.

Tran, VH, Guyot, A, Nguyen, TP and Molinie, P (1991) “Poly(vinyl chloride) dehydrochlorination via the polaron mechanism” *Polymer Degradation and Stabilisation*, 37, 209-216.

Utracki, LA (1995) “History of Commercial Polymer Alloys and Blends (From a Perspective of the Patent Literature)” *Polymer Engineering and Science*, 35(1), 1 – 17.

Van Hoang, T and Guyot, A (1990) “Polaron Mechanism in the Thermal Degradation of Poly(vinyl chloride)” *Polymer Degradation and Stabilisation*, 32, 93-103.

Vinyl2010 (2006) “Vinyl 2010. The Voluntary Commitment of the PVC industry”.

VinylPlus (2013) “Progress Report 2013. Reporting on the activities of the year 2012”.

Vymazal, Z, Czako, E, Meissner, B, and Stepek, X (1974) “Dehydrochlorination of polyvinylchloride using correction for isothermal conditions.” *Journal of Appiled Polymer Sci*ence, 18, 2861.

Wang, X and Zhang, Q (2004) “Effect of hydrotalcite on the thermal stability, mechanical properties, rheology and flame retardance of poly(vinyl chloride)” *Polymer International*, 53, 698-707.

Wen, R, Yang, Z, Chen, H, Hu, Y and Duan, J (2011) “Zn-Al-La hydrotalcite-like compounds as heating stabiliser in PVC resin” *Journal of Rare Earths*, 30 (9), 895-902.

Wheeler, RN (1981) “Poly(vinyl Chloride) Processes and Products” *Environmental Health Perspectives*, 41, 123-128.

Wilkes, CE, Summers, JW, Daniels, CA and Berard, MT (2005) *PVC handbook,* Hanser, Munich.

Wypych, G (2008) *PVC Degradation & Stabilization*, ChemTec Publishing.

Wypych, G, Kozlakowski, K, Krzeszewski, L and Roszkowski, W (1985) “Color stability measuring device.” *UK Patent Application GB 2 174 800 A*, Date of filling May 7, 1985.

Xu, ZP, Saha, SK, Braterman, PS and D’Souza, N (2006) “The effect of Zn,Al layered hydroxide on thermal decomposition of poly(vinyl chloride)” *Polymer Degradation and Stability*, 91(12), 3237-3244.

Xue, X, Zhang, H and Zhang, S (2014) “Preparation of MgAl LDHs intercalated with Amines and Effect on Thermal Behavior for Poly(vinyl chloride)” *Advances in Material Physics and* Chemistry, 4, 258-266.

Yousufzai, AHK, Zafar, MM, ul-Hasan, S (1972) “Radical Degradation of Polyvinyl Chloride”, *European Polymer Journal*, 8, 1231-1236.

Yngve, V (1940) “Stabilized Vinyl Resins” *US Patent 2,219,463*, assigned to Carbide and Carbon Chemicals, New York.

Zeng, Hy, Deng, X, Wang, YJ and Liao, KB (2009) "Preparation of Mg-Al Hydrotalcite by Urea Method and Its Catalytic Activity for Transesterification", *AIChE Journal*, 55(5), 1229-1235.

Zhang, X, Zhou, L, Pi, H, Guo, S and Fu, J (2014) “Performance of layered double hydroxides intercalated by a UV stabilizer in accelerated weathering and thermal stabilization of PVC” *Polymer Degradation and Stability*, 102, 204-211.

Zweifel, H, Maier RD and Schiller, M (2008) *Plastics Additives Handbook*, 6th Edition, Hanser, Germany.

Appendix

Appendix 1: Reaction Reagent Masses

Table A.1: LDH reaction reagents and masses used.

$CaAl\ CO_3$ LDH		$MgAlCO_3$	
Reagant	Mass (g)	Reagant	Mass (g)
CaO	652.19	MgO	449.1
$Al(OH)_3$	434.81	$Al(OH)_3$	434.81
$NaHCO_3$	236.48	$NaHCO_3$	236.48
H_2O	5500	H_2O	5500

Appendix 2: Sample Names and Stabiliser Concentrations

Table A.2: Sample names and stabiliser concentrations

Sample Name	PVC	LDH Additive	Concentration (PHR)	Dry Blend Mass (g)	Additive Mass (g)	Mixed
N1	Dry Blend 01	NONE	0	600	0	Yes
Ca0_1	Dry Blend 01	CaAlCO3 0	1	600	2.941176471	Yes
Ca1_1	Dry Blend 01	CaAlCO3 1	1	600	2.941176471	Yes
Ca2_1	Dry Blend 01	CaAlCO3 2	1	600	2.941176471	Yes
Ca6_1	Dry Blend 01	CaAlCO3 6	1	600	2.941176471	Yes
Mg0_1	Dry Blend 01	MgAlCO3 0	1	600	2.941176471	Yes
Mg1_1	Dry Blend 01	MgAlCO3 1	1	600	2.941176471	Yes
Mg2_1	Dry Blend 01	MgAlCO3 2	1	600	2.941176471	Yes
Mg6_1	Dry Blend 01	MgAlCO3 6	1	600	2.941176471	Yes
Ca0_2	Dry Blend 01	CaAlCO3 0	2	600	5.882352941	Yes
Ca1_2	Dry Blend 01	CaAlCO3 1	2	600	5.882352941	Yes
Ca2_2	Dry Blend 01	CaAlCO3 2	2	600	5.882352941	Yes
Ca6_2	Dry Blend 01	CaAlCO3 6	2	600	5.882352941	Yes
Mg0_2	Dry Blend 02	MgAlCO3 0	2	600	5.882352941	Yes
Mg1_2	Dry Blend 02	MgAlCO3 1	2	600	5.882352941	Yes
Mg2_2	Dry Blend 02	MgAlCO3 2	2	600	5.882352941	Yes
Mg6_2	Dry Blend 02	MgAlCO3 6	2	600	5.882352941	Yes
Ca0_6	Dry Blend 02	CaAlCO3 0	5	600	14.70588235	Yes
Ca1_6	Dry Blend 02	CaAlCO3 1	5	600	14.70588235	Yes
Ca2_6	Dry Blend 02	CaAlCO3 2	5	600	14.70588235	Yes
Ca6_6	Dry Blend 02	CaAlCO3 6	5	600	14.70588235	Yes
Mg0_6	Dry Blend 02	MgAlCO3 0	5	600	14.70588235	Yes
Mg1_6	Dry Blend 02	MgAlCO3 1	5	600	14.70588235	Yes

Mg2_6	Dry Blend 02	MgAlCO3 2	5	600	14.70588235	Yes
Mg6_6	Dry Blend 02	MgAlCO3 6	5	600	14.70588235	Yes
N2	Dry Blend 02	NONE	0	600	0	Yes

Appendix 3: Analysed XRD Patterns for unmilled LDH's.

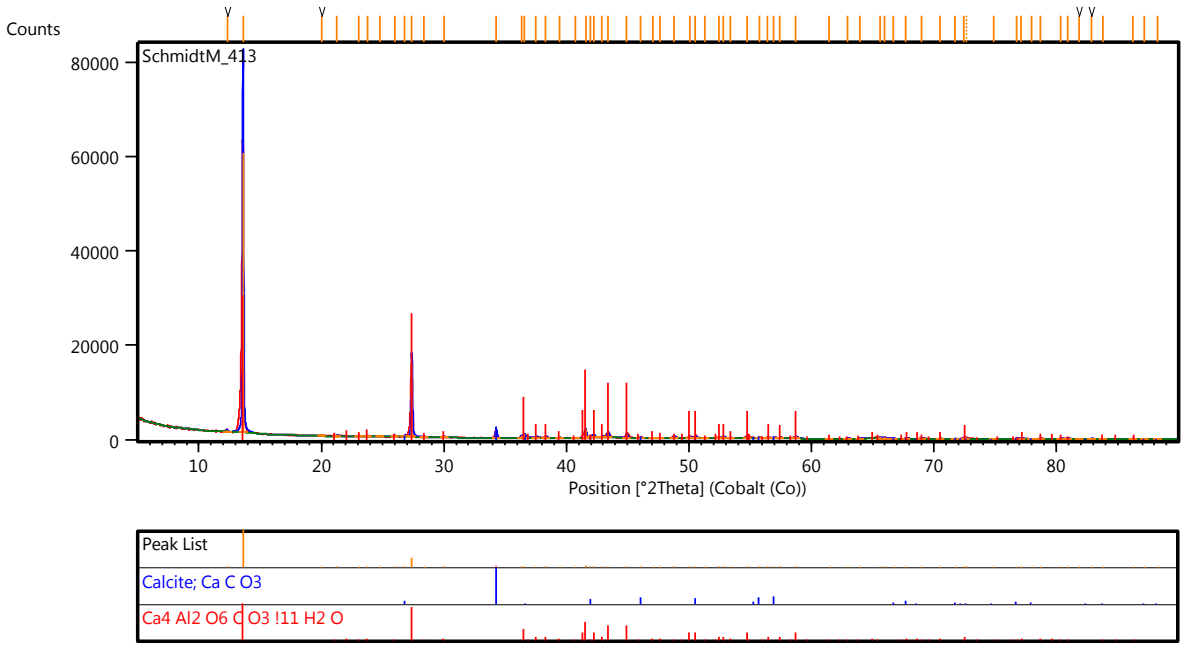

Figure A.1: Analysed XRD pattern for unmilled CaAl-CO_3 LDH.

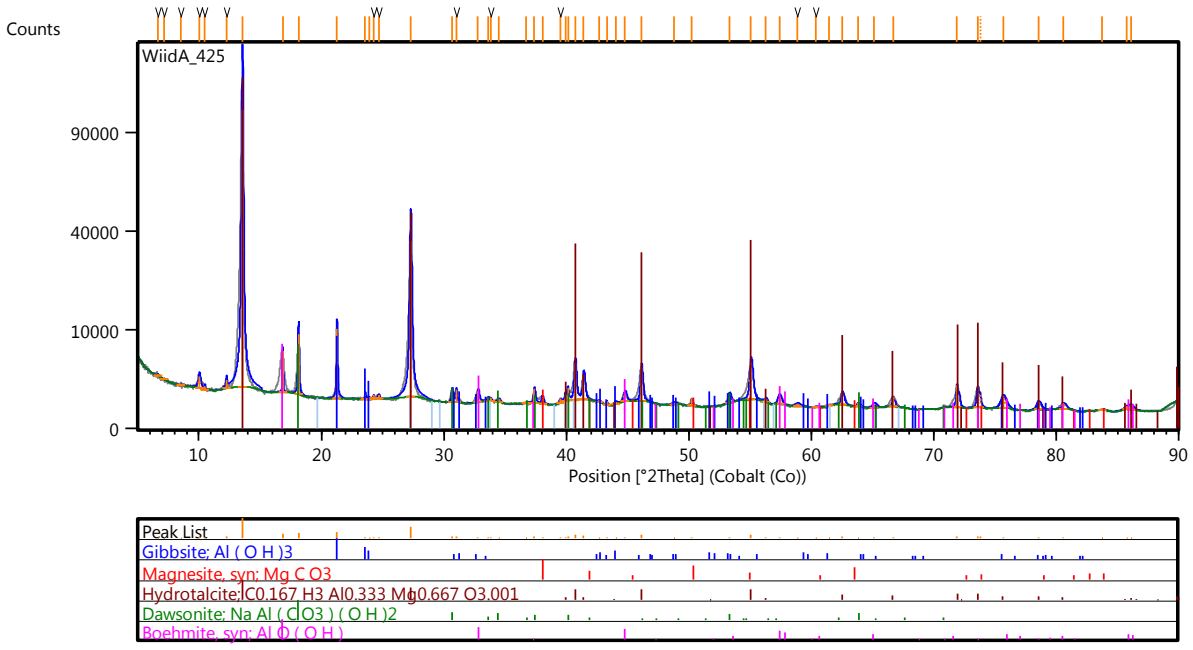

Figure A.2: Analysed XRD pattern for unmilled MgAl-CO_3 LDH.

Appendix 4: Analysed XRD Patterns for Milled LDH's.

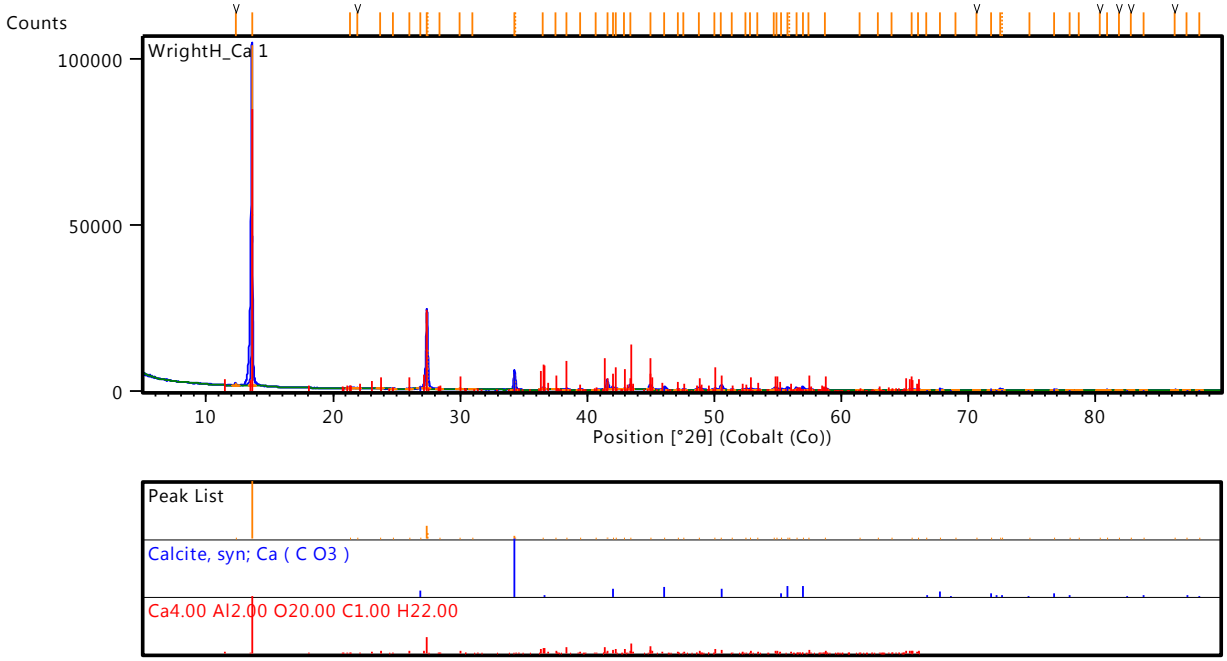

Figure A.3: Analysed XRD pattern for milled CaAl-CO_3 LDH, with one pass through the mill.

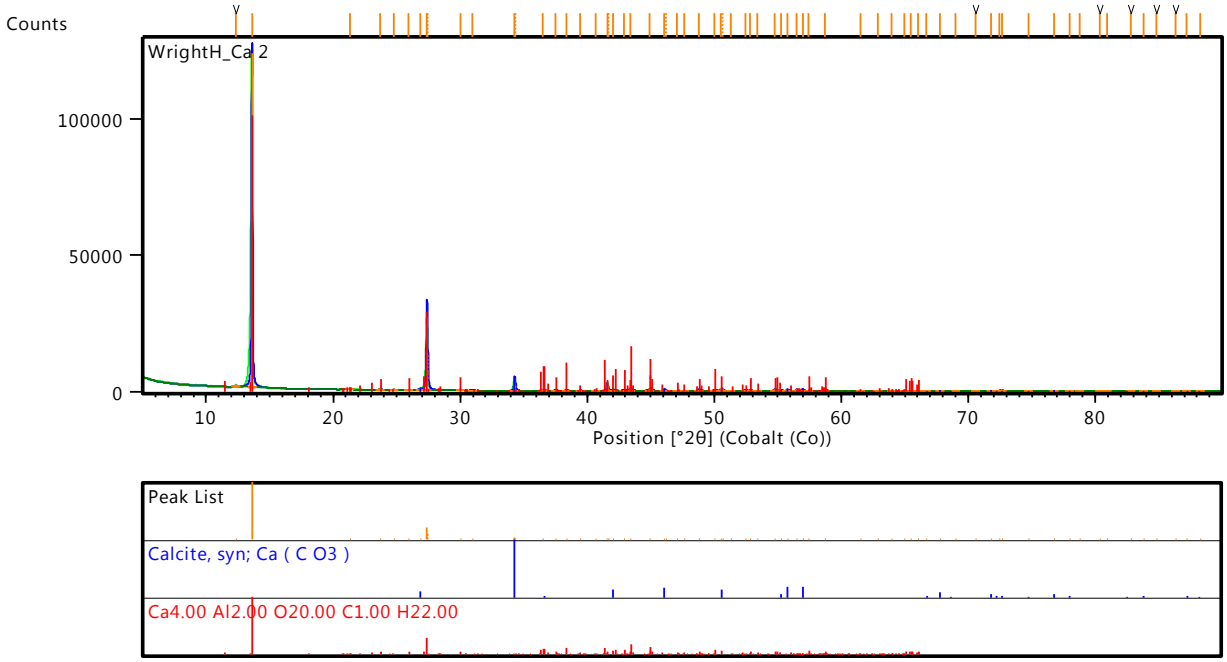

Figure A.4: Analysed XRD pattern for milled CaAl-CO_3 LDH, with two passes through the mill.

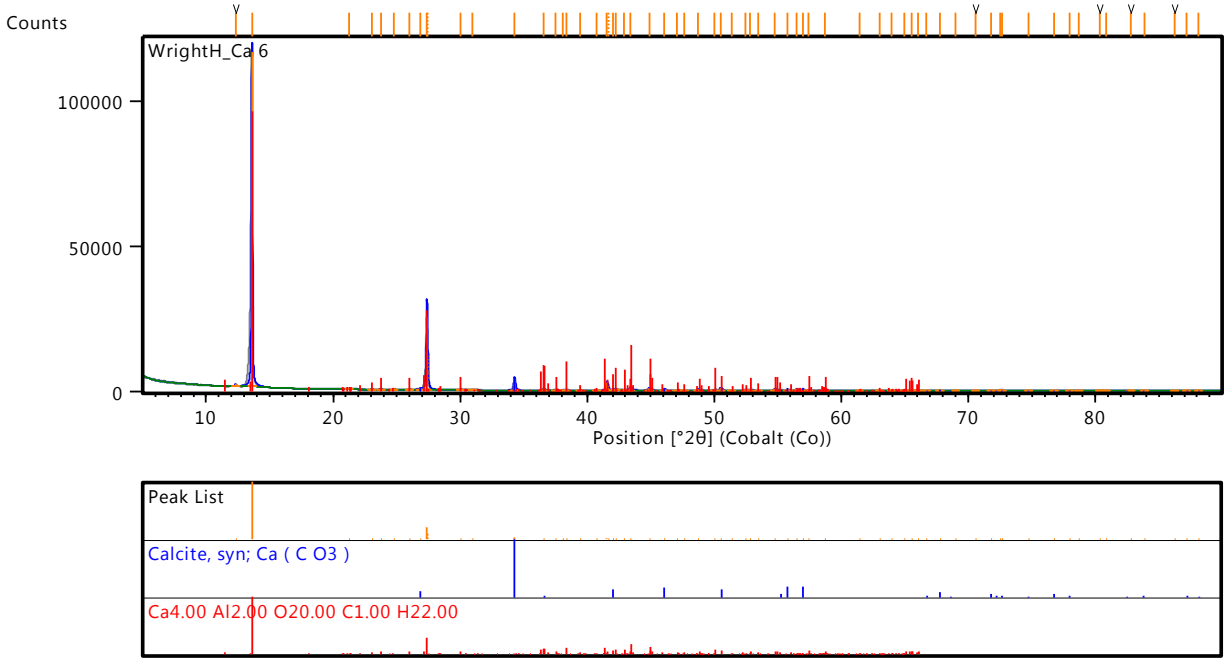

Figure A.5: Analysed XRD pattern for milled CaAl-CO_3 LDH, with six passes through the mill.

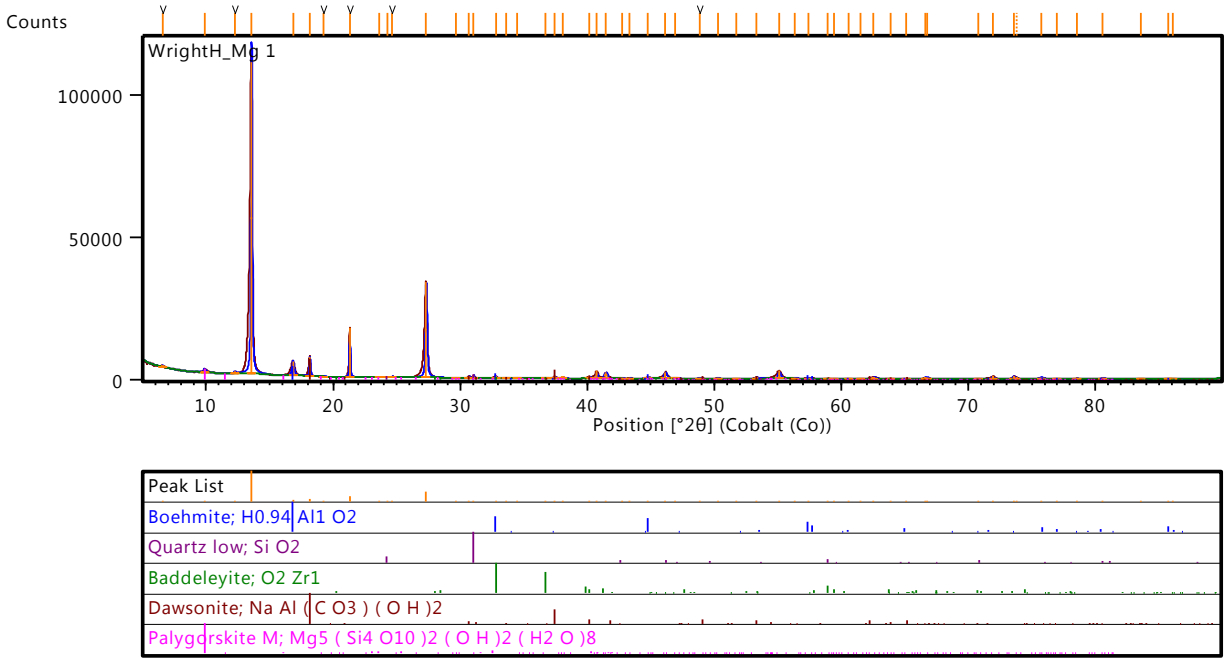

Figure A.6: Analysed XRD pattern for milled MgAl-CO_3 LDH, with one pass through the mill.

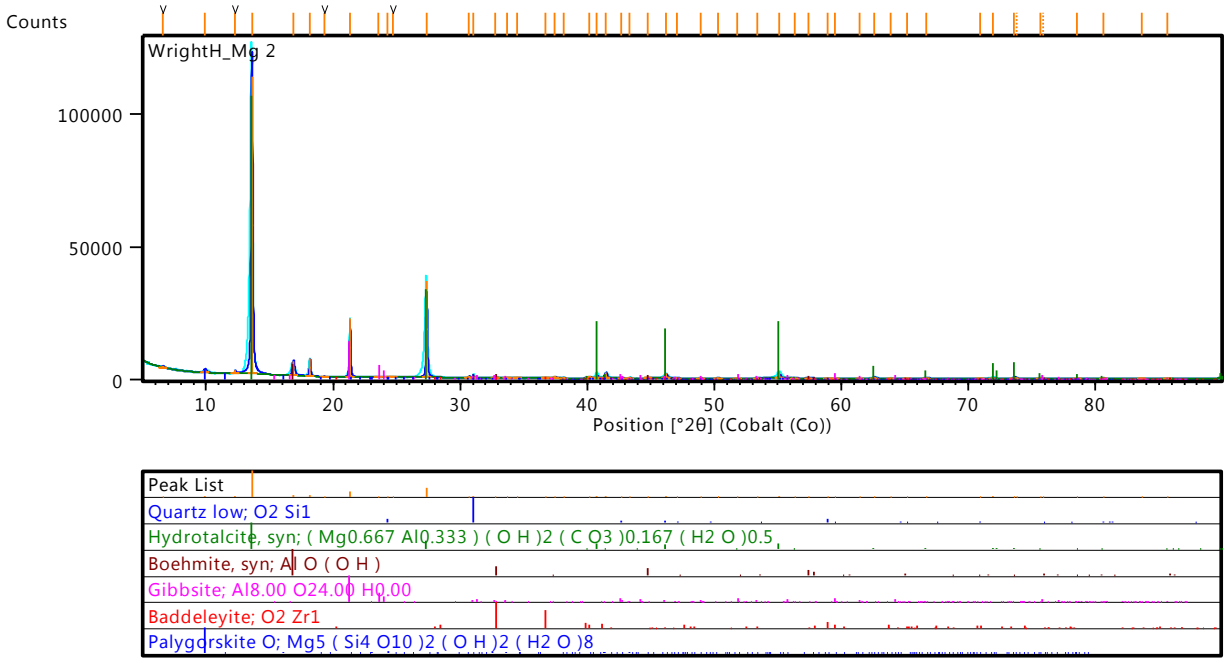

Figure A.7: Analysed XRD pattern for milled MgAl-CO_3 LDH, with two passes through the mill.

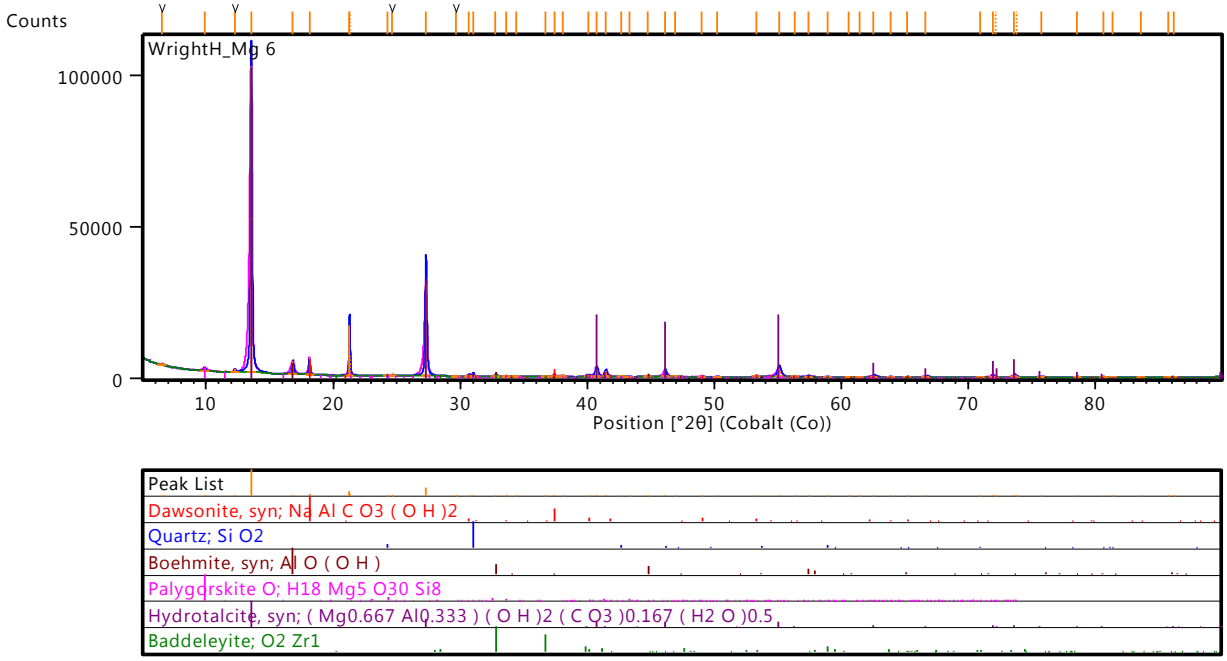

Figure A.8: Analysed XRD pattern for milled MgAl-CO_3 LDH, with six passes through the mill.

Appendix 5: Standard Deviations and Coefficient of Error for PSA tests.

Table A.3: Standard Deviation and Coefficient of Variance for PSA data

LDH Sample	Mill Passes		Run 1 (µm)	Run 2 (µm)	Run 3 (µm)	Mean (µm)	Standard Deviation	Coefficient of Variance
$MgAlCO_3$	0	D10	2.48	2.47	2.50	2.48	0.01	0.50
		D50	10.20	9.96	10.30	10.15	0.14	1.41
		D90	59.00	59.30	63.40	60.57	2.01	3.31
	1	D10	1.92	2.01	2.02	1.98	0.04	2.27
		D50	5.79	5.95	6.02	5.92	0.10	1.63
		D90	33.50	28.20	28.00	29.90	2.55	8.52
	2	D10	1.32	1.60	1.28	1.40	0.14	10.17
		D50	5.30	5.55	5.08	5.31	0.19	3.62
		D90	15.90	16.80	16.50	16.40	0.37	2.28
	6	D10	0.95	0.91	0.90	0.92	0.02	2.20
		D50	4.13	3.70	3.64	3.82	0.22	5.71
		D90	15.80	13.20	13.80	14.27	1.11	7.79
$CaAlCO_3$	0	D10	3.82	3.35	3.55	3.57	0.19	5.39
		D50	11.20	10.10	10.20	10.50	0.50	4.73
		D90	40.80	35.40	32.70	36.30	3.37	9.28
	1	D10	2.64	2.64	2.70	2.66	0.03	1.06
		D50	8.12	8.28	8.42	8.27	0.12	1.48
		D90	33.50	37.70	39.40	36.87	2.48	6.73
	2	D10	2.51	2.46	2.45	2.47	0.03	1.06
		D50	7.61	7.35	7.47	7.48	0.11	1.42
		D90	35.70	30.10	32.40	32.73	2.30	7.02
	6	D10	2.30	2.27	2.19	2.25	0.05	2.06
		D50	6.65	6.54	6.39	6.53	0.11	1.63
		D90	27.40	25.90	23.60	25.63	1.56	6.10

Appendix 6: PSA graphs for dry PSA tests.

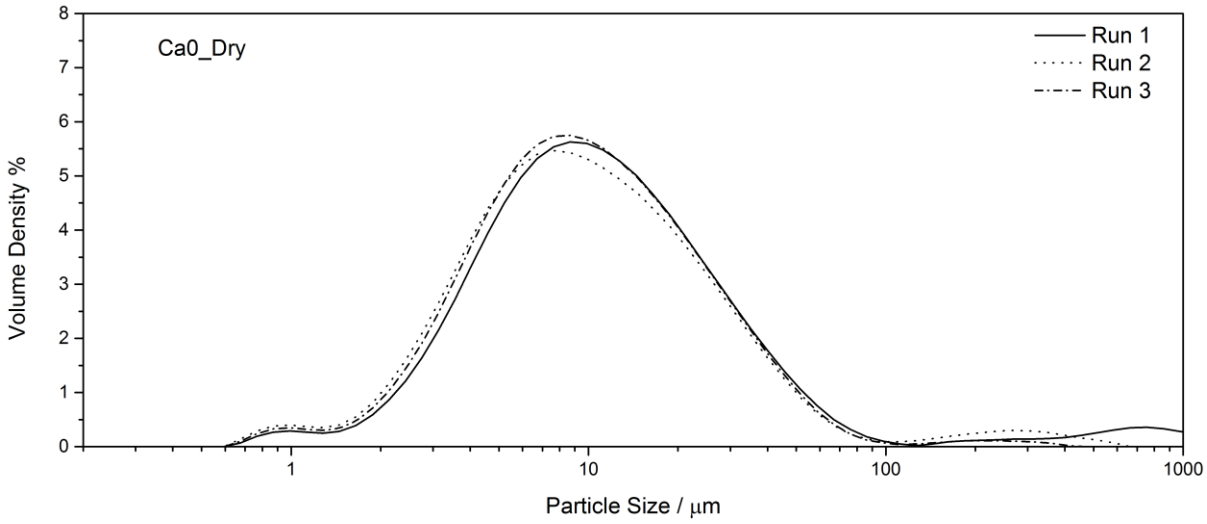

Figure A.9: Particle size distribution data for the Dry CaAl-CO_3 LDH with zero passes through the mill.

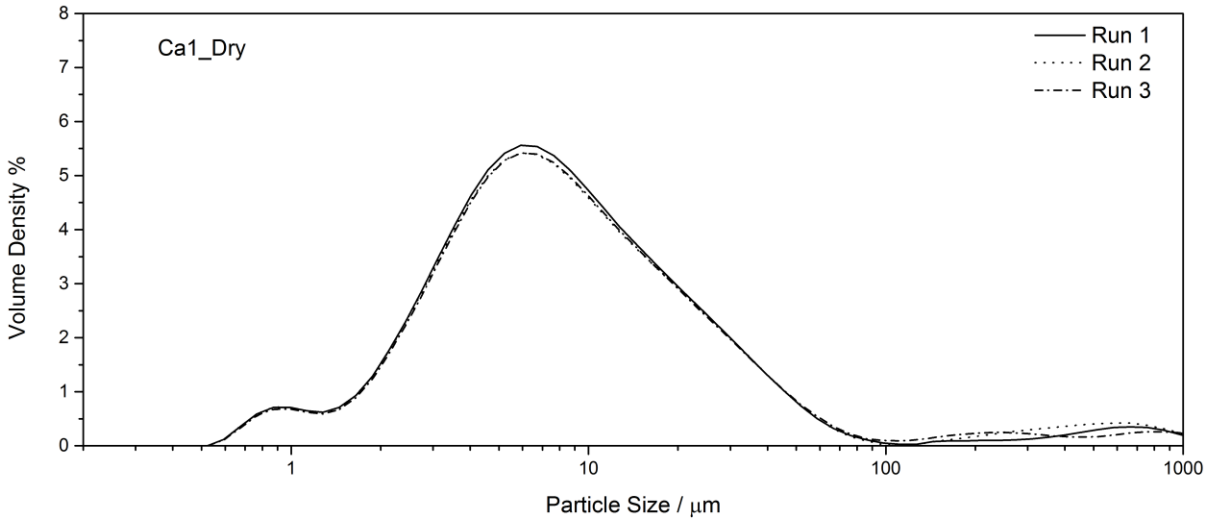

Figure A.10: Particle size distribution data for the Dry CaAl-CO_3 LDH with one pass through the mill.

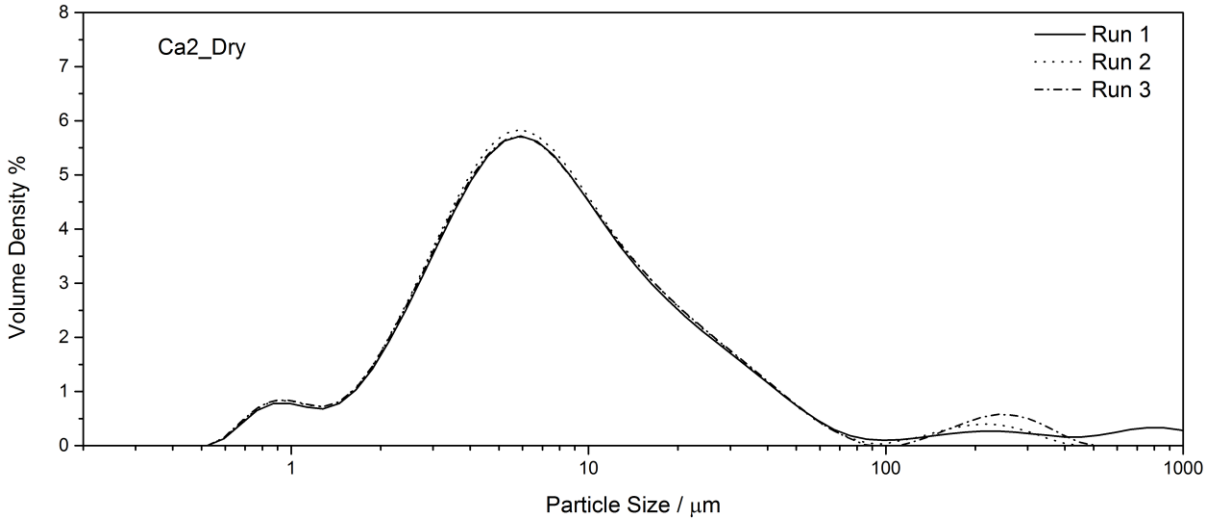

Figure A.11: Particle size distribution data for the Dry CaAl-CO_3 LDH with two passes through the mill.

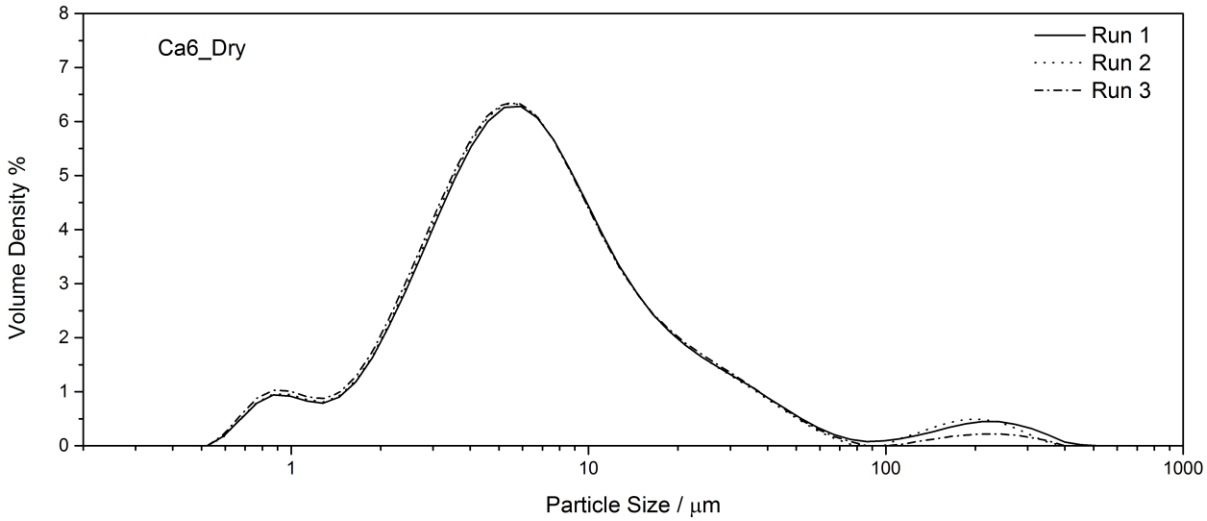

Figure A.12: Particle size distribution data for the Dry CaAl-CO_3 LDH with six passes through the mill.

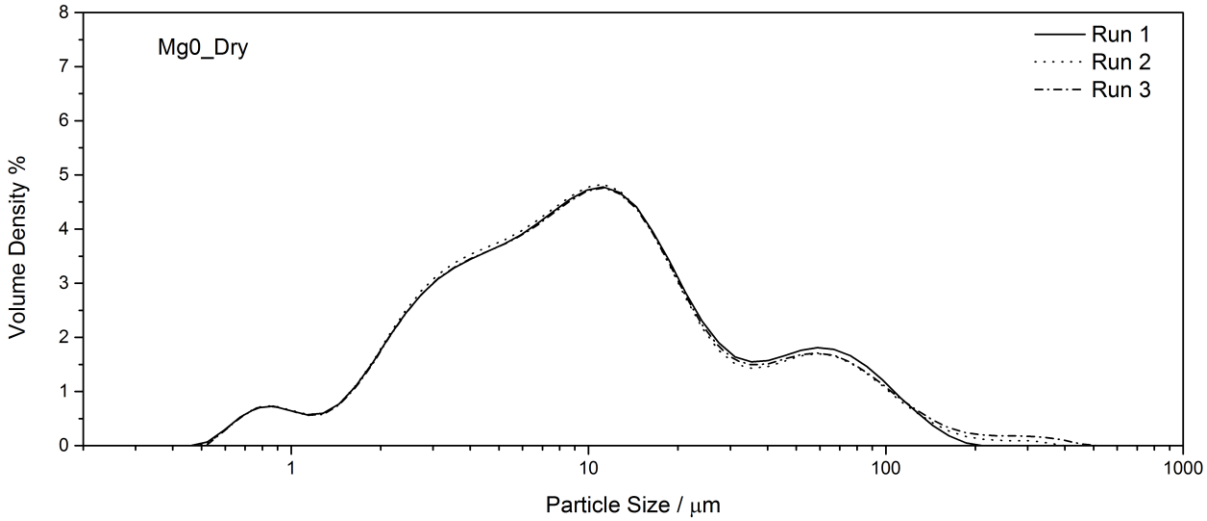

Figure A.13: Particle size distribution data for the Dry MgAl-CO_3 LDH with zero passes through the mill.

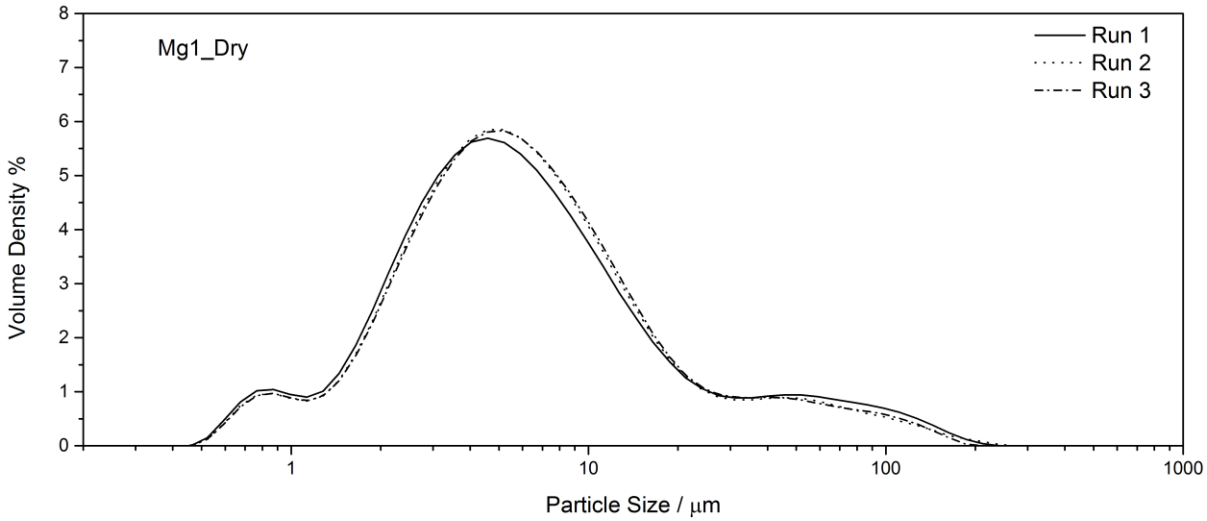

Figure A.14: Particle size distribution data for the Dry MgAl-CO_3 LDH with one pass through the mill.

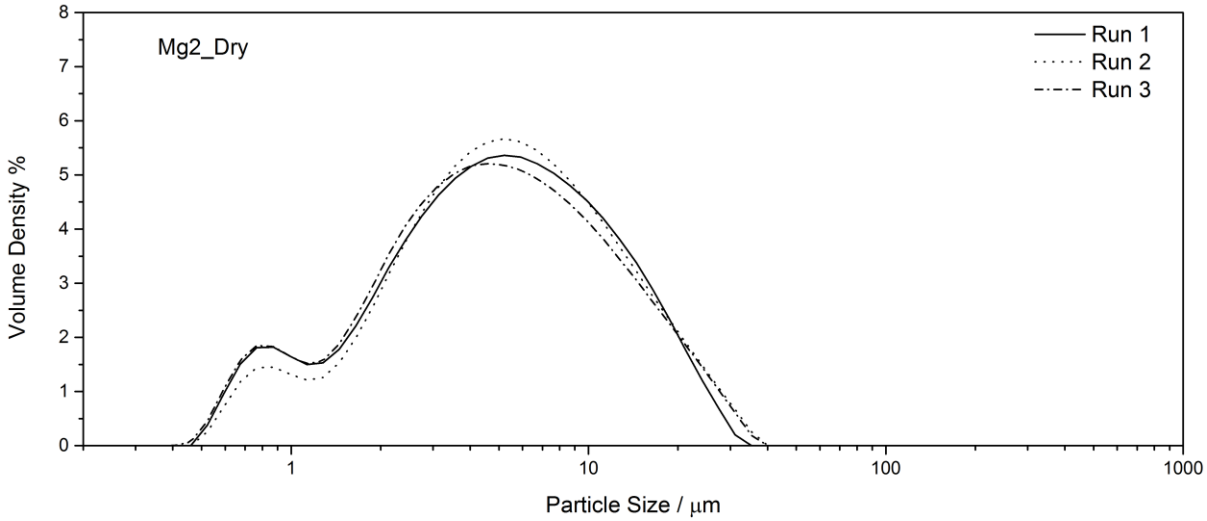

Figure A.15: Particle size distribution data for the Dry MgAl-CO_3 LDH with two passes through the mill.

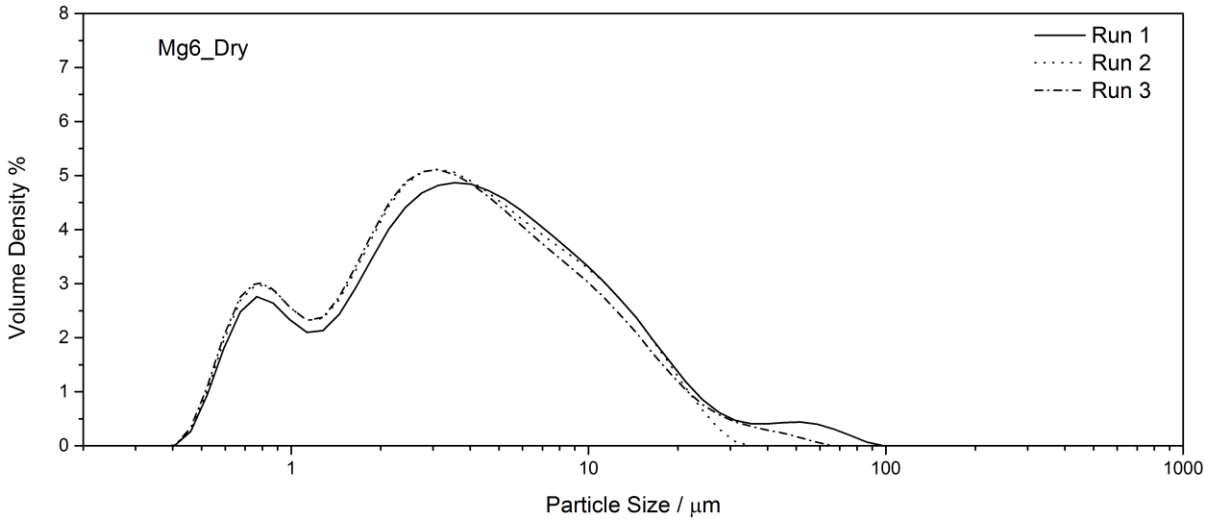

Figure A.16: Particle size distribution data for the Dry MgAl-CO_3 LDH with six passes through the mill.

Appendix 7: Acid reactivity Test Data

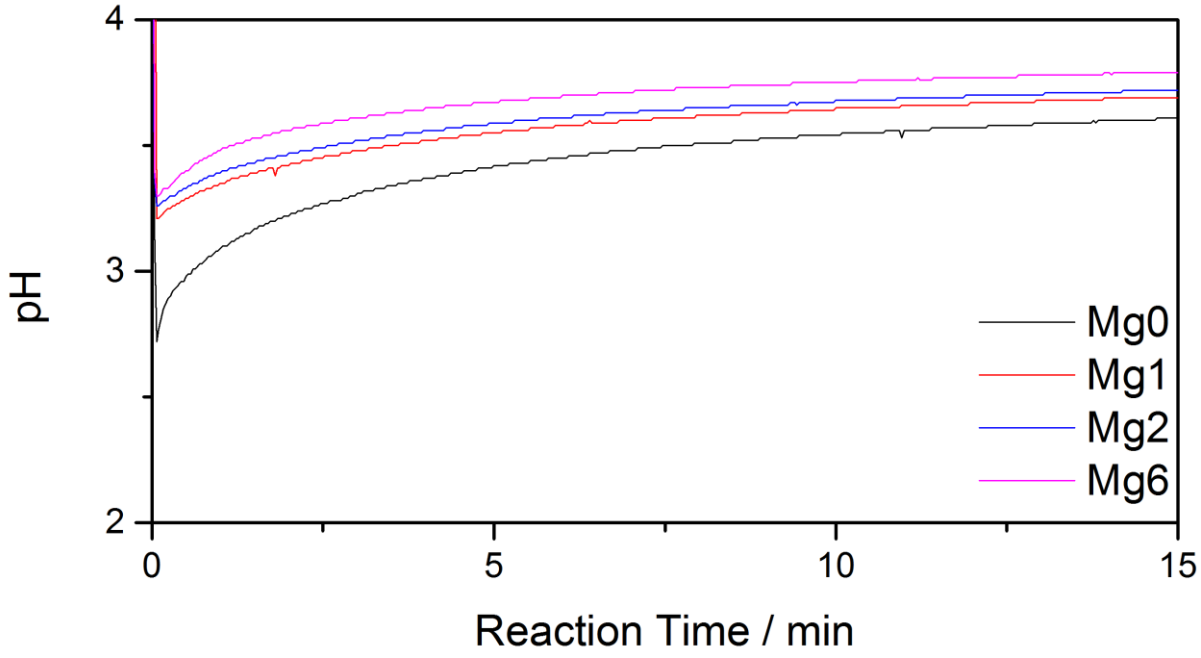

Figure A.17: Acid reactivity test data for MgAl LDH.

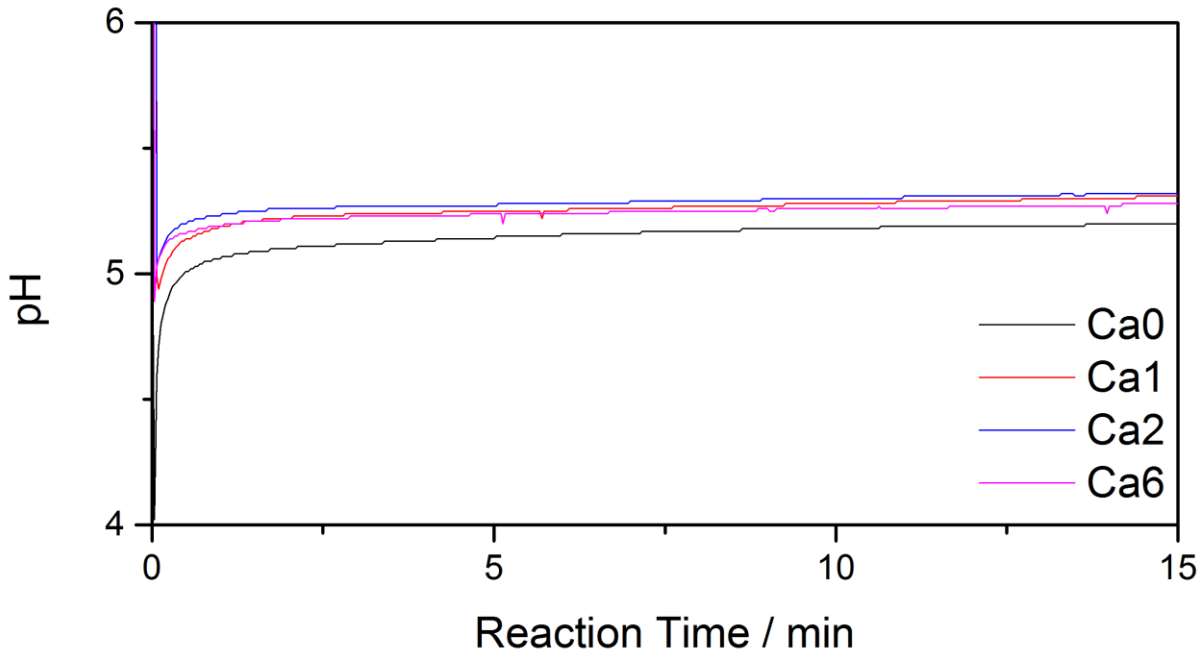

Figure A.18: Acid reactivity test data for CaAl LDH.

Appendix 8: Conductivity Data for HCl Degradation Testing.

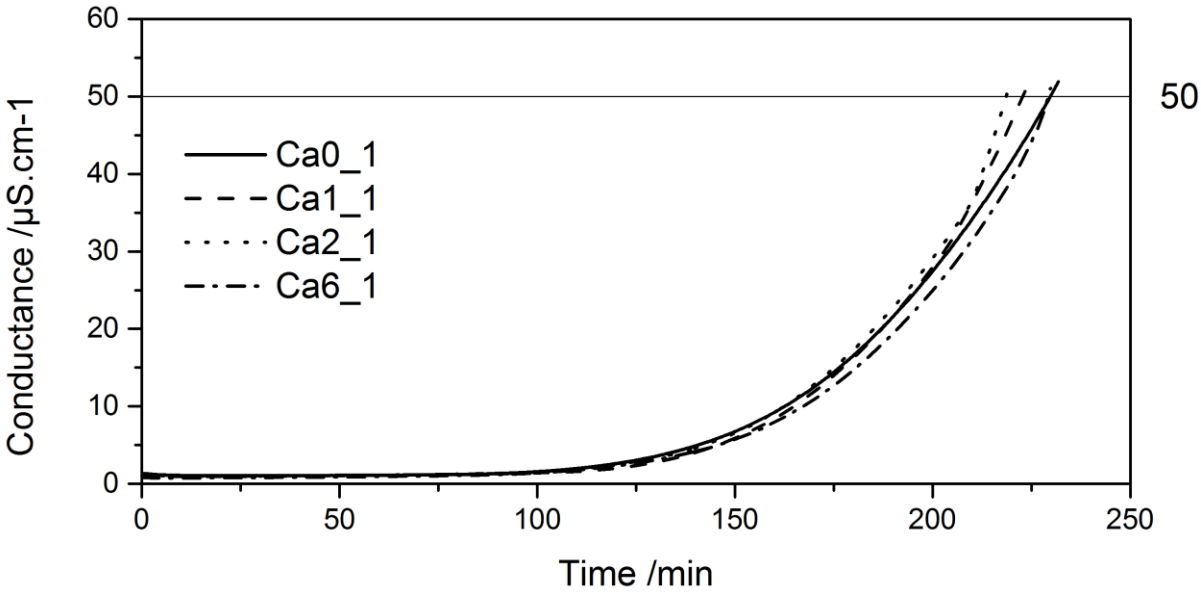

Figure A.19: PVC Thermomat conductivity data for CaAl-CO_3 LDH, at 1 PHR concentration and varying mill passes.

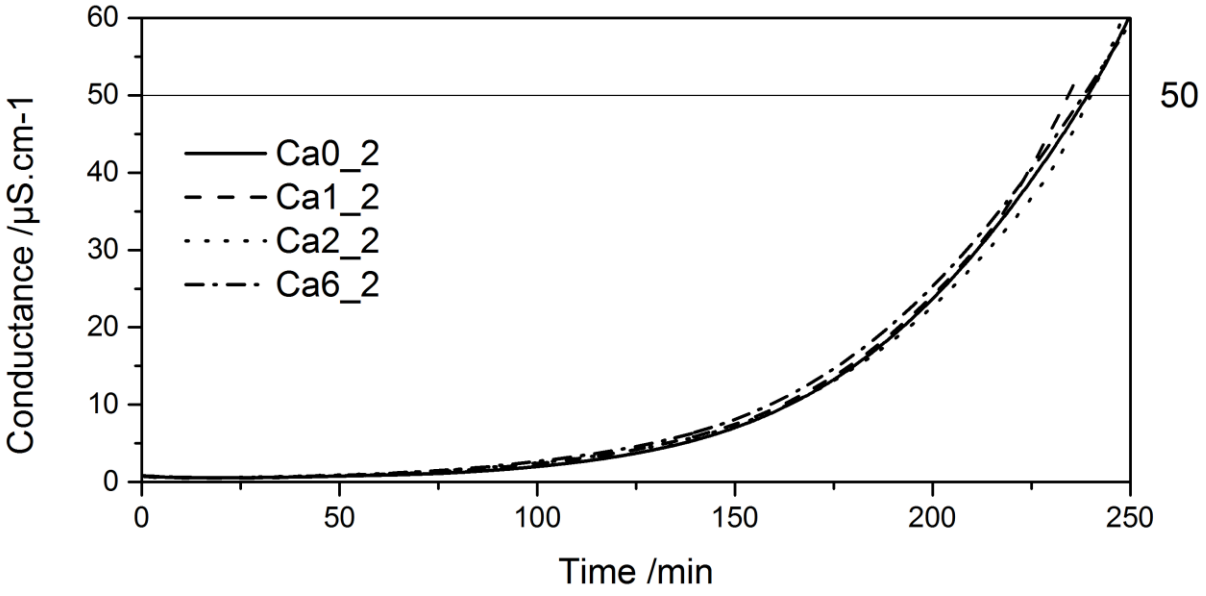

Figure A.20: PVC Thermomat conductivity data for CaAl-CO_3 LDH, at 2 PHR concentration and varying mill passes.

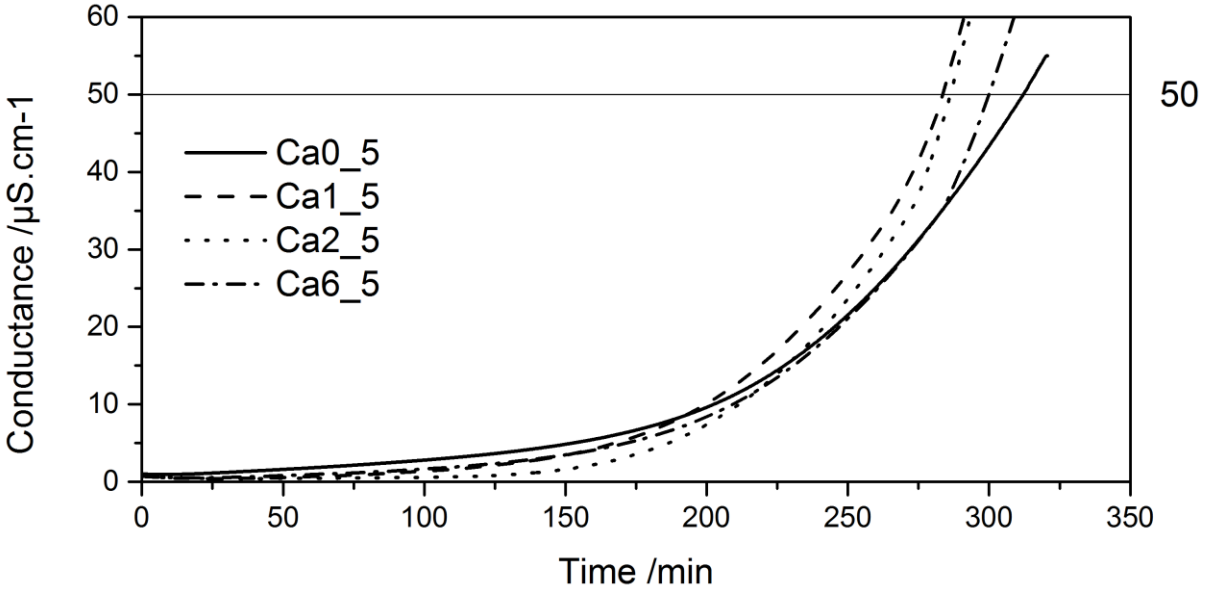

Figure A.21: PVC Thermomat conductivity data for CaAl-CO_3 LDH, at 5 PHR concentration and varying mill passes.

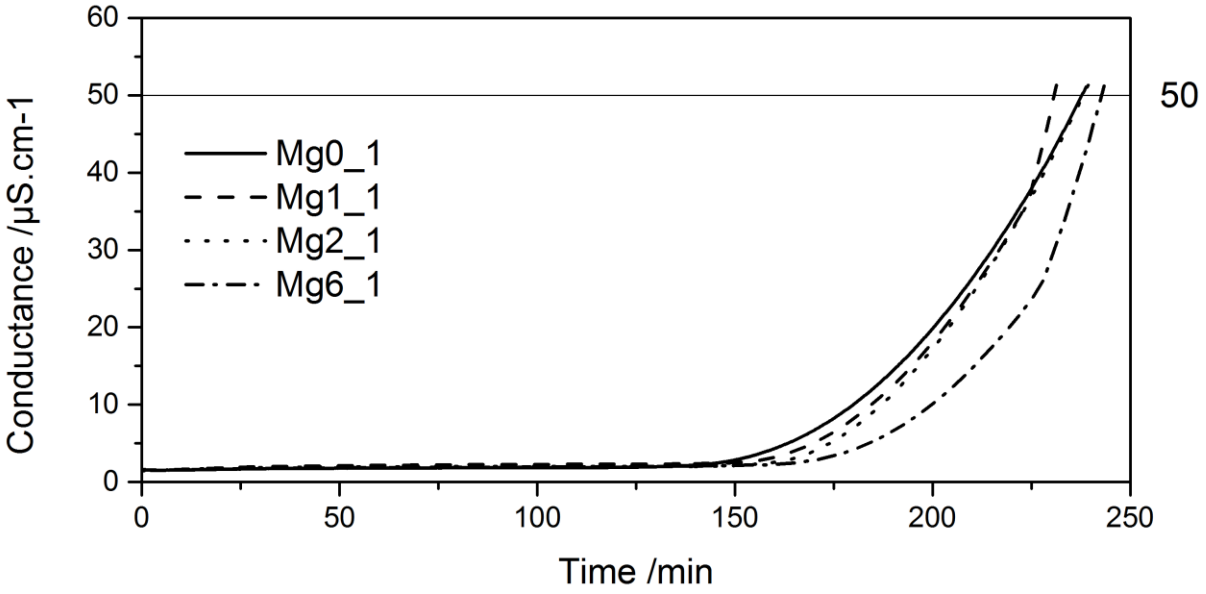

Figure A.22: PVC Thermomat conductivity data for MgAl-CO_3 LDH, at 1 PHR concentration and varying mill passes.

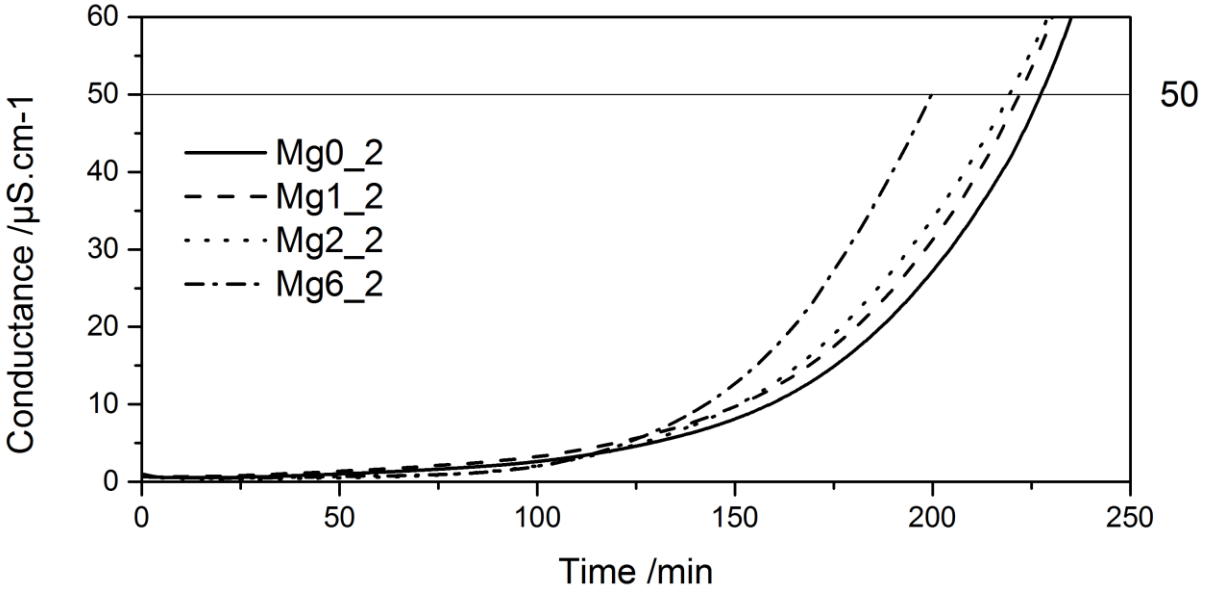

Figure A.23: PVC Thermomat conductivity data for MgAl-CO_3 LDH, at 2 PHR concentration and varying mill passes.

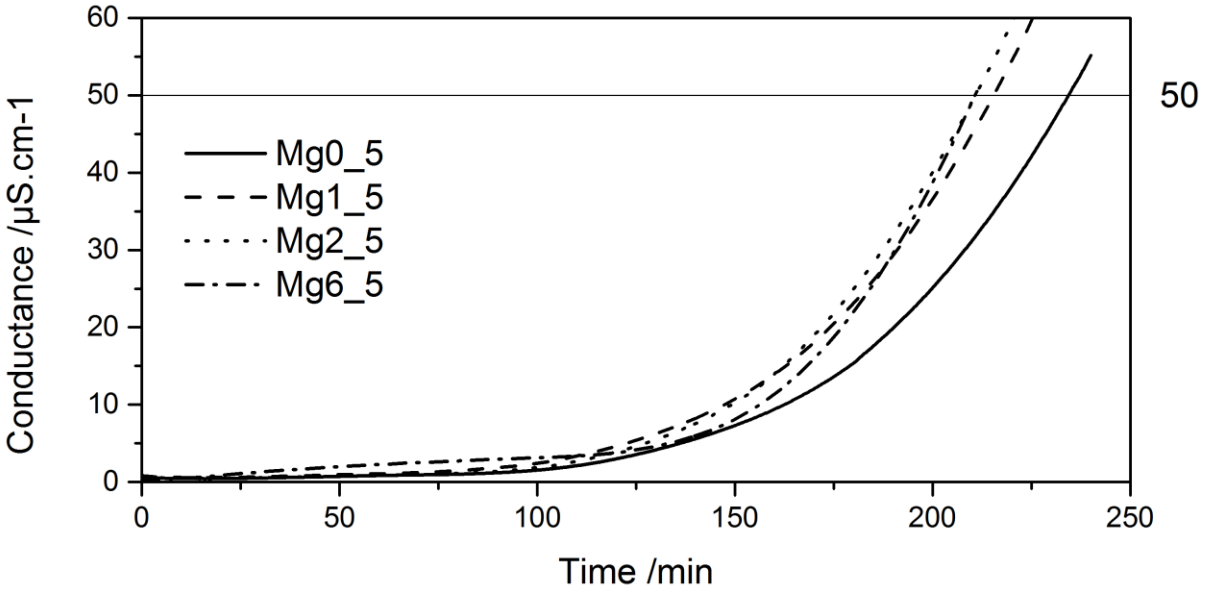

Figure A.24: PVC Thermomat conductivity data for CaAl-CO_3 LDH, at 5 PHR concentration and varying mill passes.

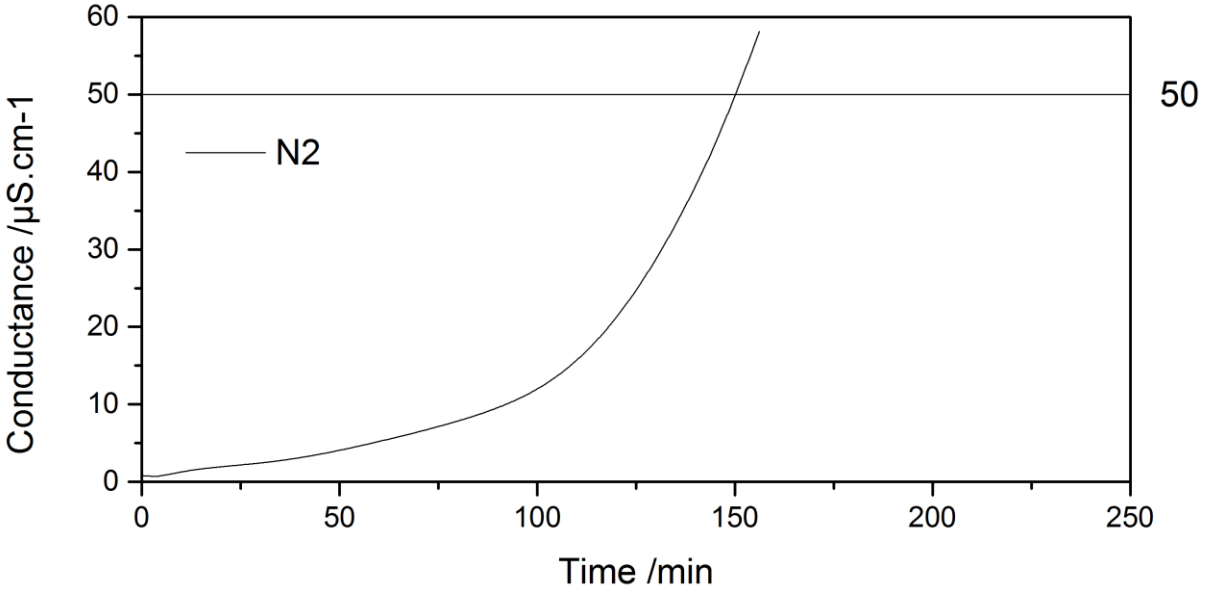

Figure A.25: PVC Thermomat conductivity data for unstabilised PVC.

Appendix 9: Raw Photos of Metrastat Degraded PVC

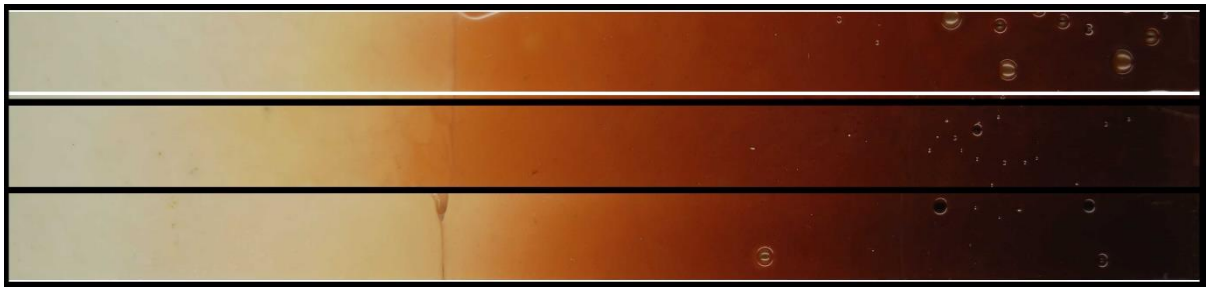

Figure A.26: Photos of PVC strips with no LDH stabiliser.

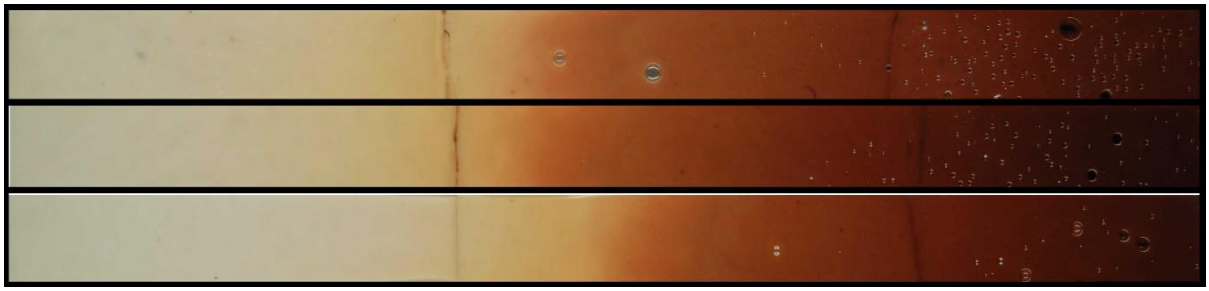

Figure A.27: Photos of PVC strips with MgAl LDH stabiliser at 1 PHR, with 0 mill passes.

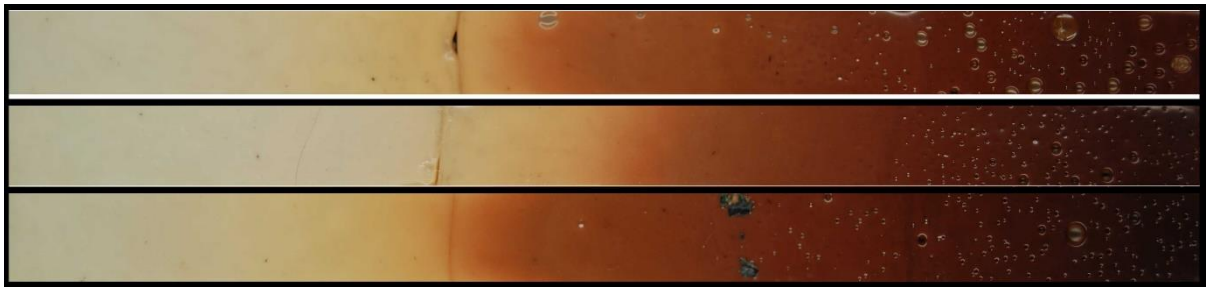

Figure A.28: Photos of PVC strips with MgAl LDH stabiliser at 1 PHR, with 1 mill pass.

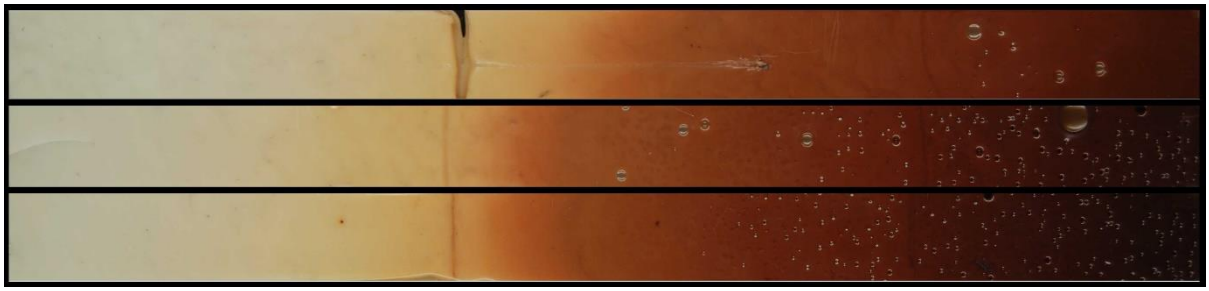

Figure A.29: Photos of PVC strips with MgAl LDH stabiliser at 1 PHR, with 2 mill passes.

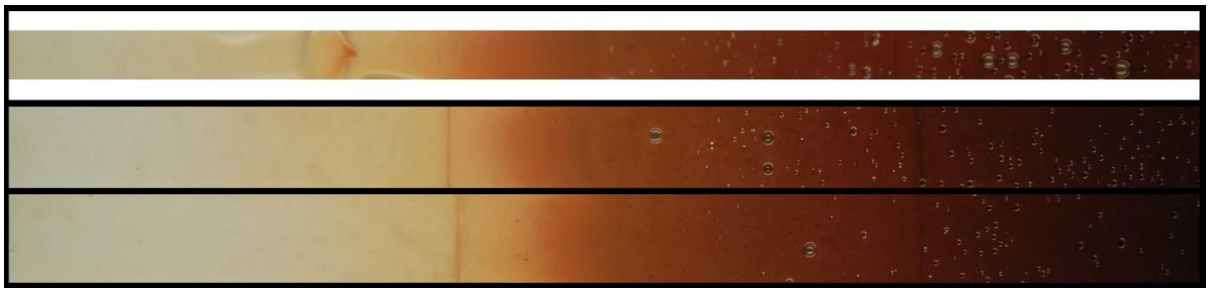

Figure A.30: Photos of PVC strips with MgAl LDH stabiliser at 1 PHR, with 6 mill passes.

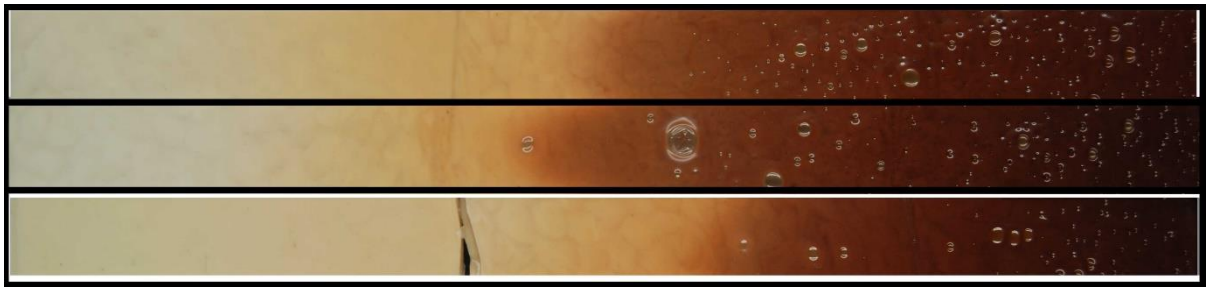

Figure A.31: Photos of PVC strips with MgAl LDH stabiliser at 2 PHR, with 0 mill passes.

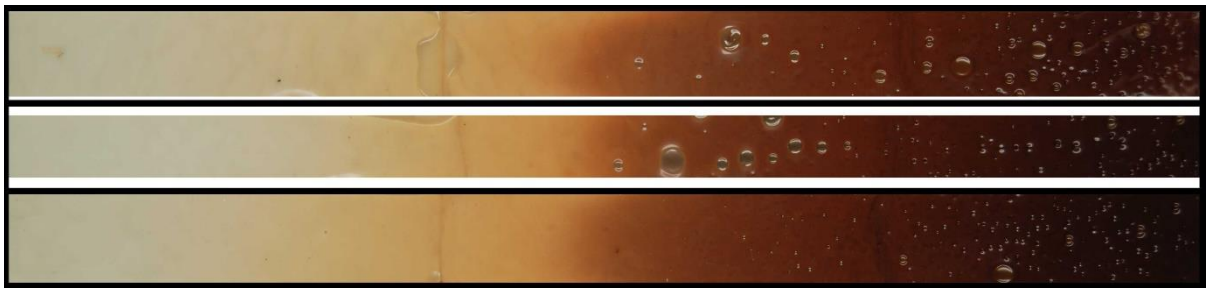

Figure A.32: Photos of PVC strips with MgAl LDH stabiliser at 2 PHR, with 1 mill pass.

Figure A.33: Photos of PVC strips with MgAl LDH stabiliser at 2 PHR, with 2 mill passes.

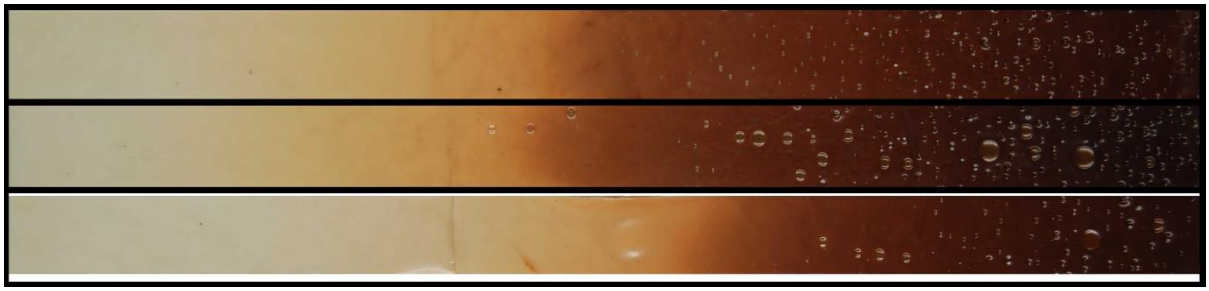

Figure A.34: Photos of PVC strips with MgAl LDH stabiliser at 2 PHR, with 6 mill passes.

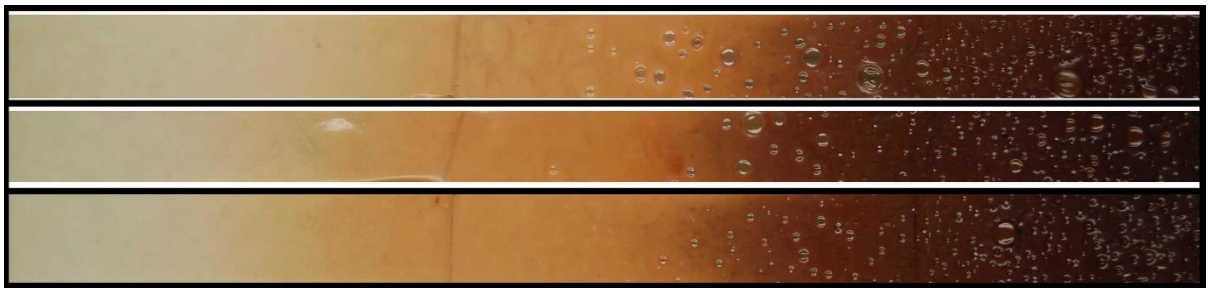

Figure A.35: Photos of PVC strips with MgAl LDH stabiliser at 5 PHR, with 0 mill passes.

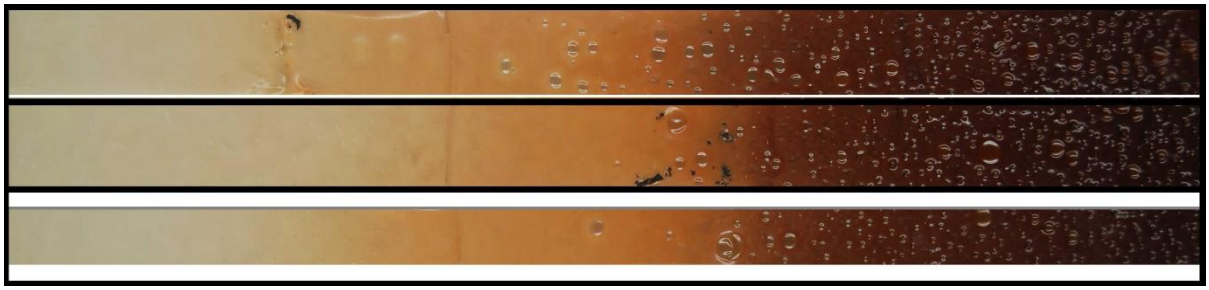

Figure A.36: Photos of PVC strips with MgAl LDH stabiliser at 5 PHR, with 1 mill pass.

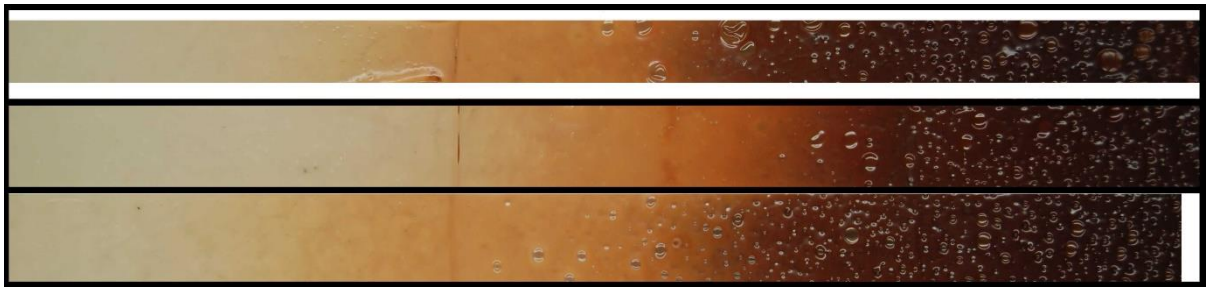

Figure A.37: Photos of PVC strips with MgAl LDH stabiliser at 5 PHR, with 2 mill passes.

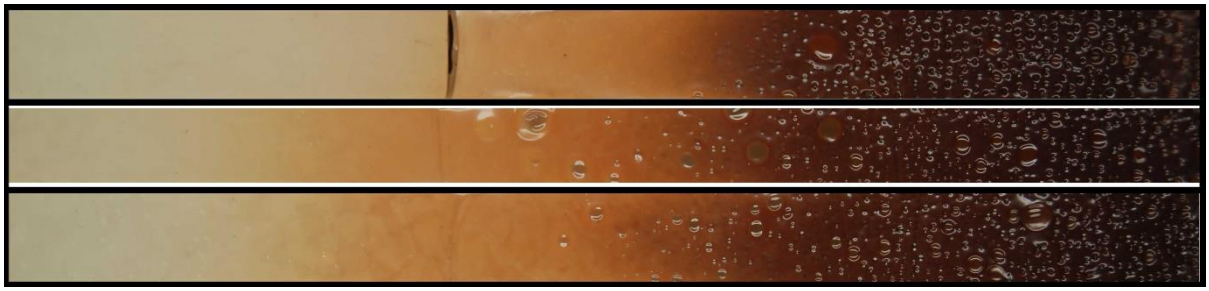

Figure A.38: Photos of PVC strips with MgAl LDH stabiliser at 5 PHR, with 6 mill passes.

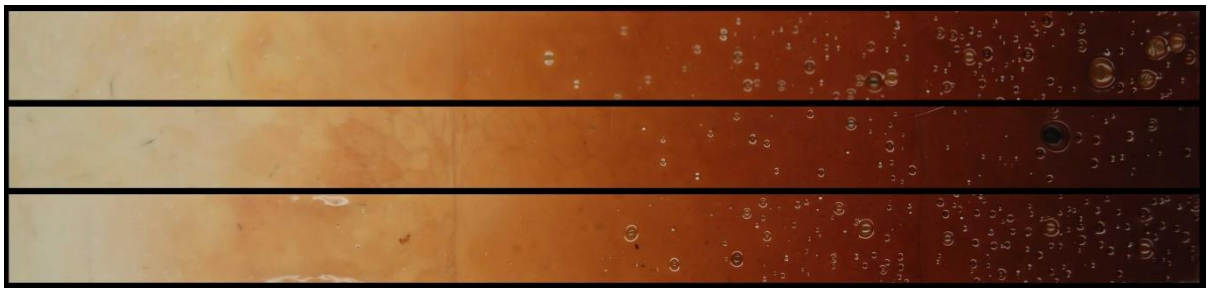

Figure A.39: Photos of PVC strips with CaAl LDH stabiliser at 1 PHR, with 0 mill passes.

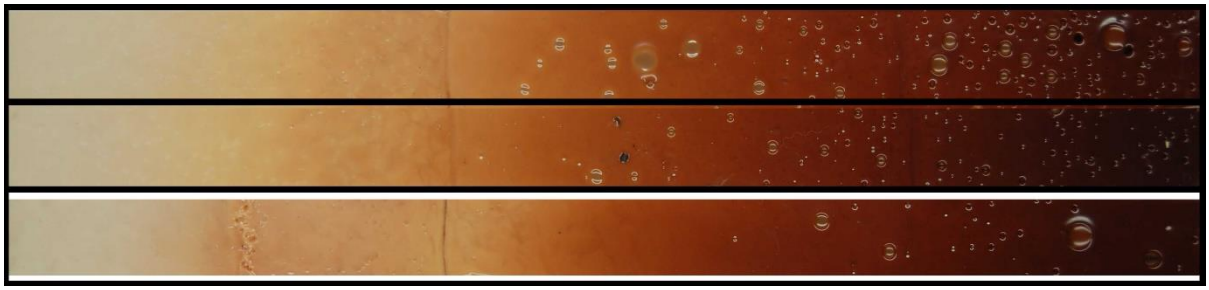

Figure A.40: Photos of PVC strips with CaAl LDH stabiliser at 1 PHR, with 1 mill pass.

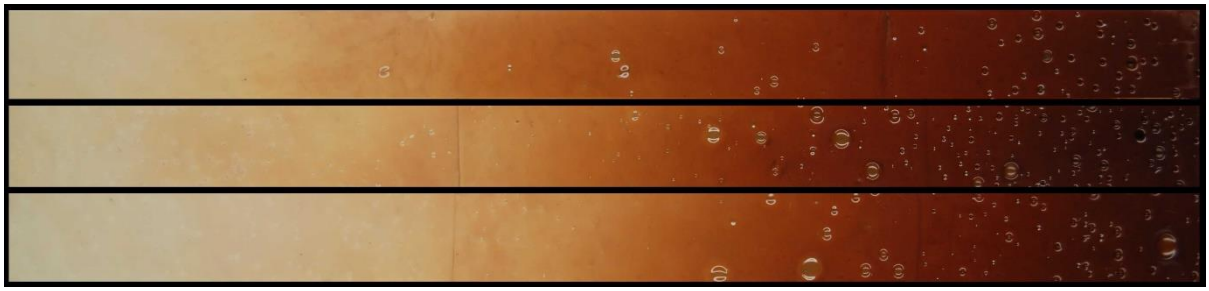

Figure A.41: Photos of PVC strips with CaAl LDH stabiliser at 1 PHR, with 2 mill passes.

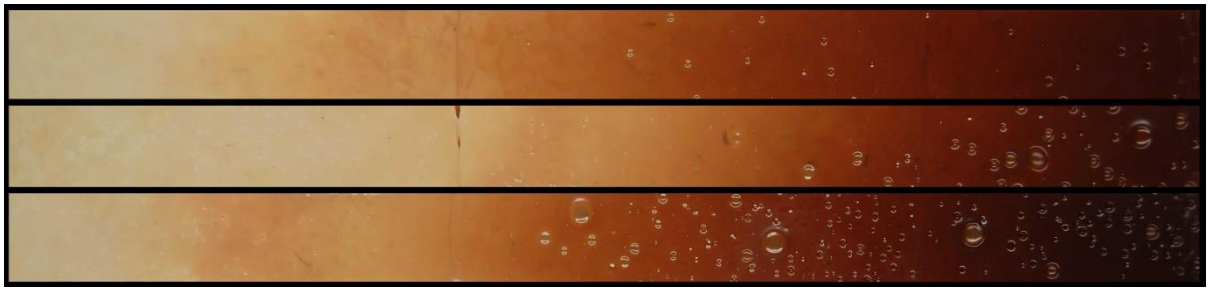

Figure A.42: Photos of PVC strips with CaAl LDH stabiliser at 1 PHR, with 6 mill passes.

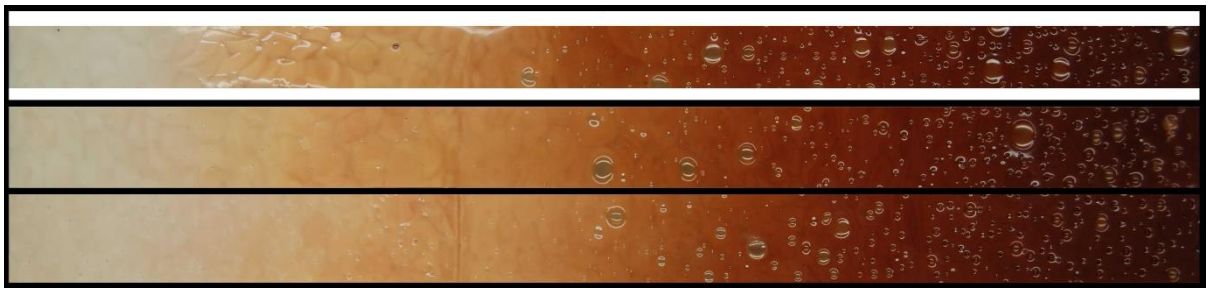

Figure A.43: Photos of PVC strips with CaAl LDH stabiliser at 2 PHR, with 0 mill passes.

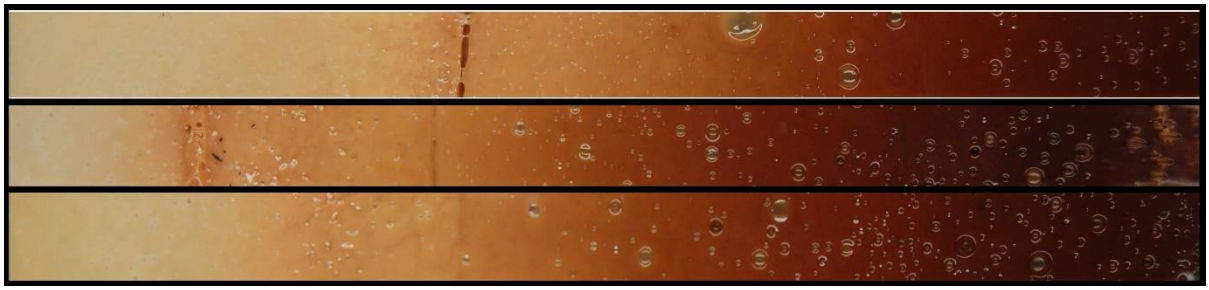

Figure A.44: Photos of PVC strips with CaAl LDH stabiliser at 2 PHR, with 1 mill pass.

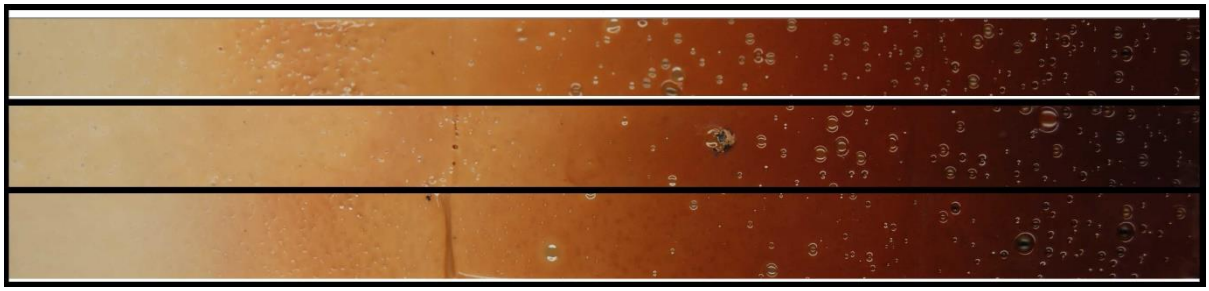

Figure A.45: Photos of PVC strips with CaAl LDH stabiliser at 2 PHR, with 2 mill passes.

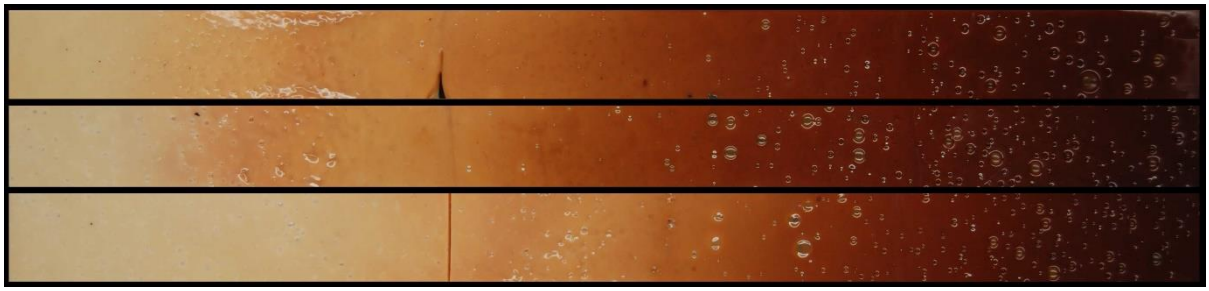

Figure A.46: Photos of PVC strips with CaAl LDH stabiliser at 2 PHR, with 6 mill passes.

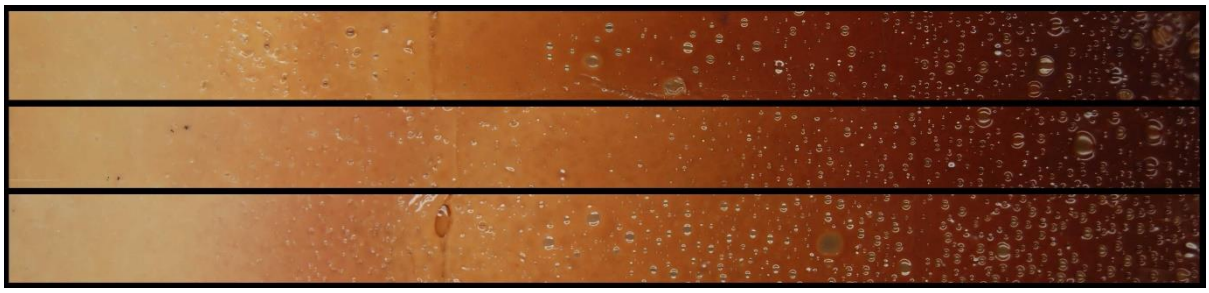

Figure A.47: Photos of PVC strips with CaAl LDH stabiliser at 5 PHR, with 0 mill passes.

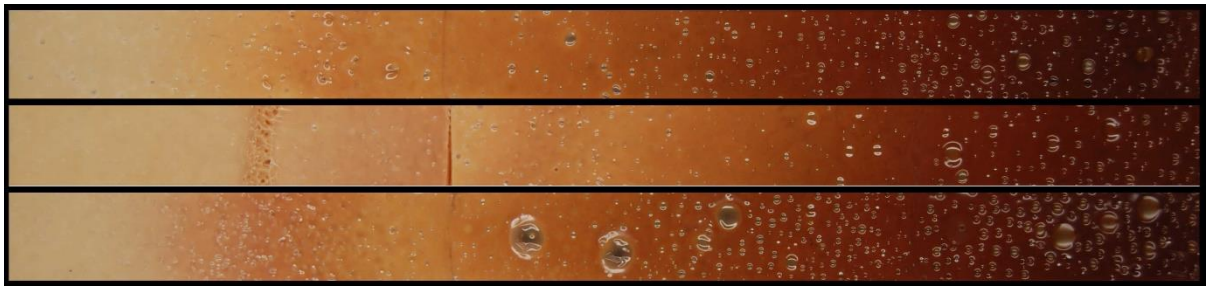

Figure A.48:: Photos of PVC strips with CaAl LDH stabiliser at 5 PHR, with 1 mill pass.

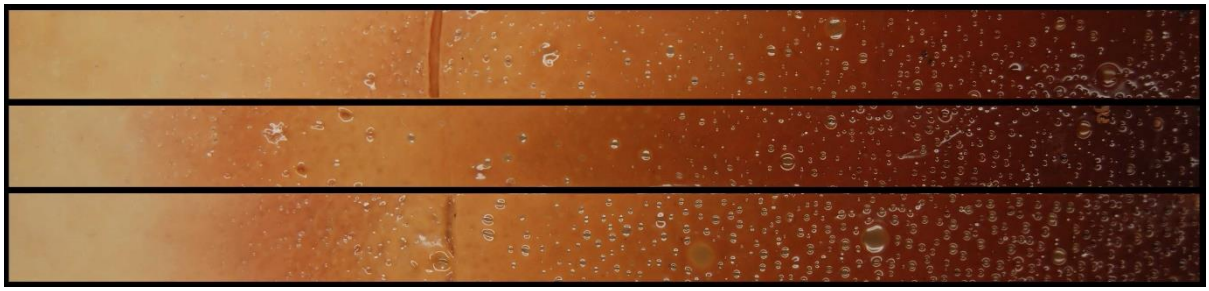

Figure A.49: Photos of PVC strips with CaAl LDH stabiliser at 5 PHR, with 2 mill passes.

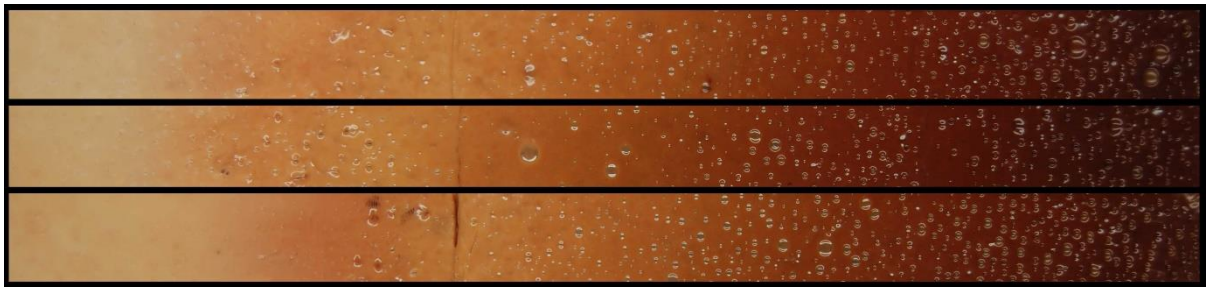

Figure A.50: Photos of PVC strips with CaAl LDH stabiliser at 5 PHR, with 5 mill passes.

Appendix 10: Raw Torque Data for the Haake Rheomix

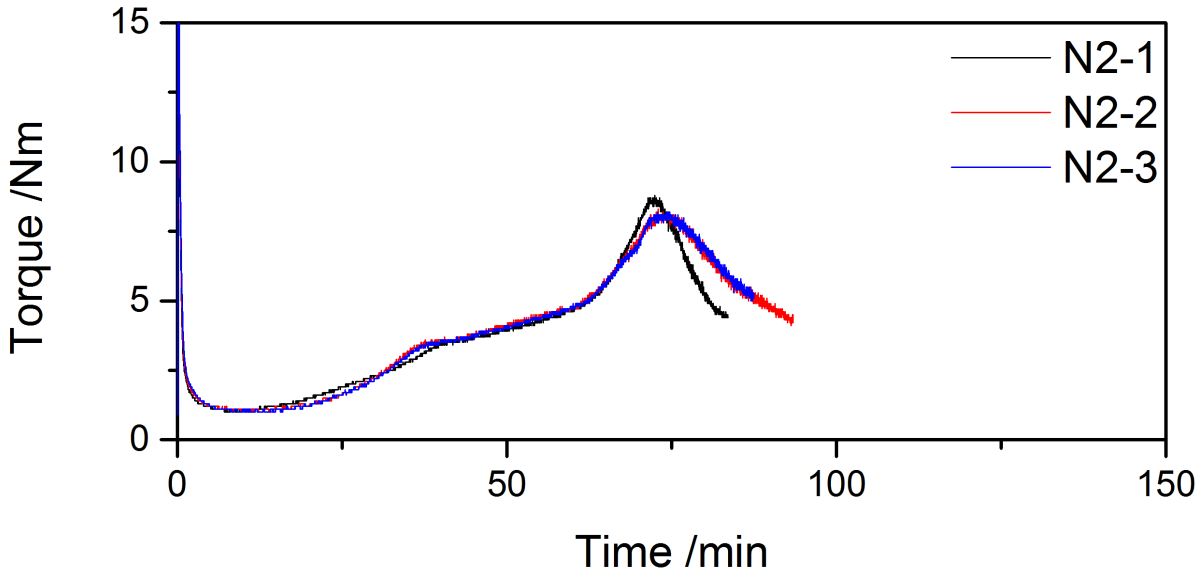

Figure A.51: Raw Torque degradation data for the PVC with no LDH stabiliser.

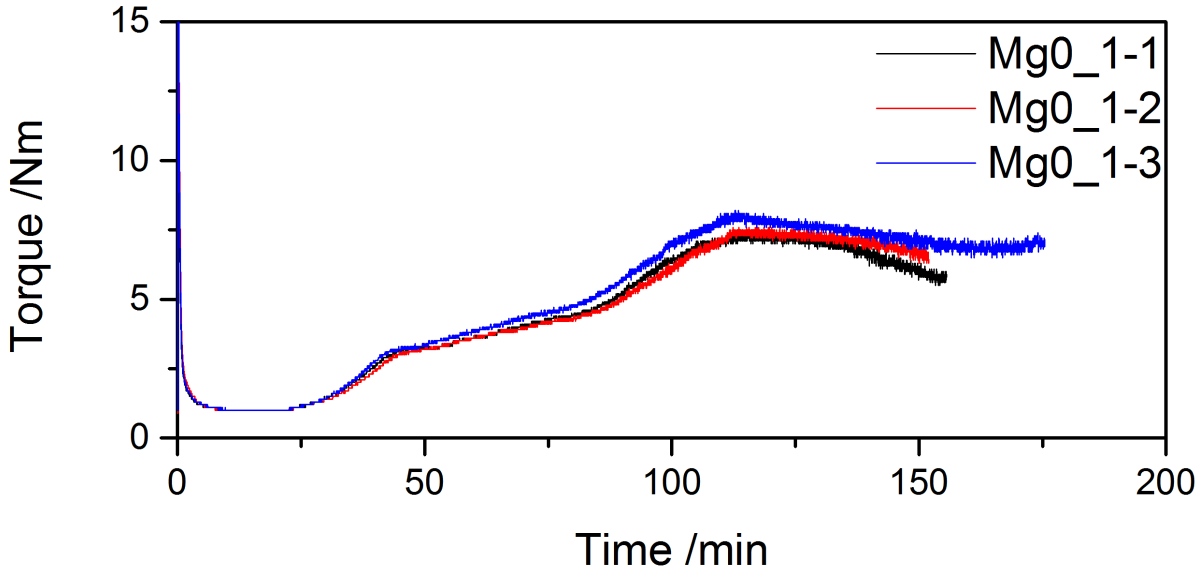

Figure A.52: Raw Torque degradation data for the MgAl LDH at 1 PHR, with 0 mill passes.

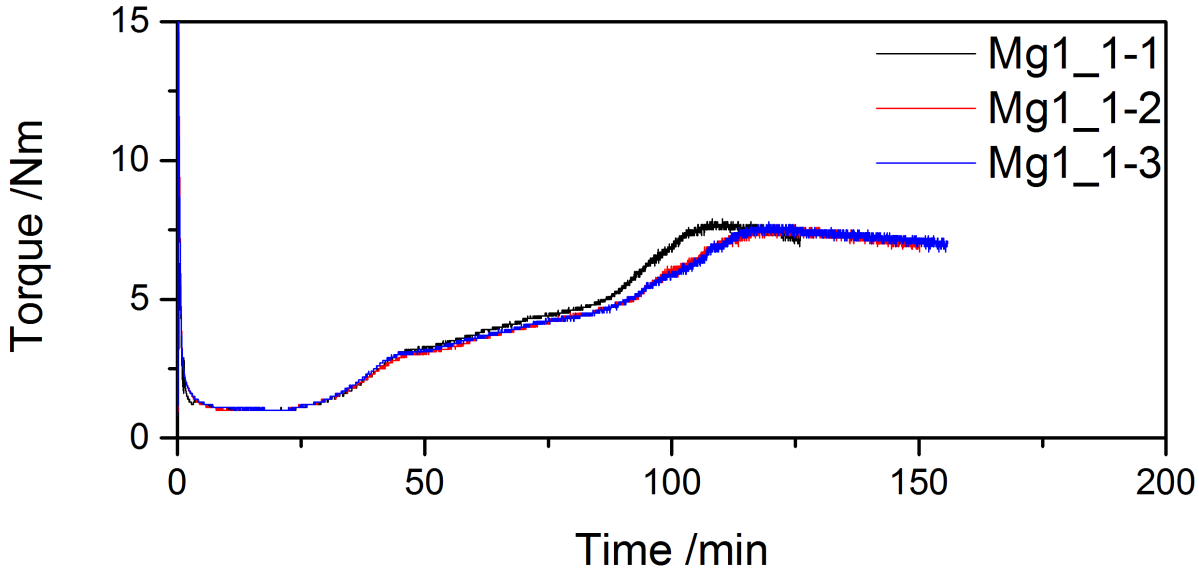

Figure A.53: Raw Torque degradation data for the MgAl LDH at 1 PHR, with 1 mill pass.

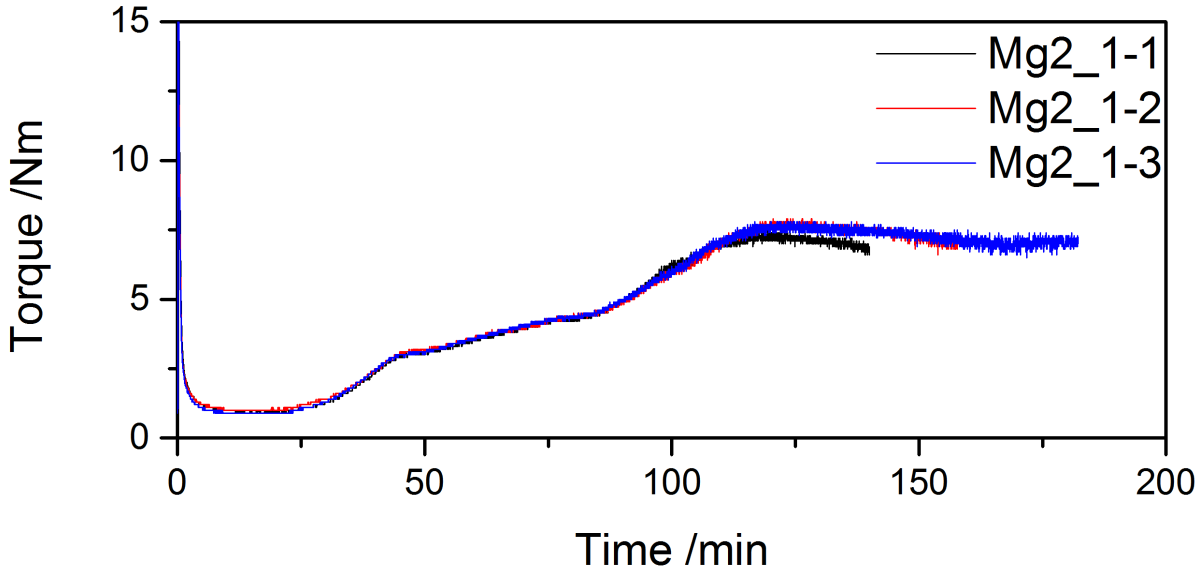

Figure A.54: Raw Torque degradation data for the MgAl LDH at 1 PHR, with 2 mill passes.

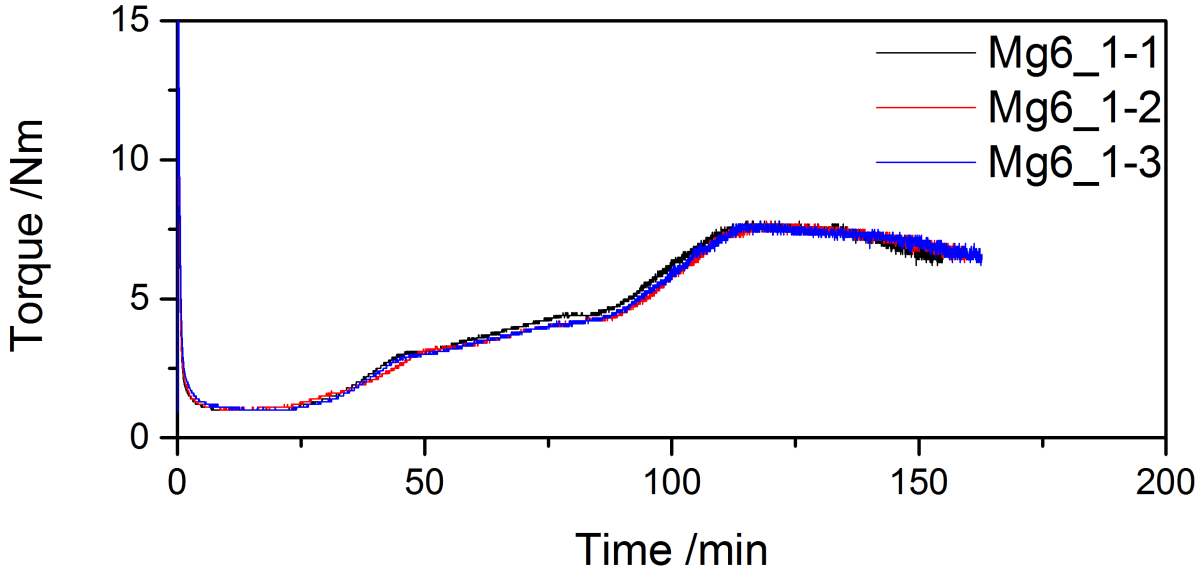

Figure A.55: Raw Torque degradation data for the MgAl LDH at 1 PHR, with 6 mill passes.

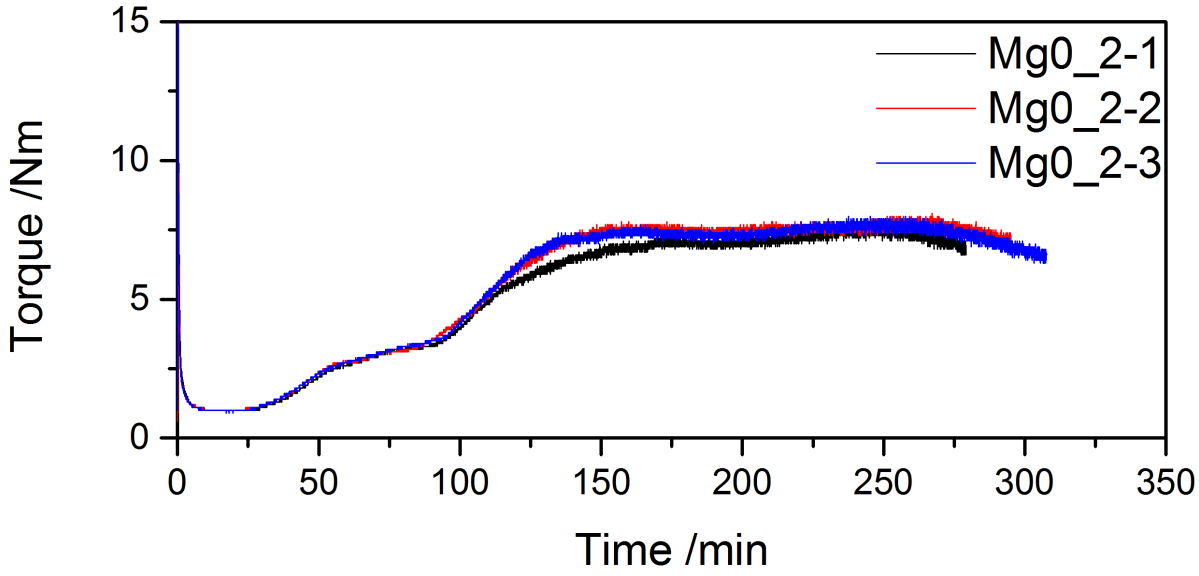

Figure A.56: Raw Torque degradation data for the MgAl LDH at 2 PHR, with 0 mill passes.

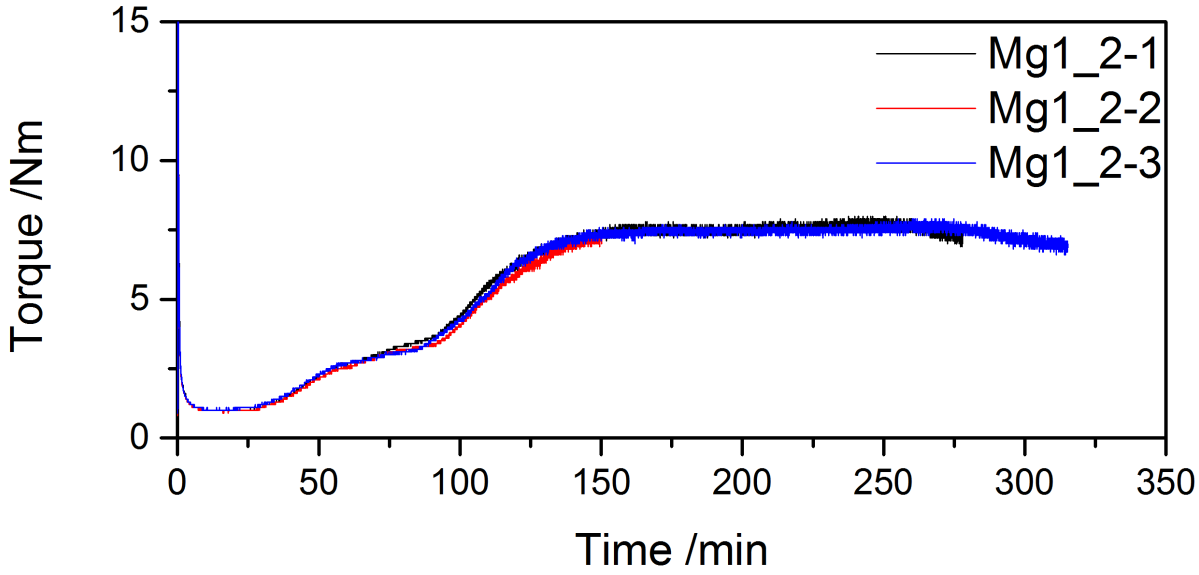

Figure A.57: Raw Torque degradation data for the MgAl LDH at 2 PHR, with 1 mill pass.

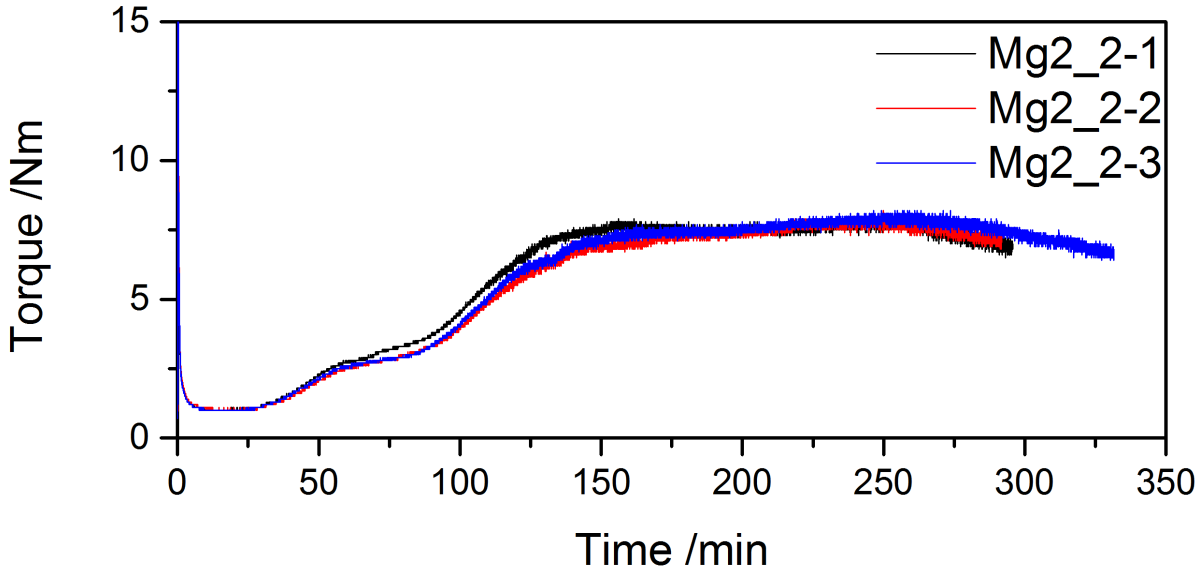

Figure A.58: Raw Torque degradation data for the MgAl LDH at 2 PHR, with 2 mill passes.

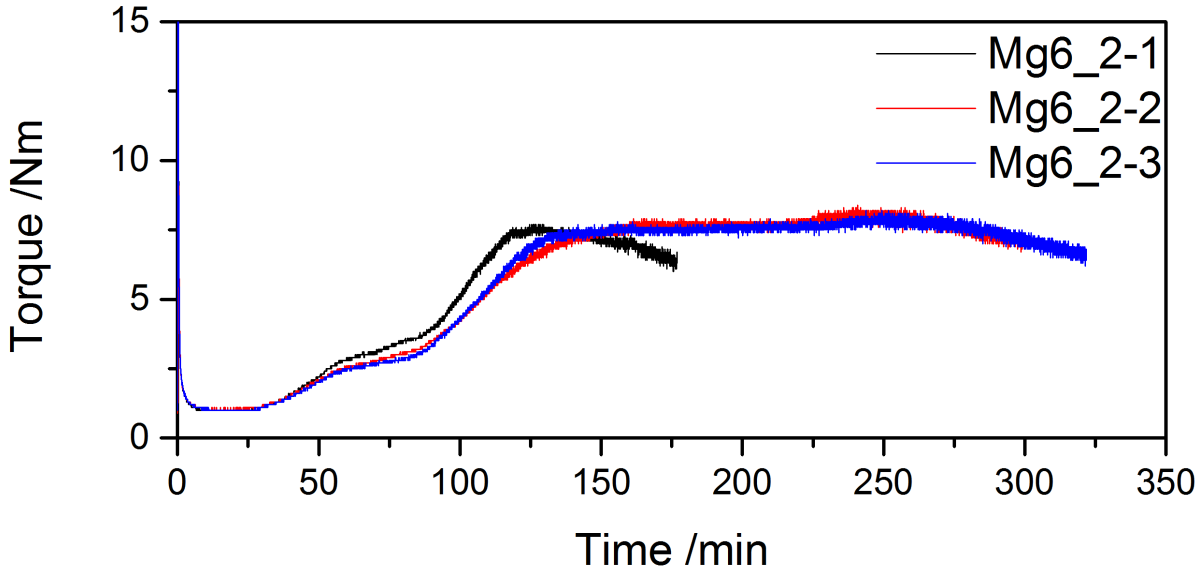

Figure A.59: Raw Torque degradation data for the MgAl LDH at 2 PHR, with 6 mill passes.

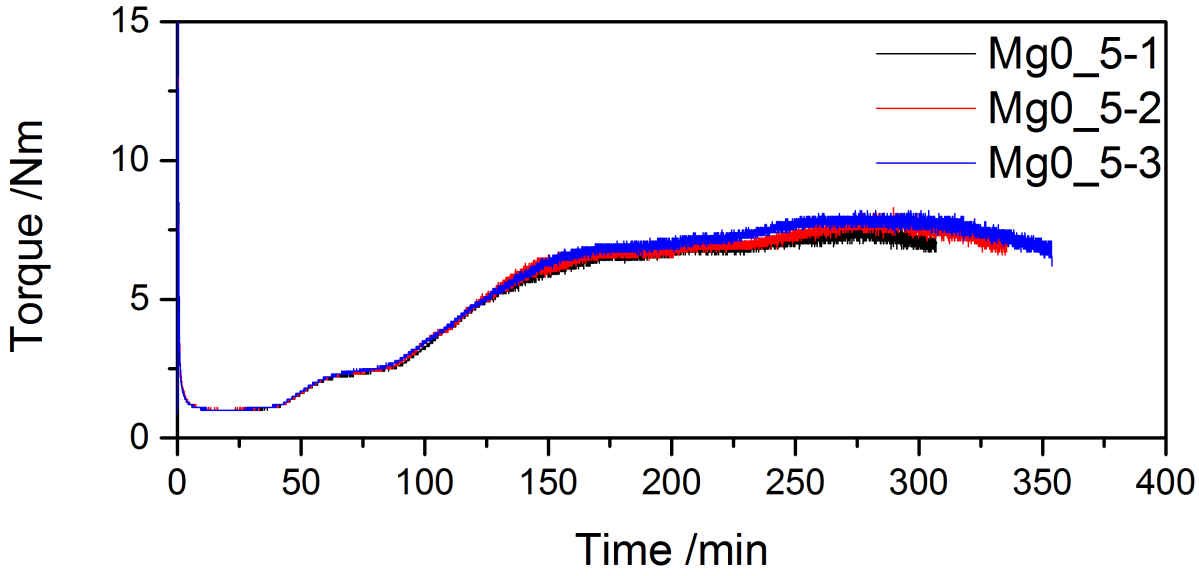

Figure A.60: Raw Torque degradation data for the MgAl LDH at 5 PHR, with 0 mill passes.

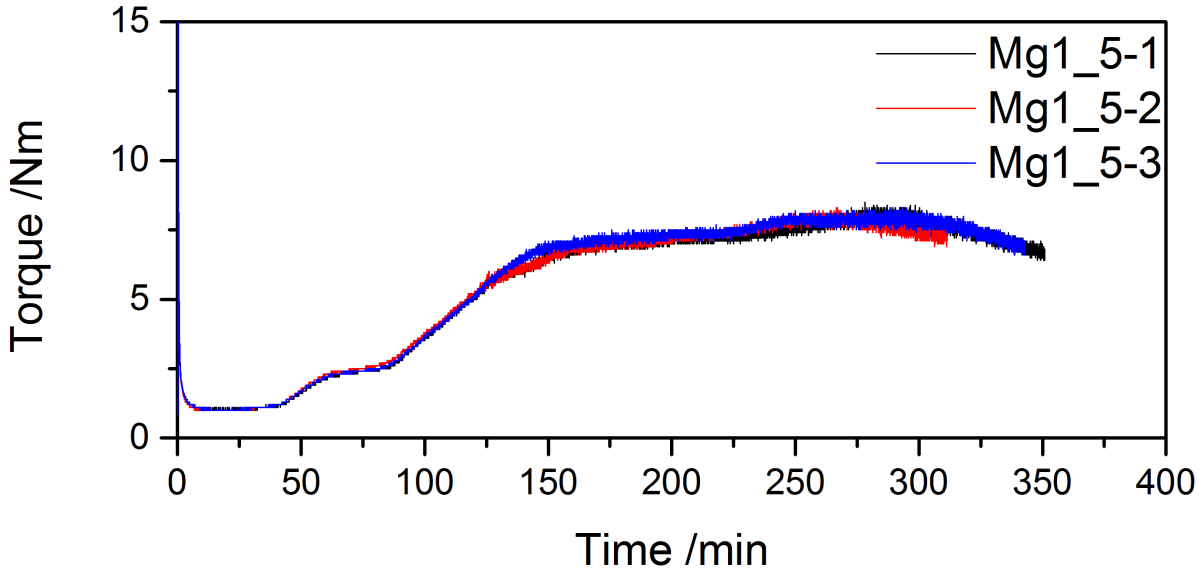

Figure A.61: Raw Torque degradation data for the MgAl LDH at 5 PHR, with 1 mill pass.

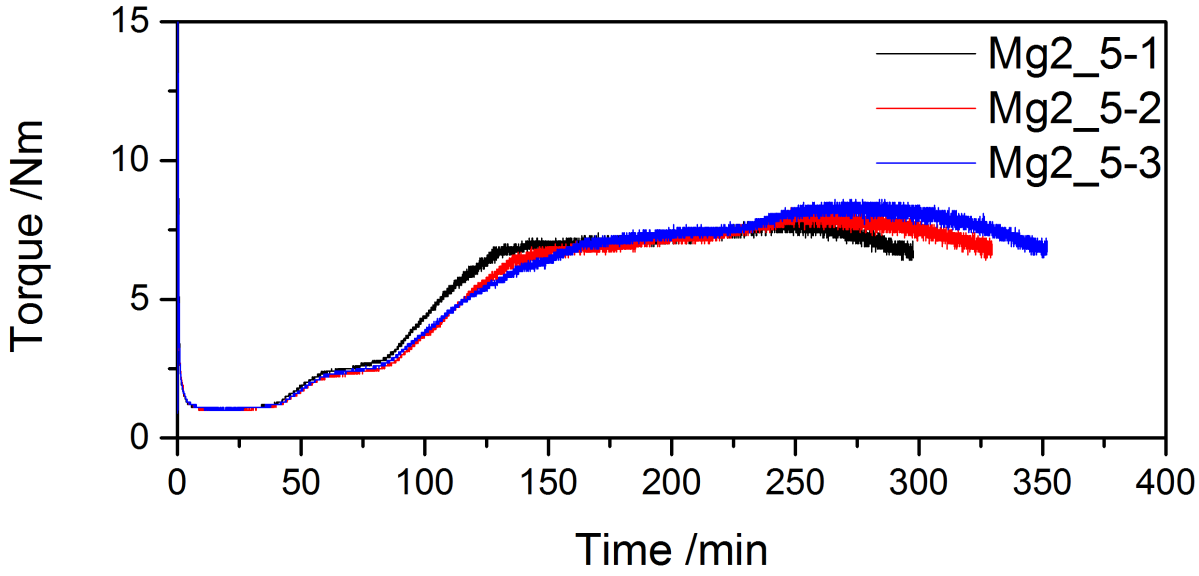

Figure A.62: Raw Torque degradation data for the MgAl LDH at 5 PHR, with 2 mill passes.

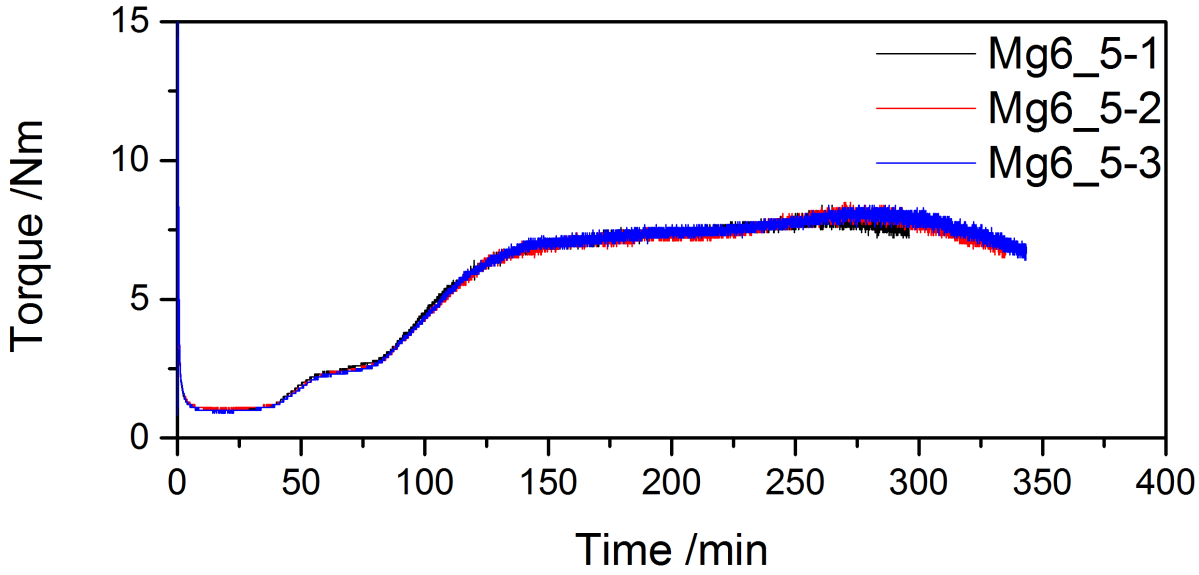

Figure A.63: Raw Torque degradation data for the MgAl LDH at 5 PHR, with 6 mill passes.

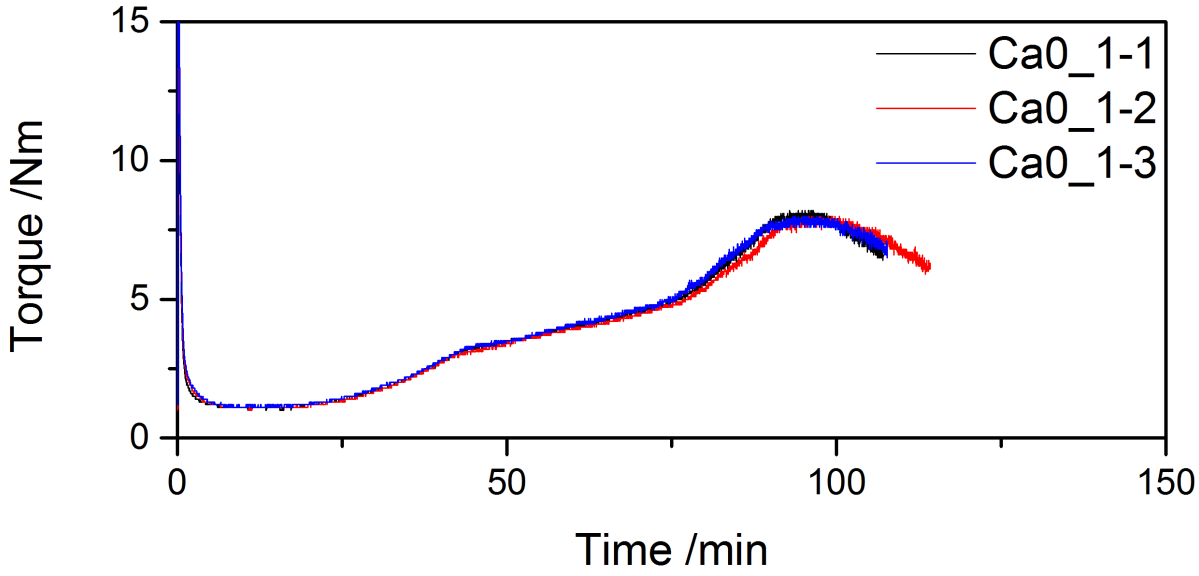

Figure A.64: Raw Torque degradation data for the CaAl LDH at 1 PHR, with 0 mill passes.

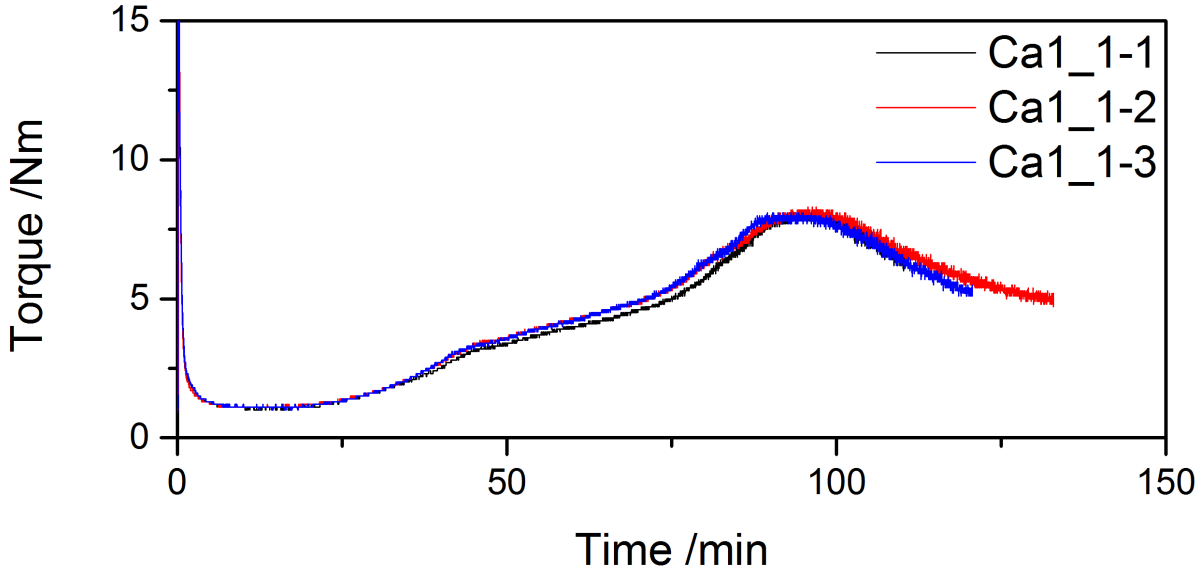

Figure A.65: Raw Torque degradation data for the CaAl LDH at 1 PHR, with 1 mill pass.

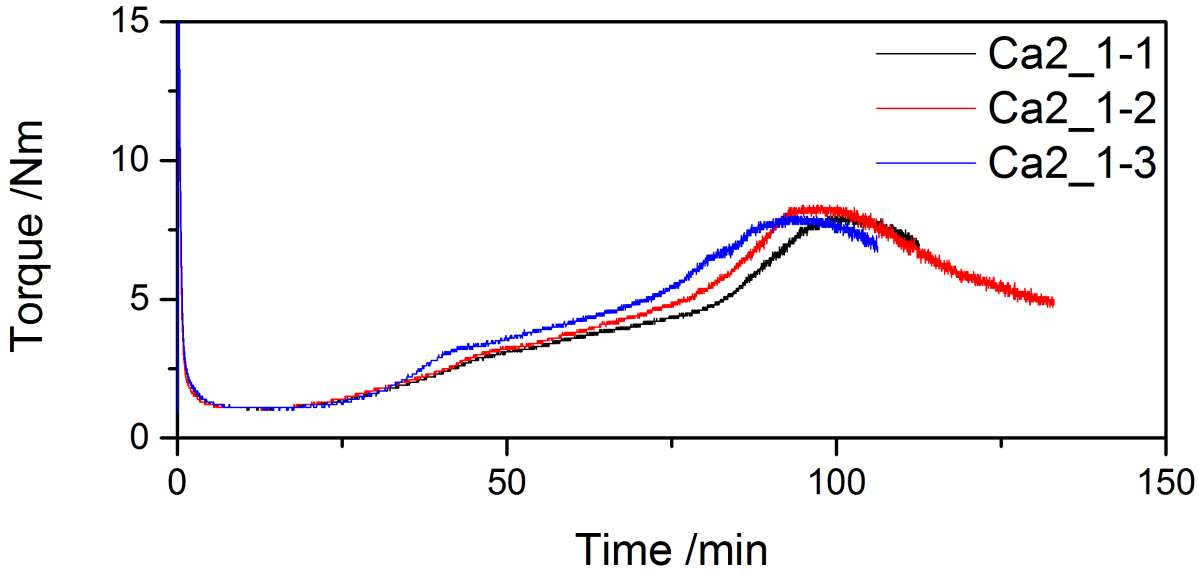

Figure A.66: Raw Torque degradation data for the CaAl LDH at 1 PHR, with 2 mill passes.

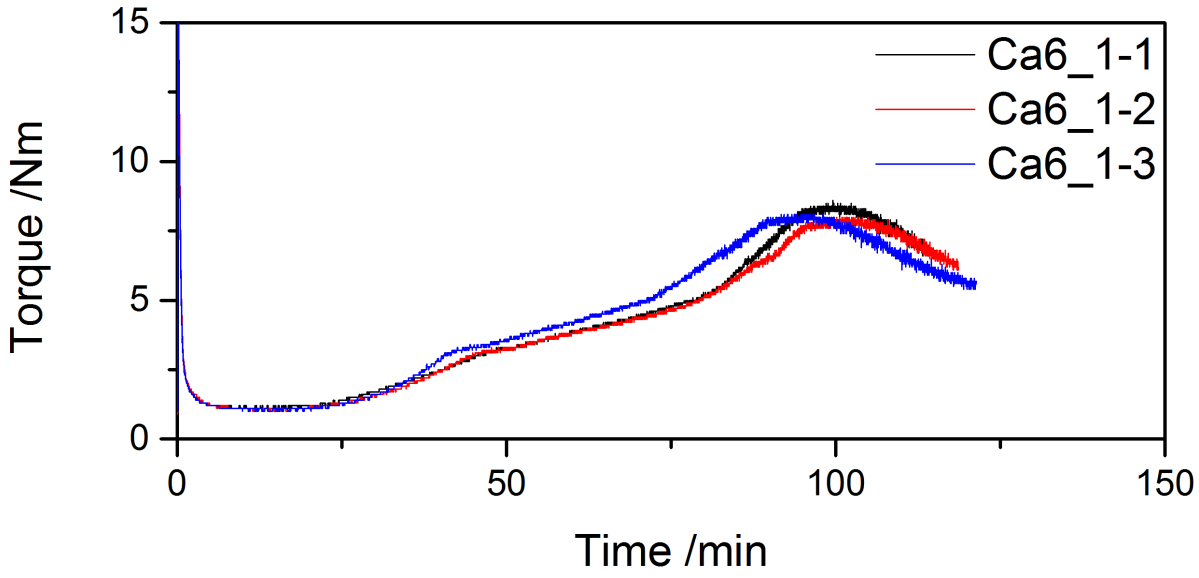

Figure A.67: Raw Torque degradation data for the CaAl LDH at 1 PHR, with 6 mill passes.

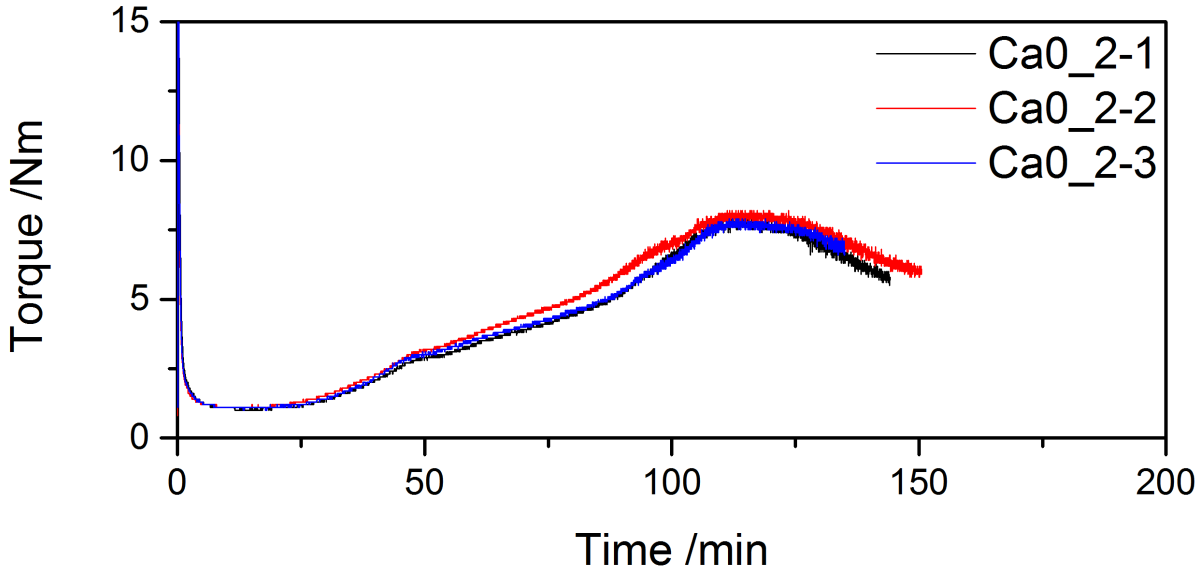

Figure A.68: Raw Torque degradation data for the CaAl LDH at 2 PHR, with 0 mill passes.

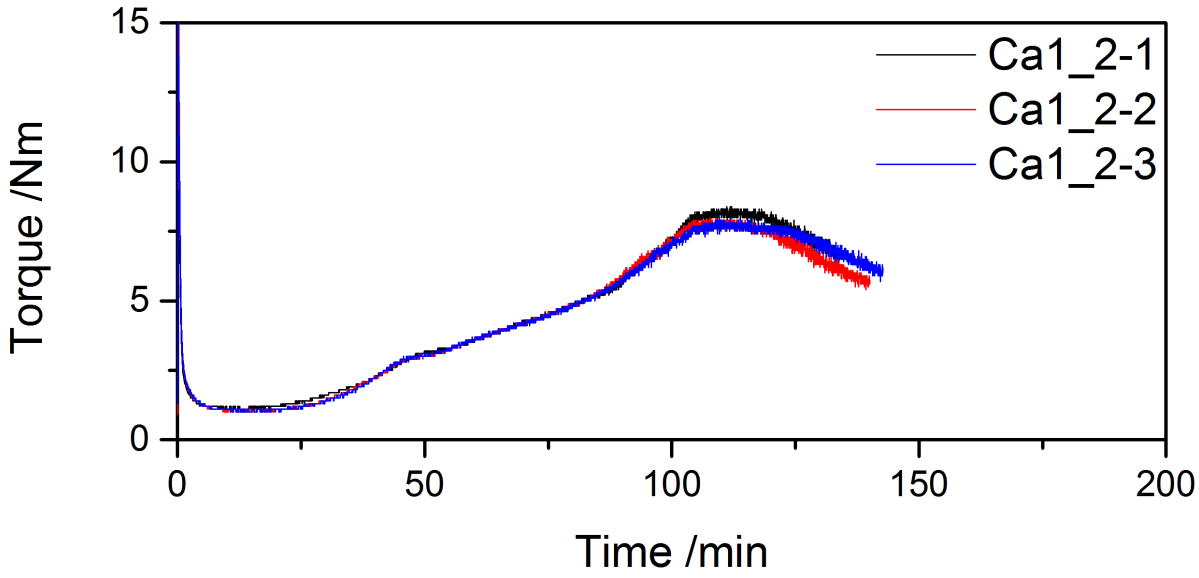

Figure A.69: Raw Torque degradation data for the CaAl LDH at 2 PHR, with 1 mill pass.

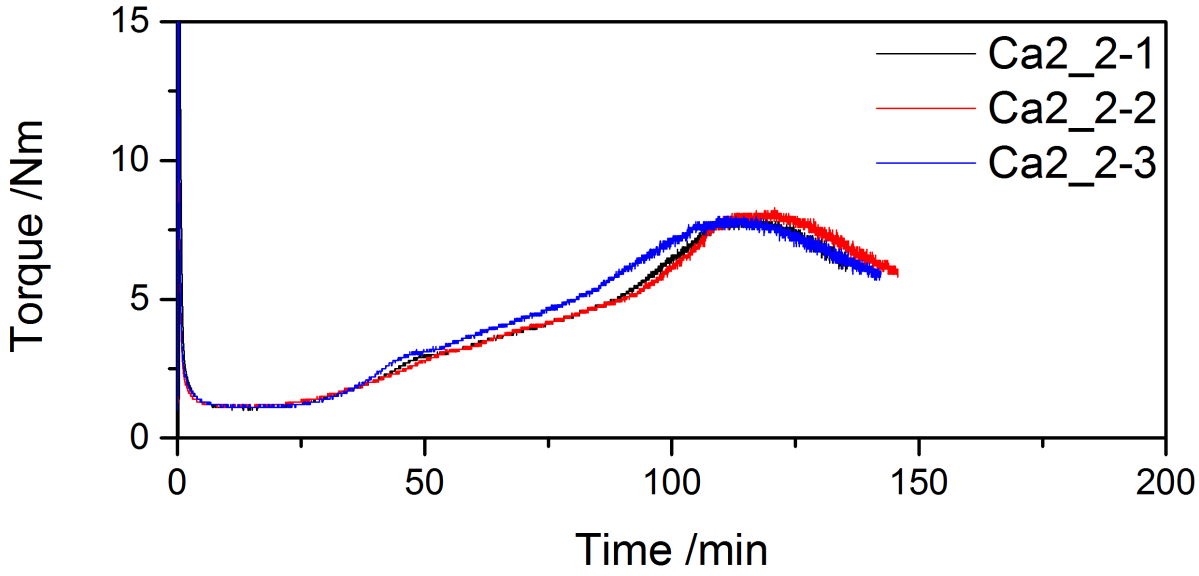

Figure A.70: Raw Torque degradation data for the CaAl LDH at 2 PHR, with 2 mill passes.

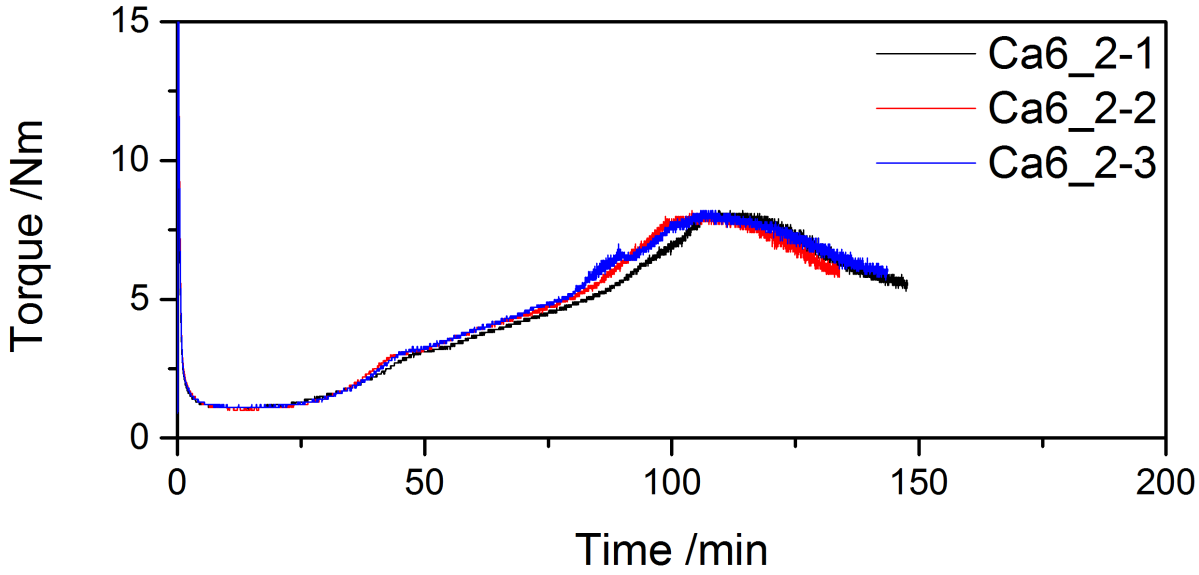

Figure A.71: Raw Torque degradation data for the CaAl LDH at 2 PHR, with 6 mill passes.

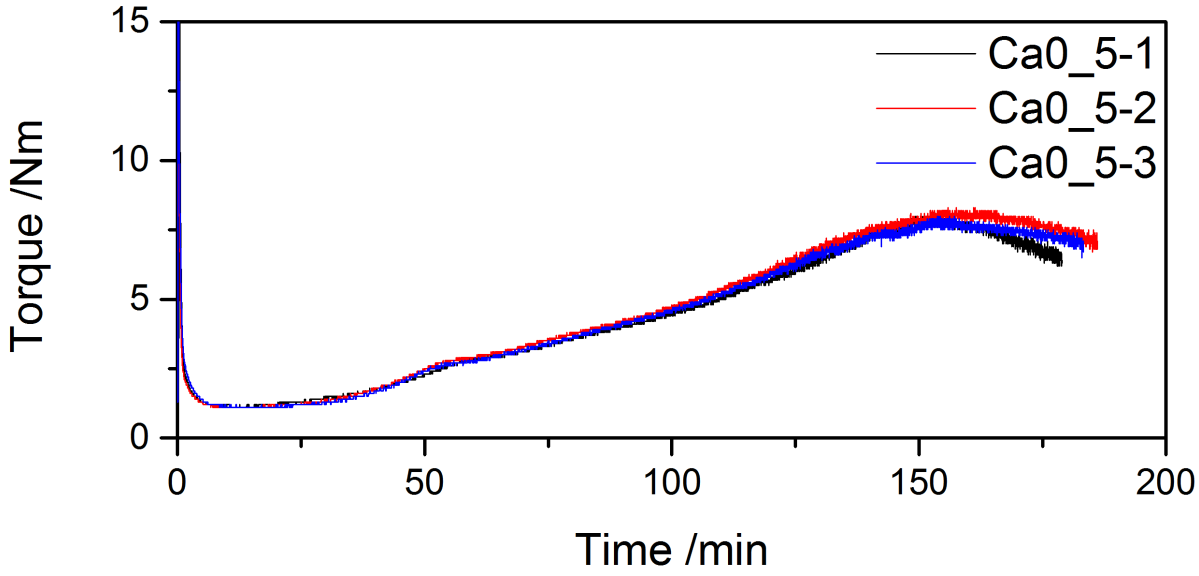

Figure A.72: Raw Torque degradation data for the CaAl LDH at 5 PHR, with 0 mill passes.

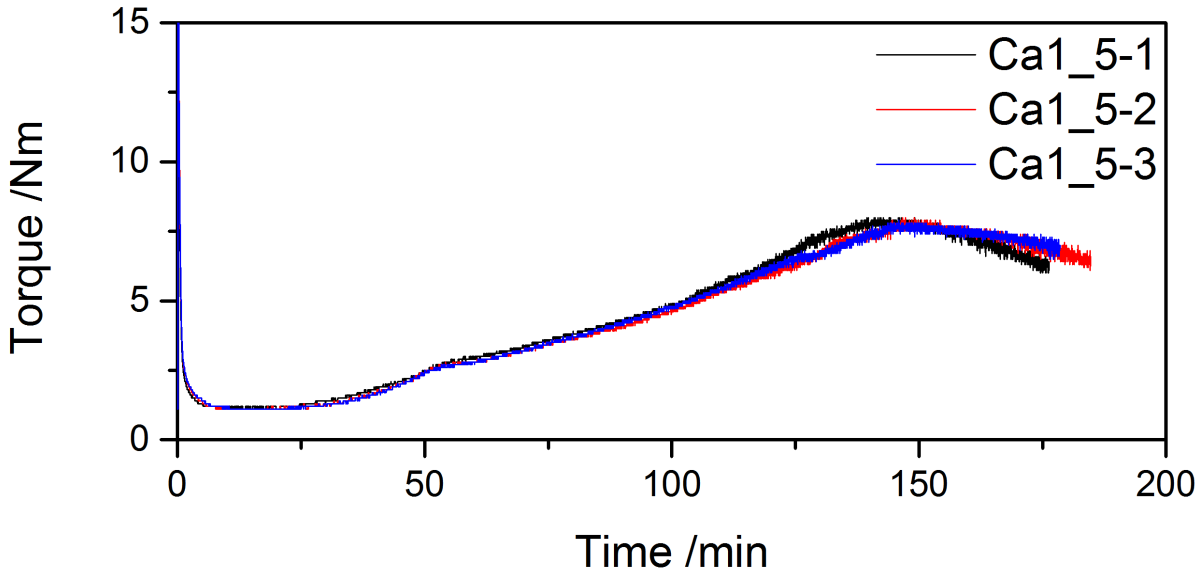

Figure A.73: Raw Torque degradation data for the CaAl LDH at 5 PHR, with 1 mill pass.

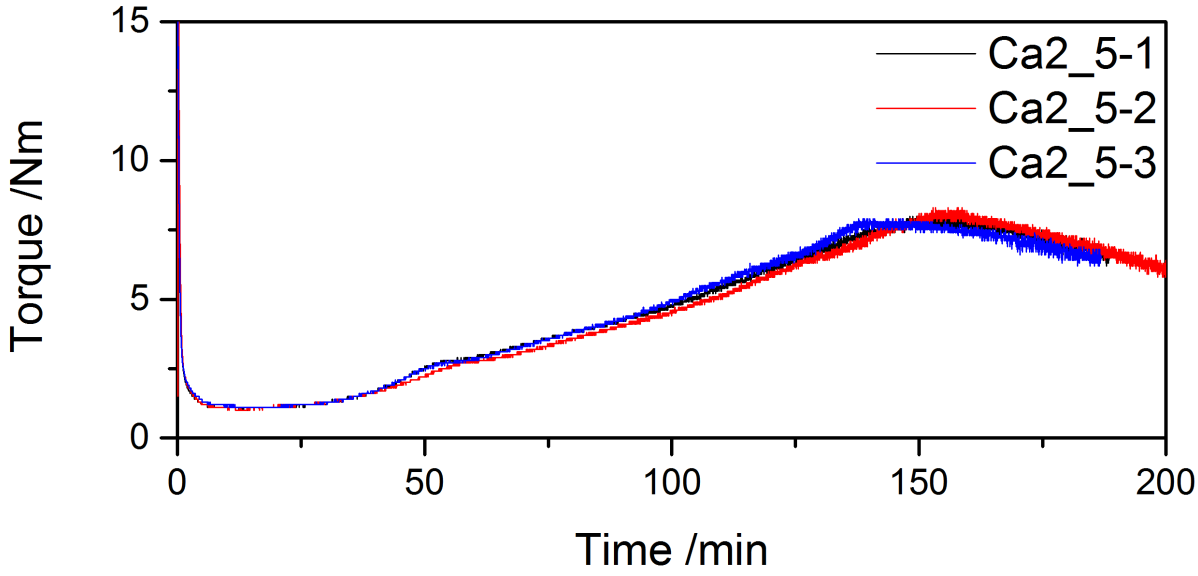

Figure A.74: Raw Torque degradation data for the CaAl LDH at 5 PHR, with 2 mill passes.

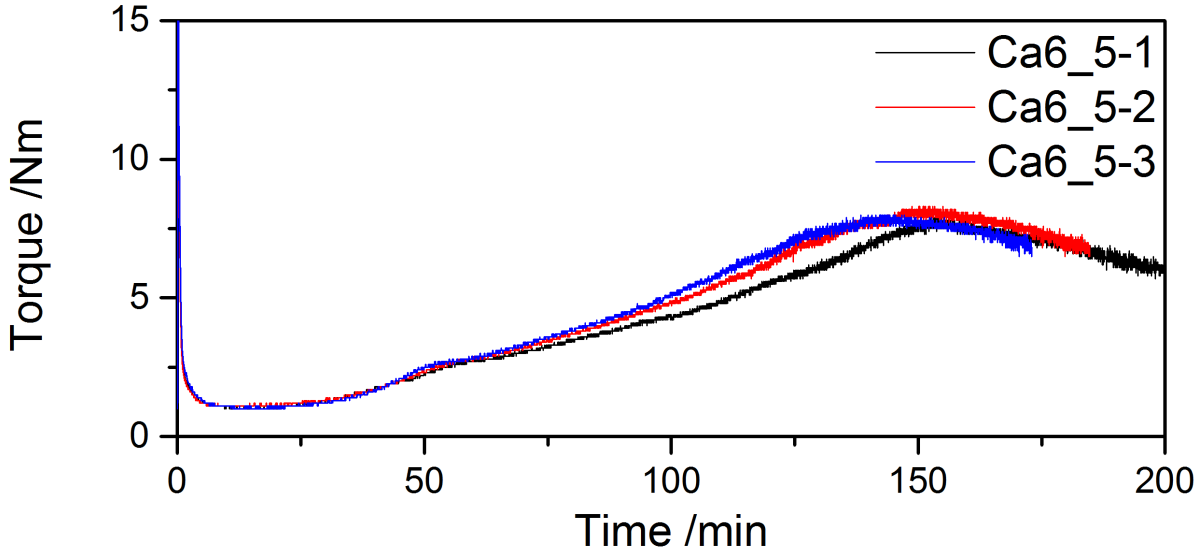

Figure A.75: Raw Torque degradation data for the CaAl LDH at 5 PHR, with 6 mill passes.